NASA Technical Paper 2872

1988

Effects of Variables Upon Pyrotechnically Induced Shock Response Spectra

Part II

James Lee Smith
George C. Marshall Space Flight Center
Marshall Space Flight Center, Alabama

National Aeronautics and Space Administration

Scientific and Technical Information Division

TABLE OF CONTENTS

LIST OF ILLUSTRATIONS

LIST OF ILLUSTRATIONS (Continued)

LIST OF ILLUSTRATIONS (Continued)

LIST OF ILLUSTRATIONS (Continued)

LIST OF ILLUSTRATIONS (Concluded)

TECHNICAL PAPER

EFFECTS OF VARIABLES UPON PYROTECHNICALLY INDUCED SHOCK RESPONSE SPECTRA – PART II

I. INTRODUCTION

Throughout the aerospace industry, large variations of 50 percent (6 dB) or more in shock response spectra (SRS) derived from pyrotechnic separation events continue to be reported from actual spaceflight data and from laboratory tests. Designers continue to over design to allow for these large variations in shock level.

One failure attributable to large shock variations occurred in June 1982. Two Solid Rocket Boosters (SRBs) were lost during the Space Transportation System Mission 4 (STS-4). The subsequent failure investigation conducted by the National Aeronautics and Space Administration's (NASA) Marshall Space Flight Center (MSFC) indicated that a water impact switch, used to cut the parachutes from the SRBs, functioned prematurely on a spurious shock signal from the SRB Frustum Separation Assembly (FSA). As a result, the parachutes were cut before deployment. The failure investigation prompted three full-scale ground tests of the FSA to be performed at MSFC.

During test one of the full-scale FSA ground tests, the water impact switch remained open. During test two the switch "chattered" but remained open. However, in test three, the switch closed! Approximately 40 channels of shock data were collected in each test. Variations of 50 percent (6 dB) or more were observed for the same measuring location from test to test. The variations raised many questions regarding the repeatability of SRS from similar explosive sources, and the accuracy and precision of the shock data. These three tests raised many questions, but provided few answers.

As a result of these tests and the STS-4 failure, NASA funded a research program for 1984 through 1986. The research team realized that the single largest problem in studying pyrotechnic shock was instrumentation. Most companies were using mounting blocks with their accelerometers. These blocks acted as mechanical filters, filtering out high frequency data and in many cases resulting in the accelerometer measuring mounting block resonance instead of the actual shock. In addition, accelerometer resonance, signal noise, lead cable failure, error from signal conditioners and amplifiers, and even accelerometer destruction due to severe environments, can result in poor signal or loss of signal.

The purpose of the 1984-1986 project was to analyze variations in pyrotechnically induced SRS and to determine if and to what degree manufacturing and assembly variables and tolerances, distance from the shock source, data acquisition instrumentation, and shock energy propagation affect the SRS. Another major goal of the project was to prove the repeatability of SRS for a given source and to show that these repeatable shocks were higher in level and in frequency content than previously believed.

First, all accelerometers used in the project were ball-drop calibrated. Next, 28 preliminary plate tests were performed to develop a basic understanding of the shock produced, to evaluate instrumentation, to determine the distance from the source to the accelerometer at which the accelerometers would survive, to determine plate size, and to generally direct the flow of the primary plate test series.

The primary test series consisted of 36 plates. Variables investigated were coreload, plate thickness, alloy variety, standoff, coupling, linear-shaped charge (LSC) apex angle, joint effects, mounting block effects, triaxial effects, and combinations of variables. Ten plates were used to develop a control case, the base reference mean SRS, and to investigate SRS repeatability.

Data from the above tests were analyzed yielding the following results: LSC variables do not affect SRS as long as the plate is completely severed. Accelerometers mounted on mounting blocks showed significantly lower levels above 5000 Hz. Lap joints do not affect SRS levels on free-free boundary plates. Since the tests plates were mounted with almost free-free boundary conditions, shock as a function of distance from the source is negligible. That is, SRS does not vary with distance from the source. Several varieties and brands of accelerometers were utilized – all varieties with one exception demonstrated very large variations in SRS for side-by-side measurements on the same plate and from plate to plate. One accelerometer gave very good repeatable results throughout the program. Instrumentation is the cause of the large variations in SRS. SRS from the same source are indeed repeatable.

The results of this study were documented in NASA TP-2603, "Effects of Variables Upon Pyrotechnically Induced Shock Response Spectra," May 1986, and Explosive Technology Final Report 0231(01)FTR, June 1986, under NASA Contract NAS8-36149.

NASA funded an additional study for 1987-1988. This study was a continuation of the previous study reference above. This paper is a summary of the additional study. The purpose of this study was to evaluate LSC-induced shock dissipation through various spacecraft structural joint types, to evaluate LSC-induced shock variation for various manufacturing and assembly variables on clamped boundary test plates, and to verify that data correction techniques are capable of accurately recovering pyroshock data from distorted data records. This study was a direct outgrowth of previous research and can be traced back to problems encountered early in the STS program as previously outlined.

Eleven pyrotechnic test plates were manufactured utilizing the SRB FSA. Five clamped boundary plate tests investigated manufacturing and assembly variables and mass loading effects. Six free-free boundary plate tests investigated shock dissipation across spacecraft joint structures.

Each free-free boundary test plate was center severed by an LSC. Two test joints were located symmetrically between the center charge and the ends of the plate, one joint on each side. Clamped boundary test plates were end severed, just as in the previous 1984-1986 research study. Therefore, data from the clamped boundary tests would be directly comparable to that of the previous study.

Data from the previous study and from the eleven plate tests in this follow-on study contained sufficient distorted raw data from side-by-side measurements for proof of principle of data correction techniques. The data corrections study results will be published as a separate paper within the next year.

All 11 tests were successfully performed completing the test phase of the research effort. Time histories from 4-msec windows (primary shock) and 20-msec windows (residual and total shock) were stored on computer disc and plotted. SRS and Fourier spectra were also calculated and plotted.

Data from all 11 plate tests and from the previous study were analyzed. Results from the joint energy dissipation tests were analyzed to aid engineers in designing to reduce pyrotechnic shock levels. Results from the manufacturing and assembly variables tests were used to determine variations in shock levels for these variables for free-free and clamped boundary plates. The minimum and maximum shock perturbation for these variables were plotted.

Distorted and non-distorted data from side-by-side measurements were utilized in the data correction techniques study. From side-by-side measurements on the same test plate, a distorted channel was corrected and compared to a non-distorted channel yielding a measure of the accuracy of the correction techniques.

II. DESCRIPTION OF EQUIPMENT

Major equipment consisted of the test fixture, test plates, and signal recording and analyzing instrumentation. Cables, connectors, switches, and other such components will not be discussed. Recommended accelerometer support instrumentation were utilized.

For a discussion of equipment used in the previous 1984-1988 study see NASA TP-2603. The previous study utilized elastomerically restrained end severed test plates. Instrumentation and support hardware were basically the same as those used in this study.

A. Test Fixture

Two distinct test setups were employed, one for the joint tests and one for the rigid mounted tests. A wood and steel work table with its central table surface portion removed served as the basic support structure for all tests.

In the joint tests, the test plates were elastomerically restrained. The plates were mounted directly to the table using elastomeric restraints with a stiffness of 2.8 lb/in. (Fig. 1).

In the rigid mounted tests, the test plates were bolted to a 1/2-in. thick mild steel plate that was in turn bolted to the test table. Ten high strength commercial fasteners were used to attach the test plate to the fixture as illustrated in Figure 2.

B. Test Plates

The test plates used for all the tests represent flat versions of the SRB frustum separation system. The aluminum 6061-T651 plates measured 4 ft in length by 1 ft in width by 1/4 in. in thickness. These are the same type of plates used in the 1984-1988 study. The separation area was machined to a thickness of 0.215 in. to simulate the actual thickness of the frustum splice ring.

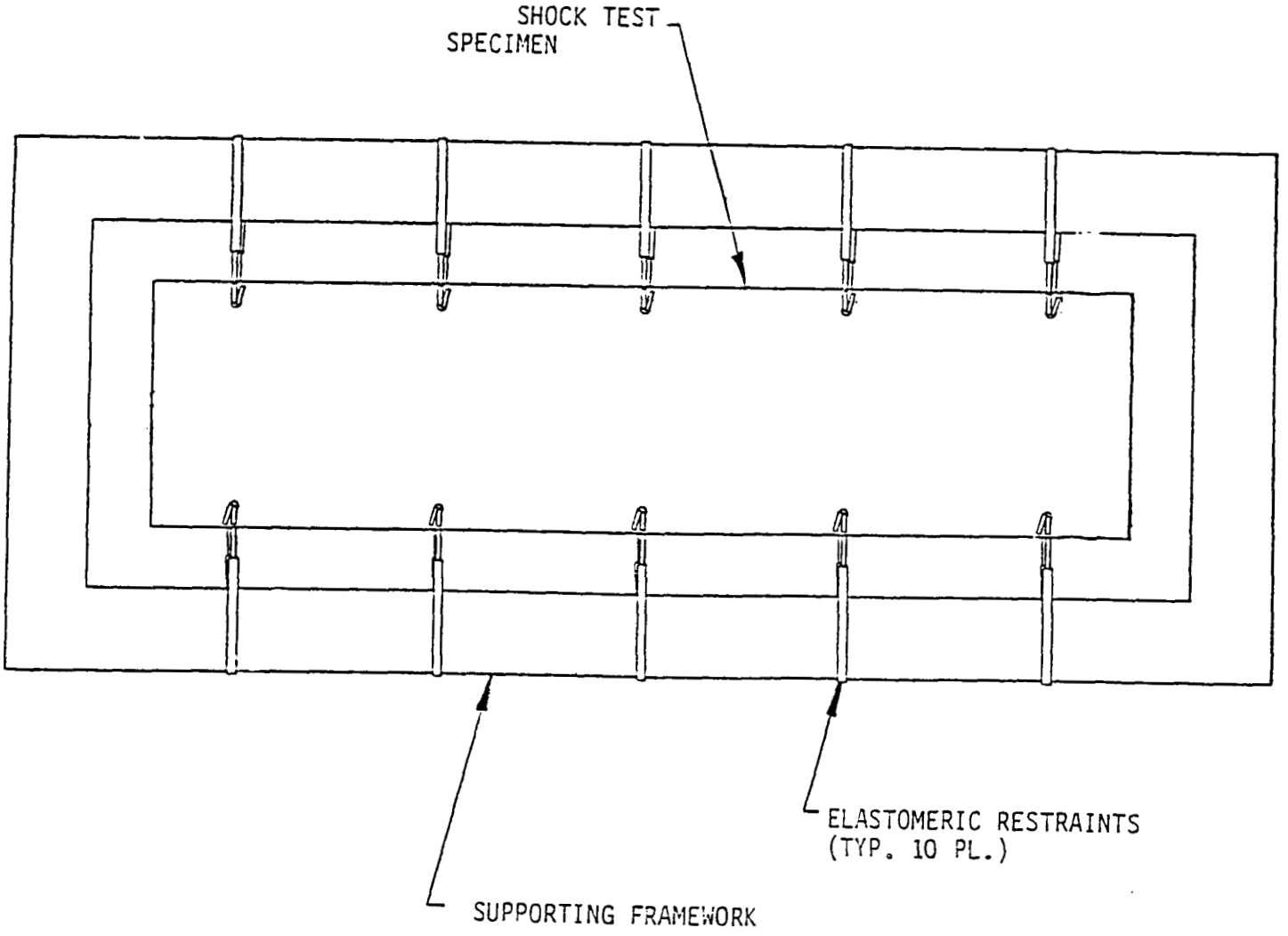

Figure 1. Test setup: NASA shock study.

1018 Mild Steel
72 x 34 x 1/2-inch thick,
WT = 251 lbs (after cut)

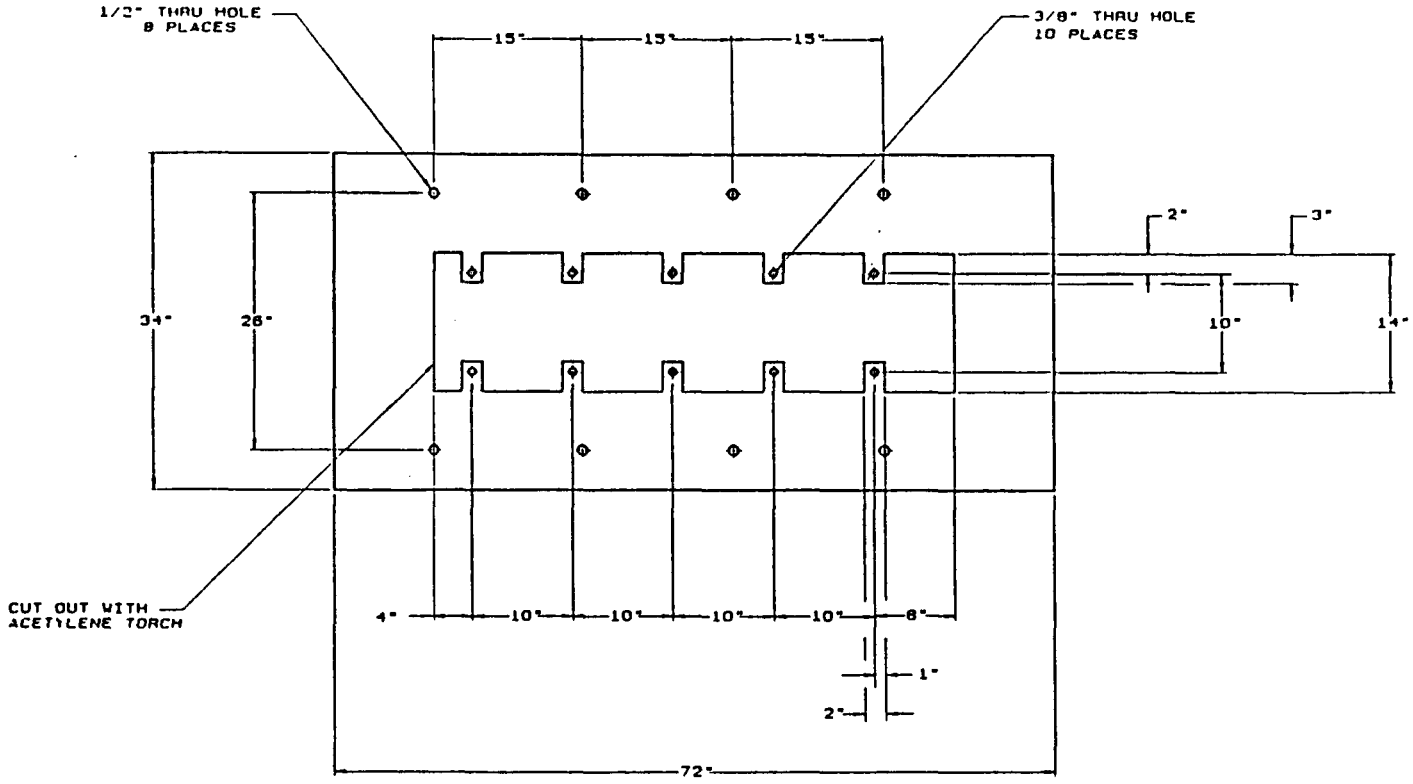

Figure 2. Rigid shock fixture.

Test plate number 11 (the overload test) was severed using RL-40-J- LSC, 40 grains per foot of RDX explosive in a lead sheath. All other plates were severed using HL-30-J LSC, 30 grains per foot of HMX explosive in a lead sheath.

Although the same plates were utilized throughout the program, they were configured differently depending upon the type of test.

All LSC were initiated using non-electric blasting caps and non-conductive TLX firing lines to prevent the possibility of introducing electrical noise from the firing signal into the transducers.

The joint plates were configured to study the reduction in shock energy across typical structural joint types and for comparison with data from the previous study. The rigid mount plates were configured such that the effects of severe edge-dampening upon SRS could be assessed.

1. Joint Tests

Test plates 1 through 6 were configured for the joint tests. Figure 3 illustrates the configuration for the joint tests. All joint test plates were center severed cutting the plate into two 2-ft sections. The LSC were enclosed in a rubberized charge holder that was glued to the test plate. Aluminum angle was

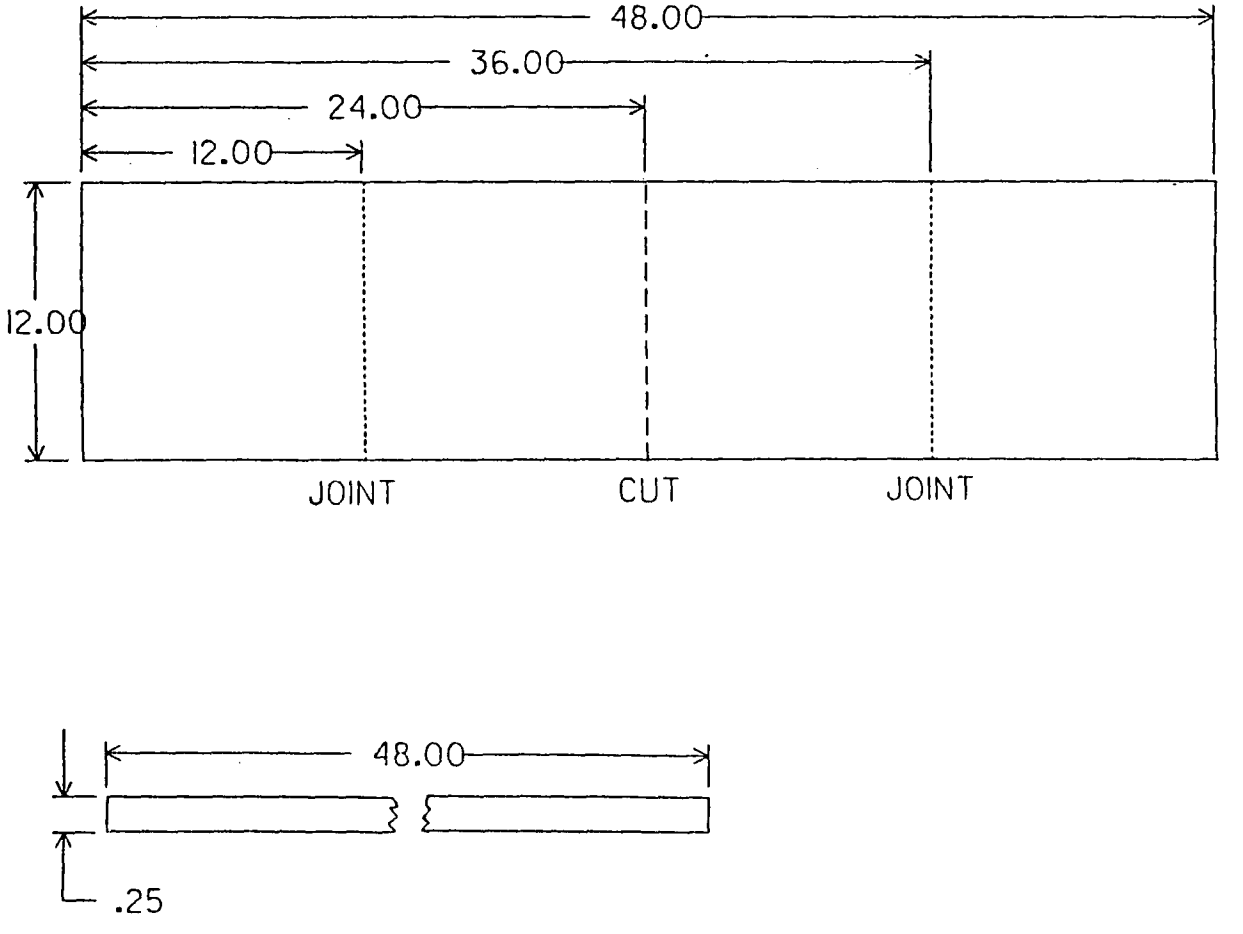

Figure 3. Joint test drawing.

bolted on both sides of the LSC charge to function as a blast shield for the accelerometers and cables. This will help prevent scrapnel from damaging instrumentation (Fig. 4).

A test joint was located 1 ft from each end, two joints per test plate (Fig. 5). Tests 1 and 2 were experimental controls – there were no joints. Tests 3 through 6 consisted of two joints per plate. Joint test variables were as follows.

Test Number	Variables
1	Control
2	Control
3	Simple Lap Joints: 3 in. and 6 in.
4	Double Lap Joints: 3 in. and 6 in.
5	Simple Lap Joints: 3 in. and 6 in. with a 1 in. Joint Gap
6	Double Lap Joints: 3 in. and 6 in. with Shims and a 1 in. Gap

Figures 6 through 13 illustrate the joint test configurations. The joint tests plates were elastomerically restrained.

2. Rigid Mount Tests

Test plates 7 through 11 were used for the rigid mount tests. These plates were bolted to a mild steel test fixture as previously specified. This produced a highly damped, fixed boundary system for comparison to the free-free boundary tests conducted in the previous study. These plates were configured just as those used in the previous 1984-1988 program. The plates were end severed and an aluminum charge holder was utilized. This charge holder was bolted to the plate fitting over the rubber charge holder which contains the LSC (Fig. 14). The variables utilized were as follows:

Test Number	Variables
7	Control
8	Control: A steel cube weighing 133.57 lb was mounted in the center of the plate
9	Maximum SRS: Maximum coreload tolerance, maximum chargeholder coupling, minimum LSC standoff
10	Minimum SRS: Minimum coreload tolerance, minimum chargeholder coupling, maximum LSC standoff
11	Charge Overload: 40 grains per foot instead of 30 grains per foot, an unamplified accelerometer to be discussed later

Figures 15 and 16 illustrate the test plates used in the rigid mount tests.

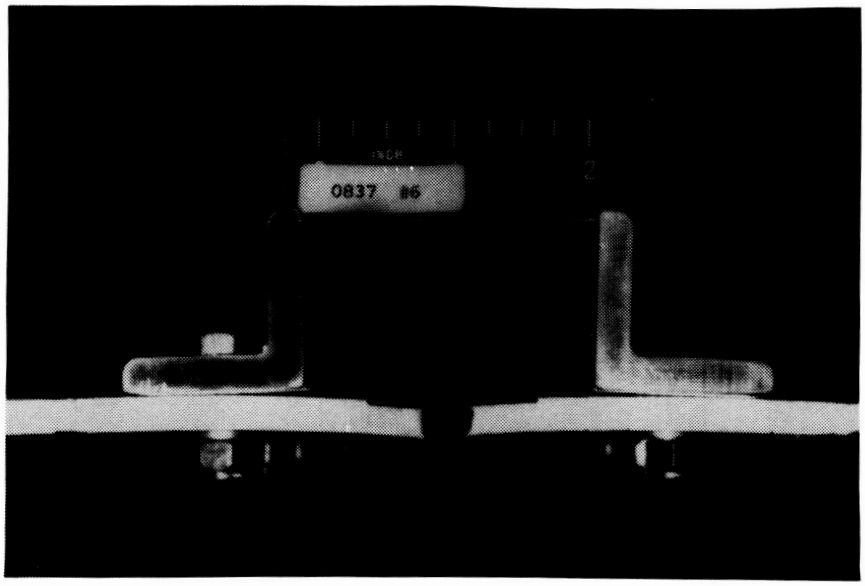

Figure 4. Joint test blast shield.

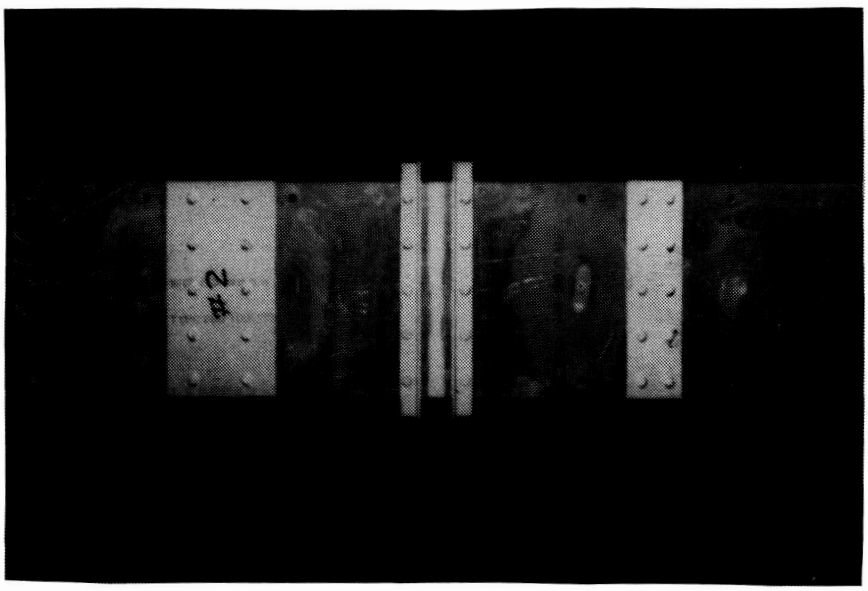

Figure 5. Joint test plate.

Figure 6. Joint test control plate.

Figure 7. Joint test plate with joints.

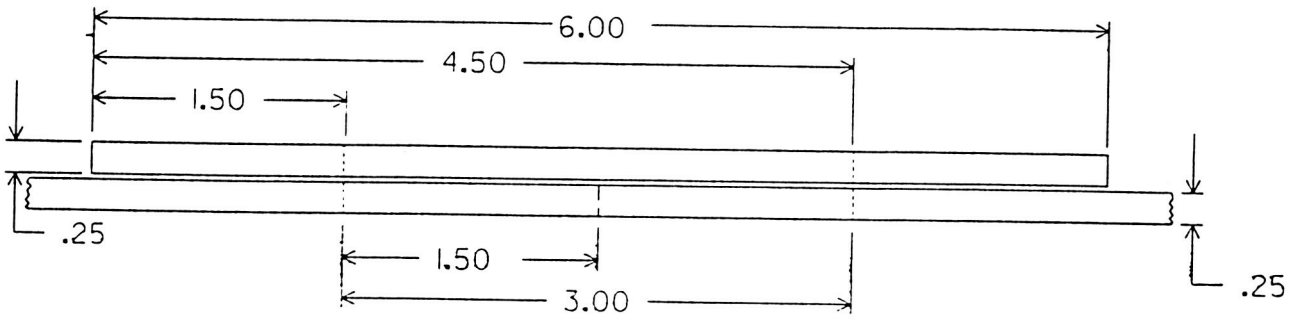

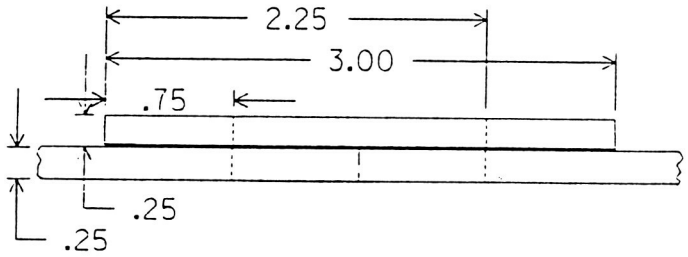

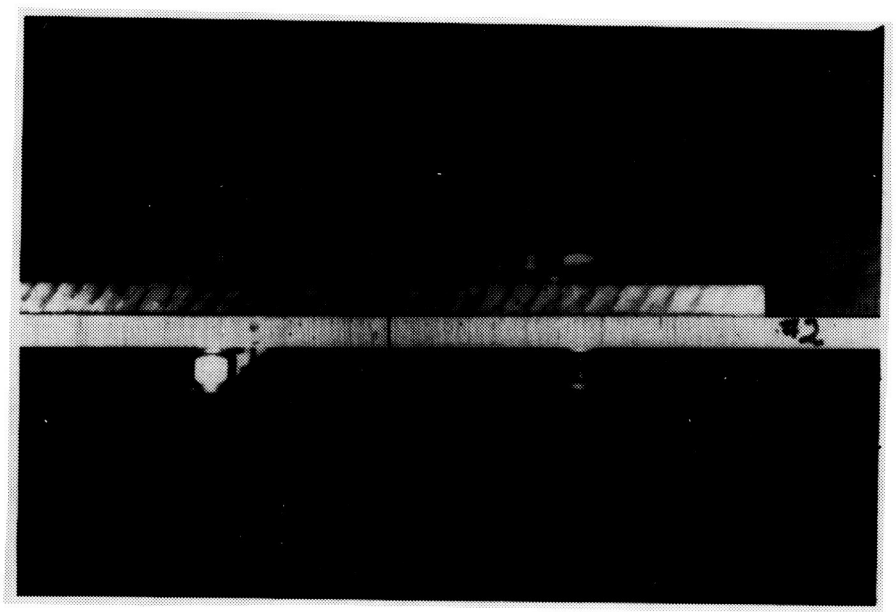

Figure 8. Joint test plate No. 3.

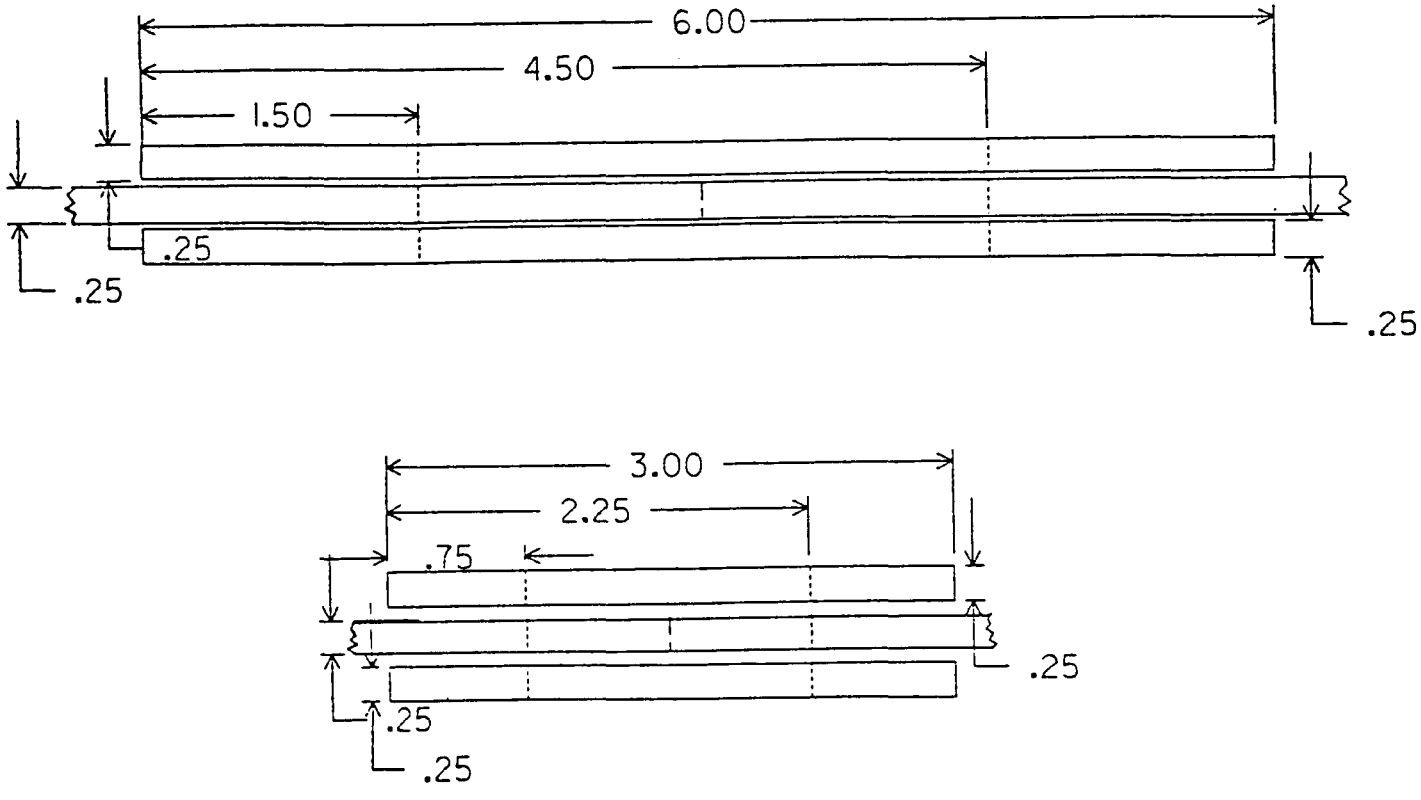

Figure 9. Joint test plate No. 4.

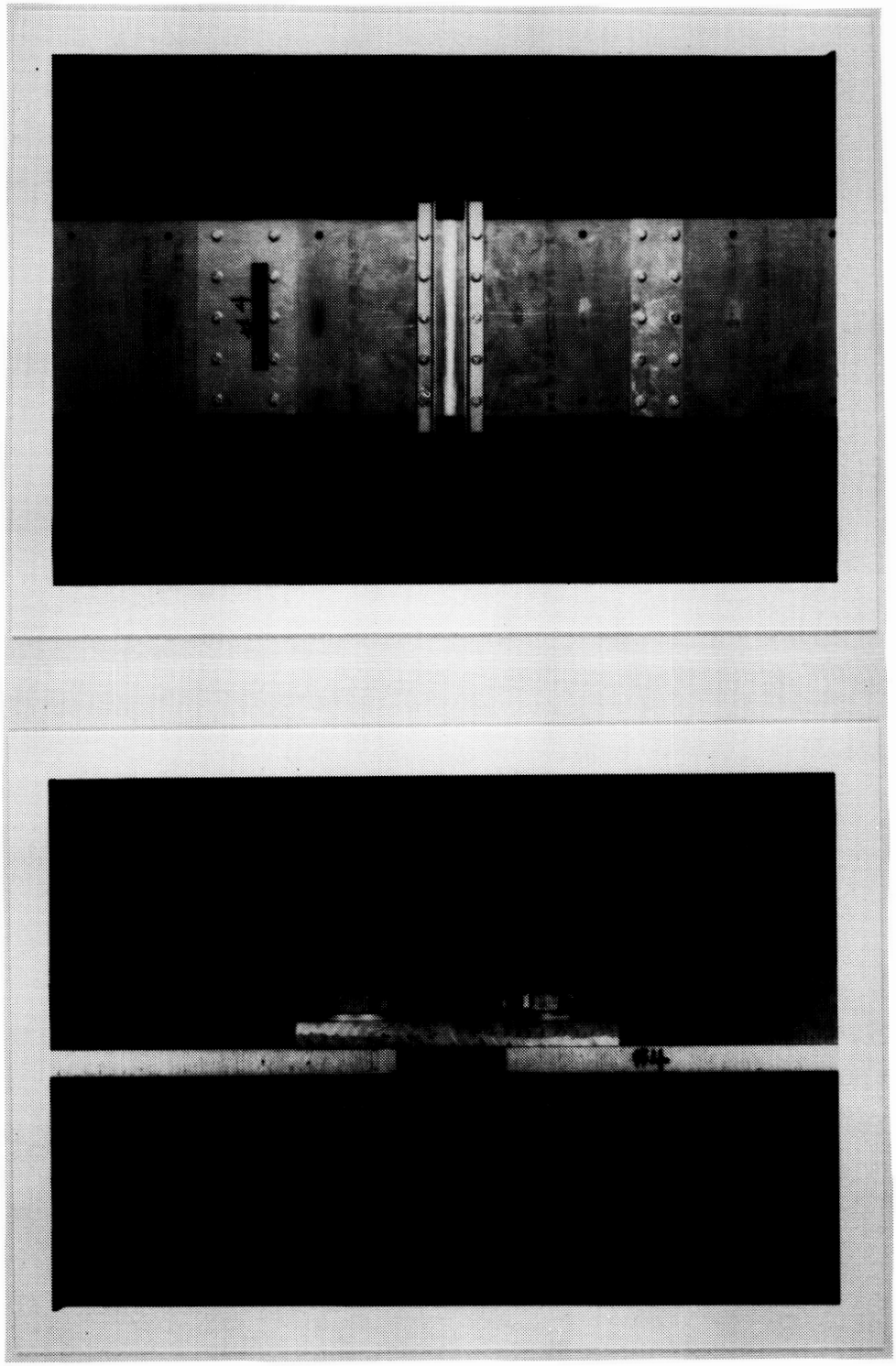

Figure 10. Joint test plate No. 5.

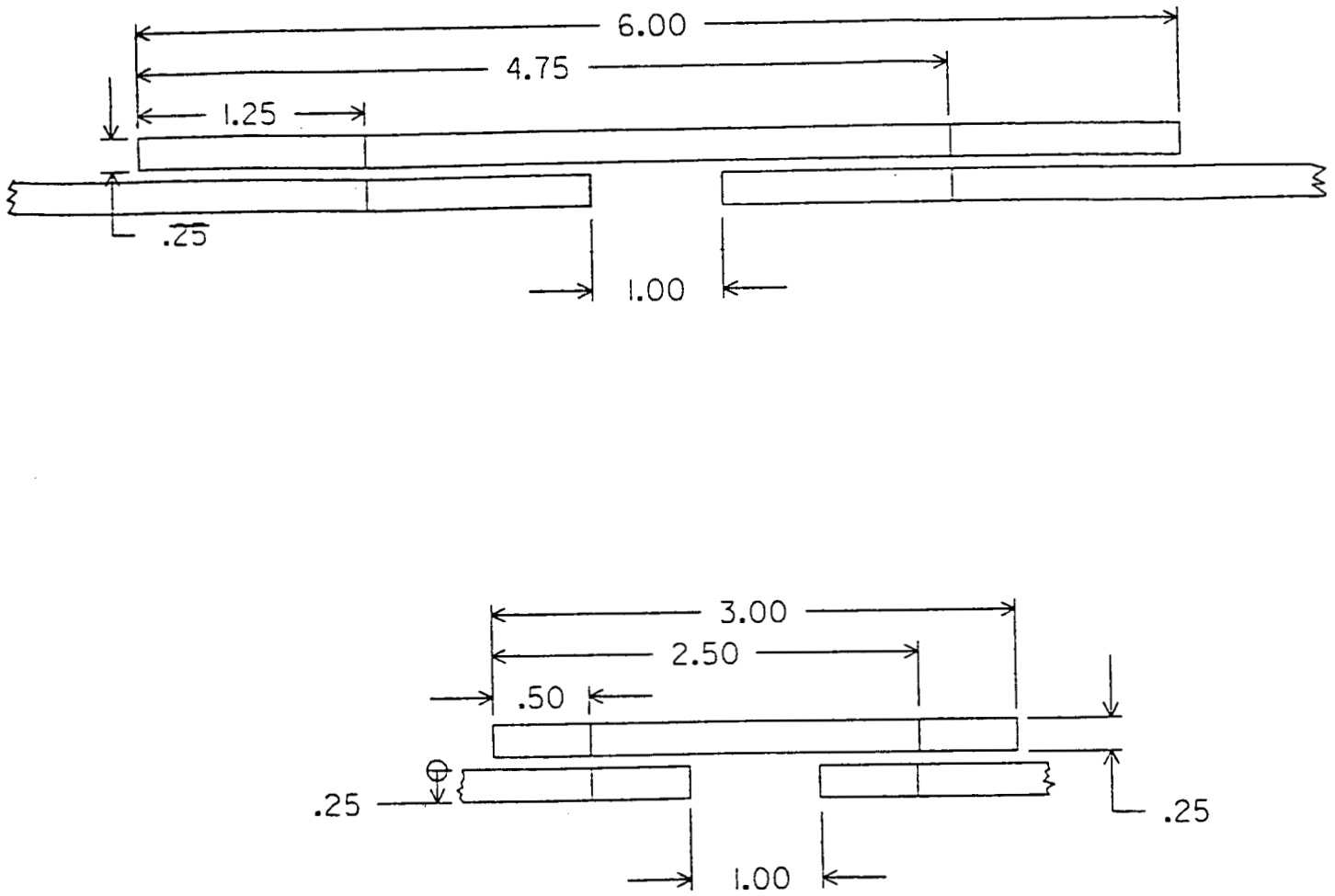

Figure 11. Joint test plate No. 5.

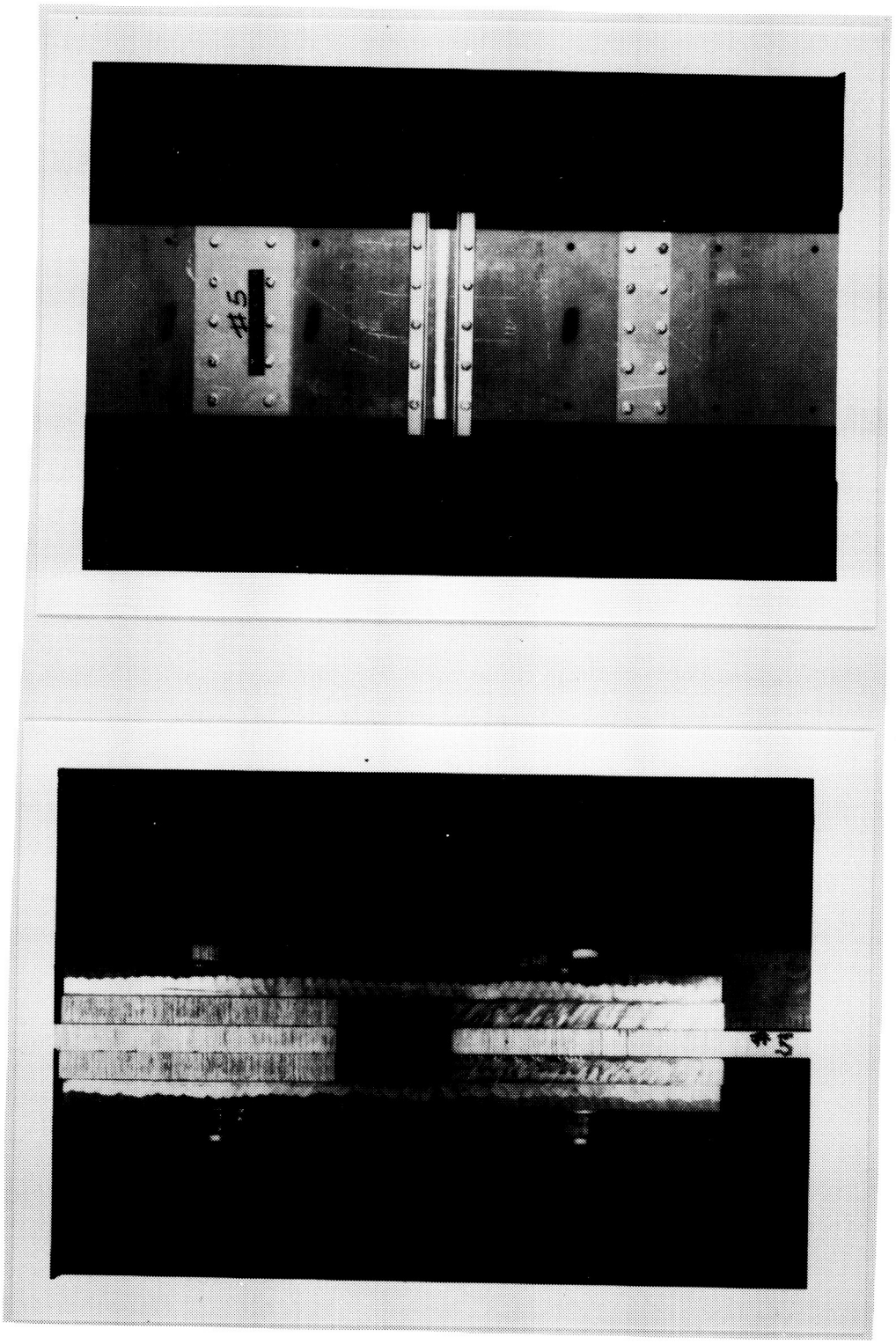

Figure 12. Joint test plate No. 6.

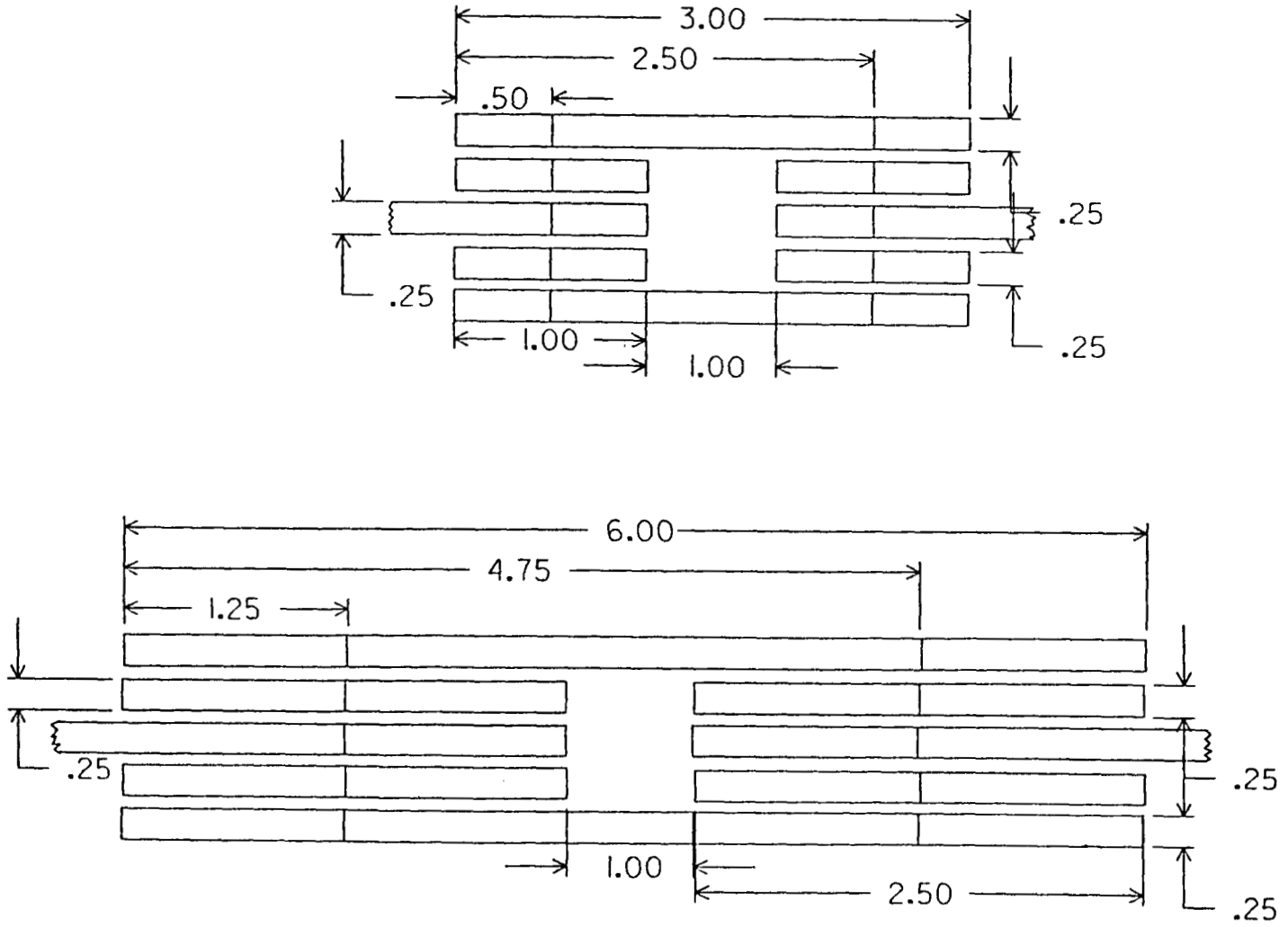

Figure 13. Joint test plate No. 6.

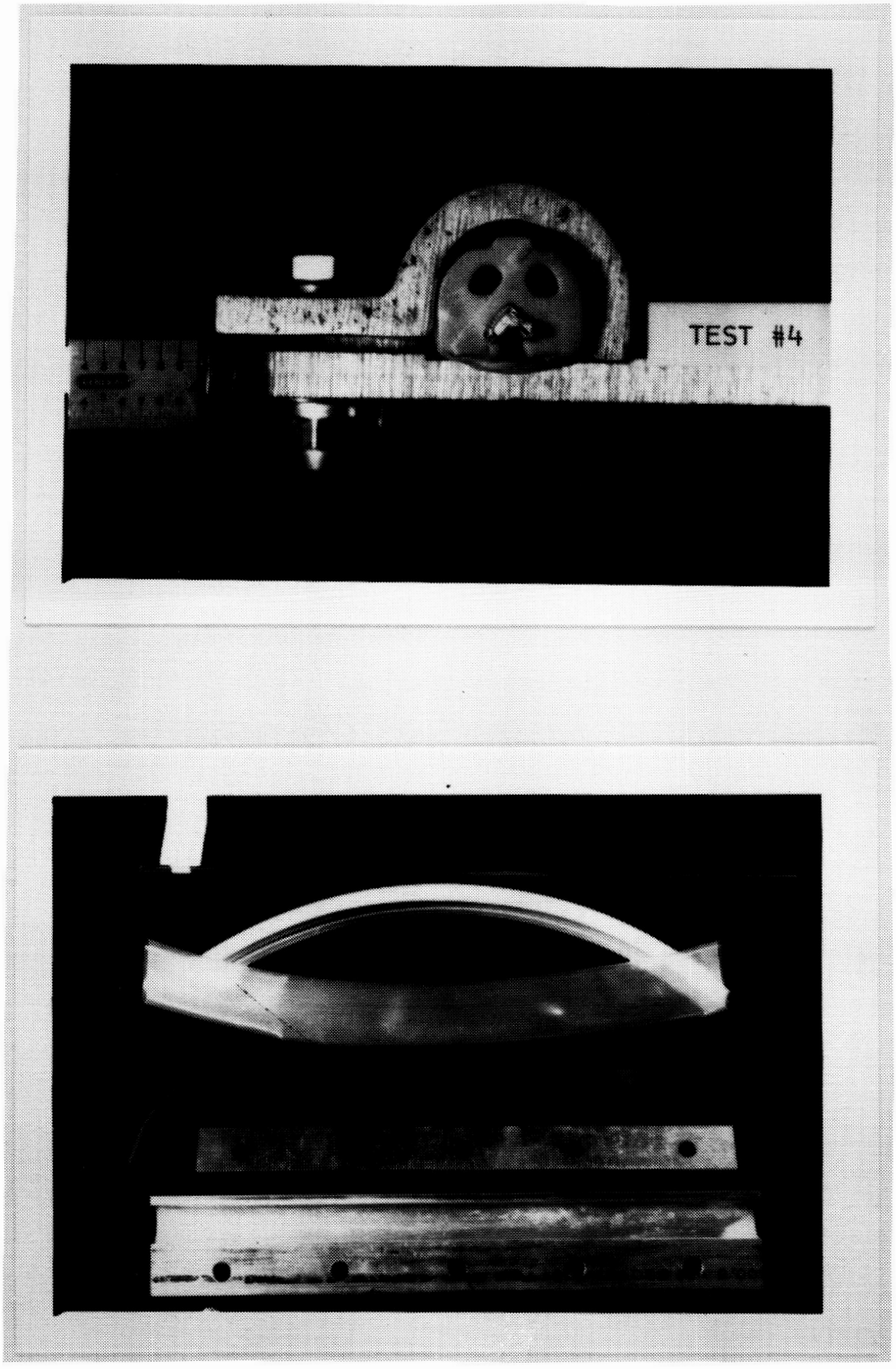

Figure 14. Rigid test charge holder end and expanded views.

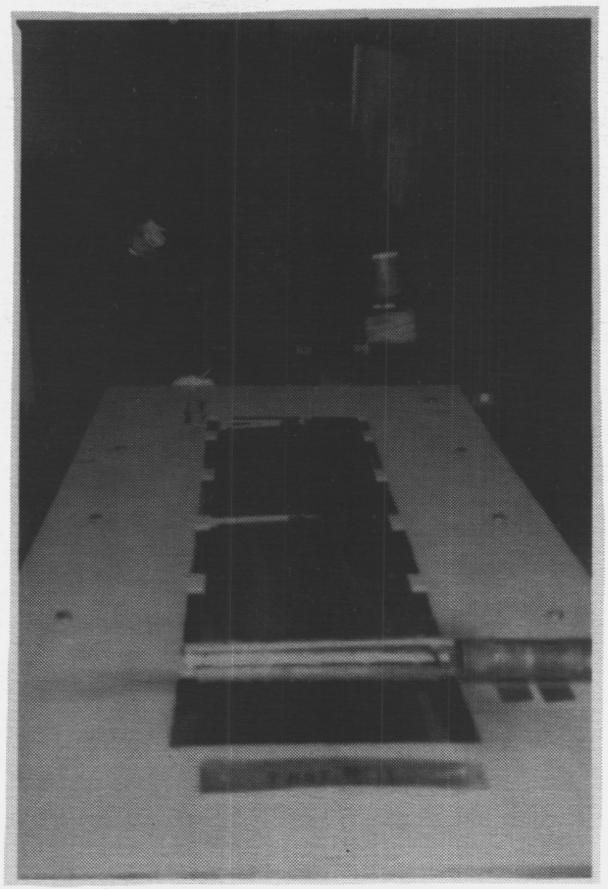

Figure 15. Rigid test plate.

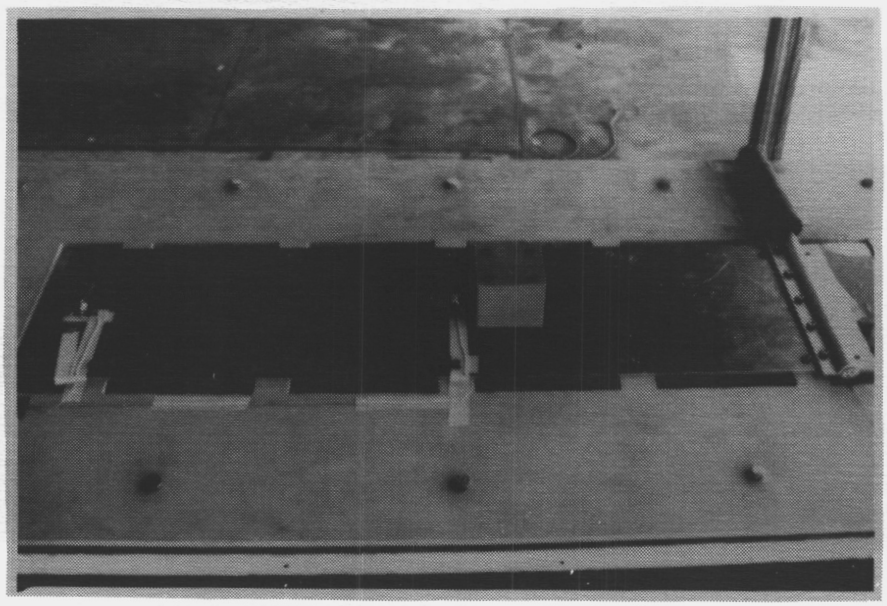

Figure 16. Rigid test plate mass loaded.

C. Signal Recording and Analyzing Equipment

On the joint test plates, four accelerometers were mounted, two on either side of the LSC 8 in. from the charge, and one between each test joint and the end of the plate, 16 in. from the LSC (Fig. 17).

On the rigid mount test plates, two accelerometers were mounted, one 22 in. and one 44 in. from the LSC. Test 11 added an extra accelerometer for the unamplified experiment, two of the accelerometers were side-by-side. All accelerometers were mounted in the longitudinal centerline of the plate for both joint and rigid mount test plates. Figure 18 shows accelerometer locations for the rigid tests.

Based upon knowledge and experience gained in the previous study, only Endevco 7270 high-shock accelerometers were used in this study. Only those accelerometers with sensitivities between 1.25 and 1.50 microvolts per G were selected. This range yielded the best signal-to-noise ratio and accelerometer survival rate for the shock levels of the program. The same accelerometers were used throughout the program with only one failure early in the program.

Accelerometer signals were amplified by Endevco 2740A or 2740B amplifiers. The signals were captured and stored by two memory systems. Zonic AE-101/102 memory systems with a sampling frequency of 200,000 Hz and a window of 20 msec were utilized – the Zonic system provides usable data up to approximately 50,000 Hz. Nicolet 2090-III digital oscilloscopes with a sampling frequency of 1,000,000 Hz and a window of 4 msec provided usable data up to 200,000 Hz. For comparison purposes, 100,000 Hz SRS were calculated from both memories, even though Zonic data begins to roll-off above 50,000 Hz. All the SRS presented in this paper are from the Nicolet. In this case the SRS based upon 4 msec is the same or greater than the SRS based upon the 20 msec window at all frequencies.

In test 11 of the rigid mount test, the unamplified accelerometer was located side-by-side to an amplified accelerometer. The unamplified accelerometer was powered by a Power Design power supply set at 1 Vdc. The signal by-passed the Endevco signal conditioning equipment. Figures 19 and 20 are illustrations of the instrumentation.

III. EXPERIMENTAL PROCEDURES

This section describes the techniques used to obtain the shock data and the variables investigated. Testing consisted of joint tests and rigid mount tests. In joint testing, variables were various spacecraft joint types and an experimental control. The rigid mount variables were charge overload, maximum SRS combination, minimum SRS combination, mass loading, unamplified accelerometer, and experimental control. In both test series, the control case was used to derive a basic SRS for comparison purposes. The actual test procedure was the same for both series.

A. Standard Firing Procedure

The firing procedure utilized in this program is outlined in the Explosive Technology Standard Test Firing Panel, PN80012, Operating Procedure Manual.

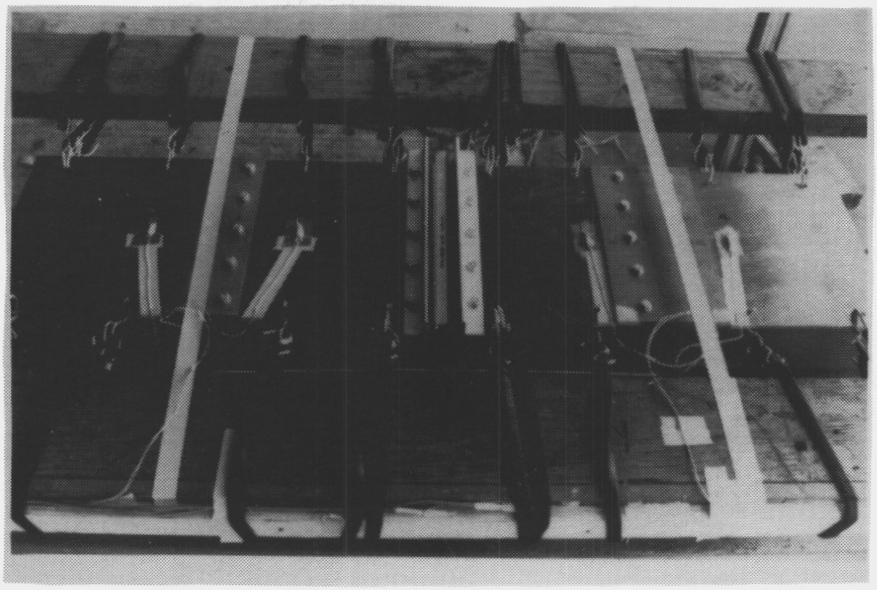

Figure 17. Joint test accelerometer locations.

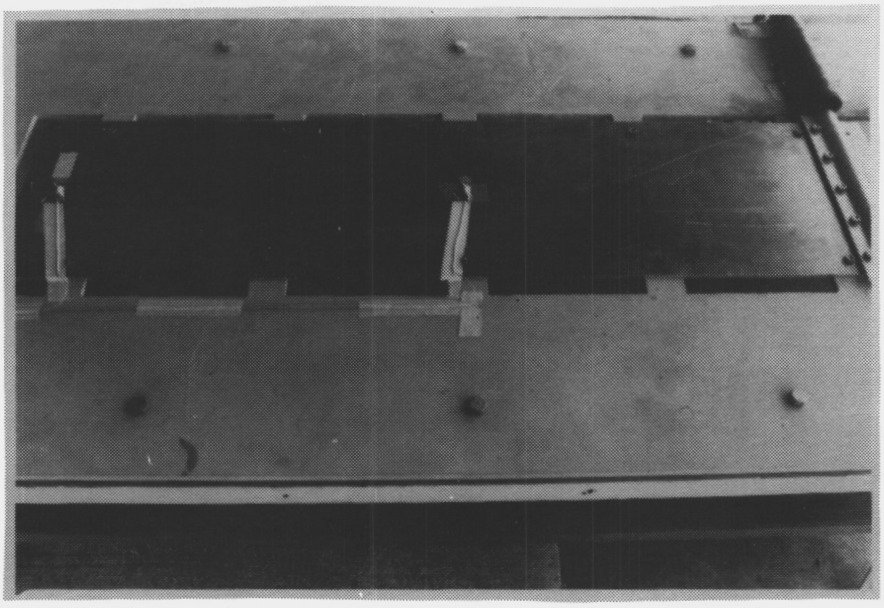

Figure 18. Rigid test accelerometer locations.

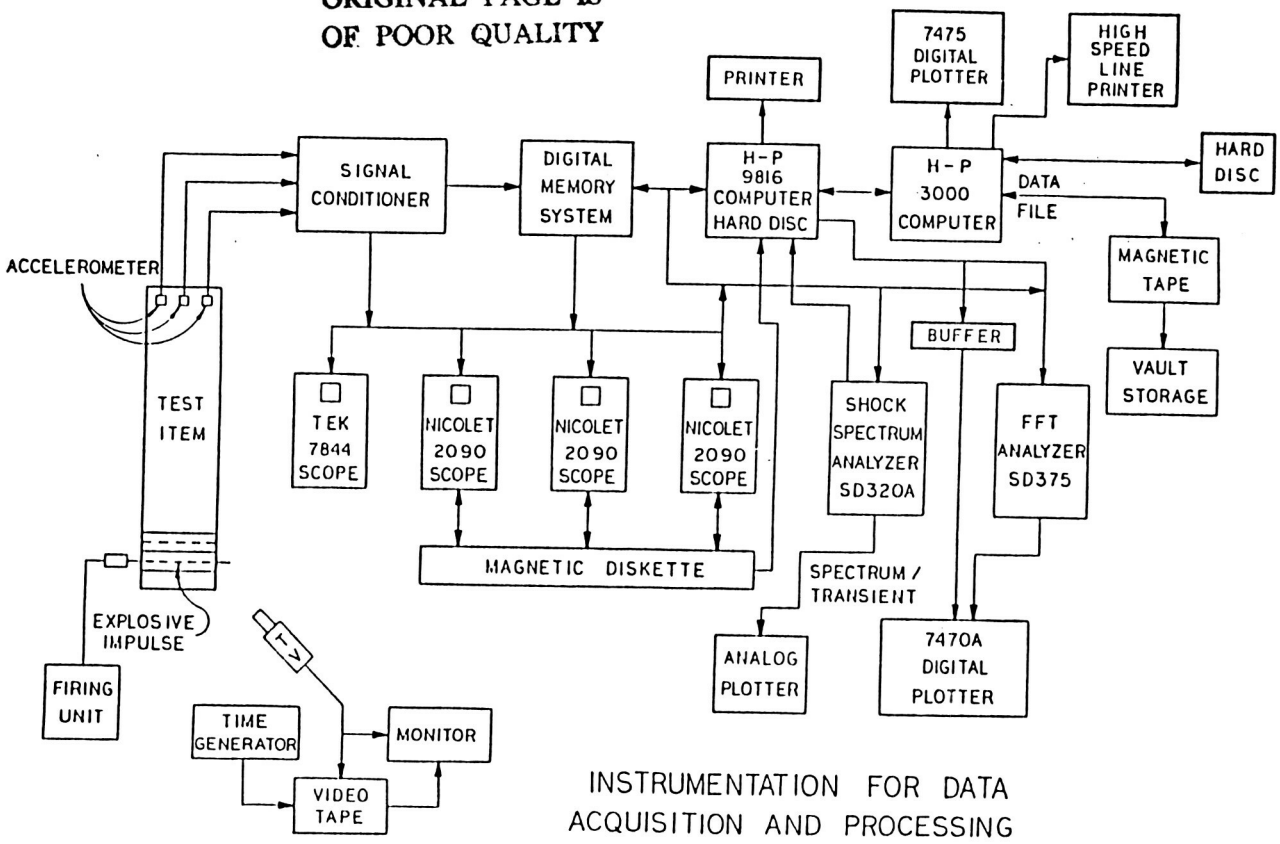

Figure 19. Instrumentation schematic.

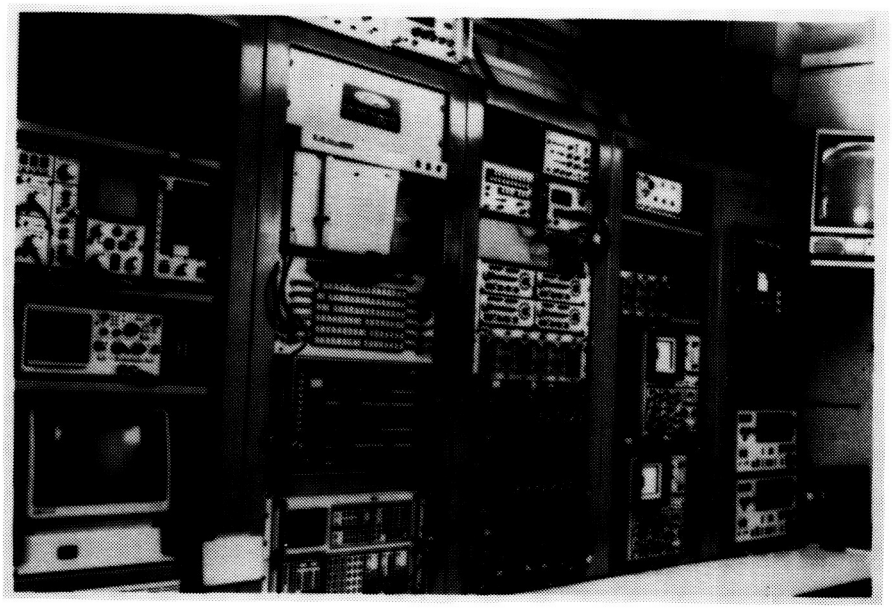

Figure 20. Instrumentation photograph.

B. Plate Tests

Plate tests were set up as previously specified in the equipment section. Other than the differences specified in setting up the equipment, the experiments were carried out using the exact same procedures. The plates were severed using standard firing procedure. From two to four accelerometers were used to capture the shock transient. The signal was recorded on computer disc and in the digital memories. Real time Fourier analysis was accomplished. Time histories were captured using 4- and 20-msec windows. The 4-msec window was used to derive the primary high-frequency SRS. The 20-msec window was used to derive the residual and low-frequency SRS. Previous study had shown that windows beyond 20-msec did not produce any variation in SRS. All SRS data were maximax with a Q of 10 or 5 percent damping.

Variables were previously defined in the equipment section. The values for variables and tolerances in the rigid mount test are based upon NASA design specifications and quality control standards.

IV. DATA ANALYSIS AND RESULTS

The following section summarizes the results of the 1984-1986 study, the joint tests, the rigid mount tests, the mass loaded test, and the unamplified accelerometer test. Because of the large quantities of data, only samples of time histories were included. The main analysis tool included in the paper is the 100,000 Hz SRS.

Both SRS and Fast Fourier Transforms (FFT) were calculated for all time histories. Initial SRS plots were derived using a Spectral Dynamics Model SD-320A shock spectrum analyzer. The final SRS plots were calculated using an SRS algorithm on a Hewlett-Packard 9000, Series 300 computer. These plots are the ones included in this report. FFT plots were taken from a Spectral Dynamics Model SD-375 Dynamic Analyzer. SRS plots were calculated, from both the Zonic and Nicolet memories, up to 100,000 Hz. One should note that because the instrumentation was ranged for very high acceleration levels (400,000 Gs), the low frequency data, below 400 to 500 Hz, were below the noise floor. FFT plots were calculated to 100,000 Hz from the Nicolet memories and to 20,000 Hz from the Zonic memories. As previously noted, Zonic data is not valid beyond 50,000 Hz. Time histories were plotted for each channel. These time histories were also recorded on computer tape and diskettes. These methods and techniques were followed both in the previous 1984-1986 study and the study reported in this paper. For a complete set of data, the reader should refer to the following references: For the previous 1984-1986 study – Explosive Technology Test Report 0231(01)FTR, and for the present study – Explosive Technology Test Report 0837(01)TR. These references are listed as References 67 and 68 in the bibliography of this paper.

Test levels from the previous 1984-1986 study, and from both the joint and rigid mount tests of this study were comparable as far as overall levels were concerned.

A. Results From the 1984-1986 Study

The previous study was a major research effort organized to analyze variations in pyrotechnically induced SRS and to determine if and to what degree manufacturing and assembly tolerances, distance from the charge, data acquisition instrumentation, and shock energy propagation affect the SRS.

The test program was divided into three areas: precision and accuracy, basic SRS, and variability. Precision and accuracy consisted of ball drop calibration testing of the test accelerometers and test firing of 28 preliminary plate tests. All plate tests in this study were elastomerically restrained resulting in near free-free boundary conditions. The results of the plate tests were used to direct the flow of the remaining test program. Data from the entire test program were used to evaluate instrumentation. The Endevco 7270 accelerometer was the only accelerometer that consistently yielded quality data. Accelerometer error as a function of frequency was documented. The Endevco 7270 demonstrated the highest level of survivability during the entire program.

Basic SRS consisted of ten plate tests used as an experimental control. The only variables involved were aluminum alloy variety and plate target area thickness. Analysis indicated that alloy variety would not affect the SRS. Analysis also indicated that target thickness would not affect the SRS as long as the plate was completely severed. The data from the Endevco 7270 were very repeatable. Other accelerometers were used side-by-side with the Endevco 7270's for the purpose of evaluating accelerometers. Most of the other accelerometers yielded baseline shifted or erratic data, or did not survive the firing. A base reference mean SRS was derived from the ten tests. This SRS was used in variability for a control comparison.

Variability consisted of 26 plate tests used to evaluate manufacturing and assembly variables and supplementary variables. LSC variables consisted of coreload, standoff, coupling, apex angle, and gross overload. These were evaluated by test individually. Data indicated that none of these variables affected the SRS to a degree that is measurable. Combination of coreload, standoff, and coupling yielded the same results. Two joint tests were performed (simple lap joints with a 3-in. overlap) that indicated that the ultra-high frequency energy decreased slightly. Two accelerometer mounting tests (flat versus block mounted) indicated a significant decrease in high frequency energy when mounting blocks are used. The final supplementary tests indicated that the plate response to pyroshock is about the same for all axes. The final result is that SRS do not vary with manufacturing and assembly tolerances, and instrumentation is the one major problem associated with pyrotechnic shock measurement.

Figures 21 through 25 are the SRS from the previous study that will be used for comparison in the present study. Included are the base reference SRS, maximum combination, minimum combination, charge gross overload, and joint effects near the source and across the joint from the source. Figures 26, 27, and 28 illustrate the old joint test plate used in the 1984-1986 program.

Several conclusions may be drawn from the previous study. Unlike popular belief, SRS from the same source are very repeatable when proper instrumentation is utilized. The 50 percent (6 dB) or more variations encountered in most previous studies were probably due to instrumentation. New accelerometer designs should eliminate many of the large variations. Shock levels are much higher overall than expected, especially in the high frequency region above 10,000 Hz. These high frequency, high acceleration levels are very capable of destroying electrical and electronic components, especially accelerometers. Baseline shifts and accelerometer resonances have distorted most pyroshock data in the

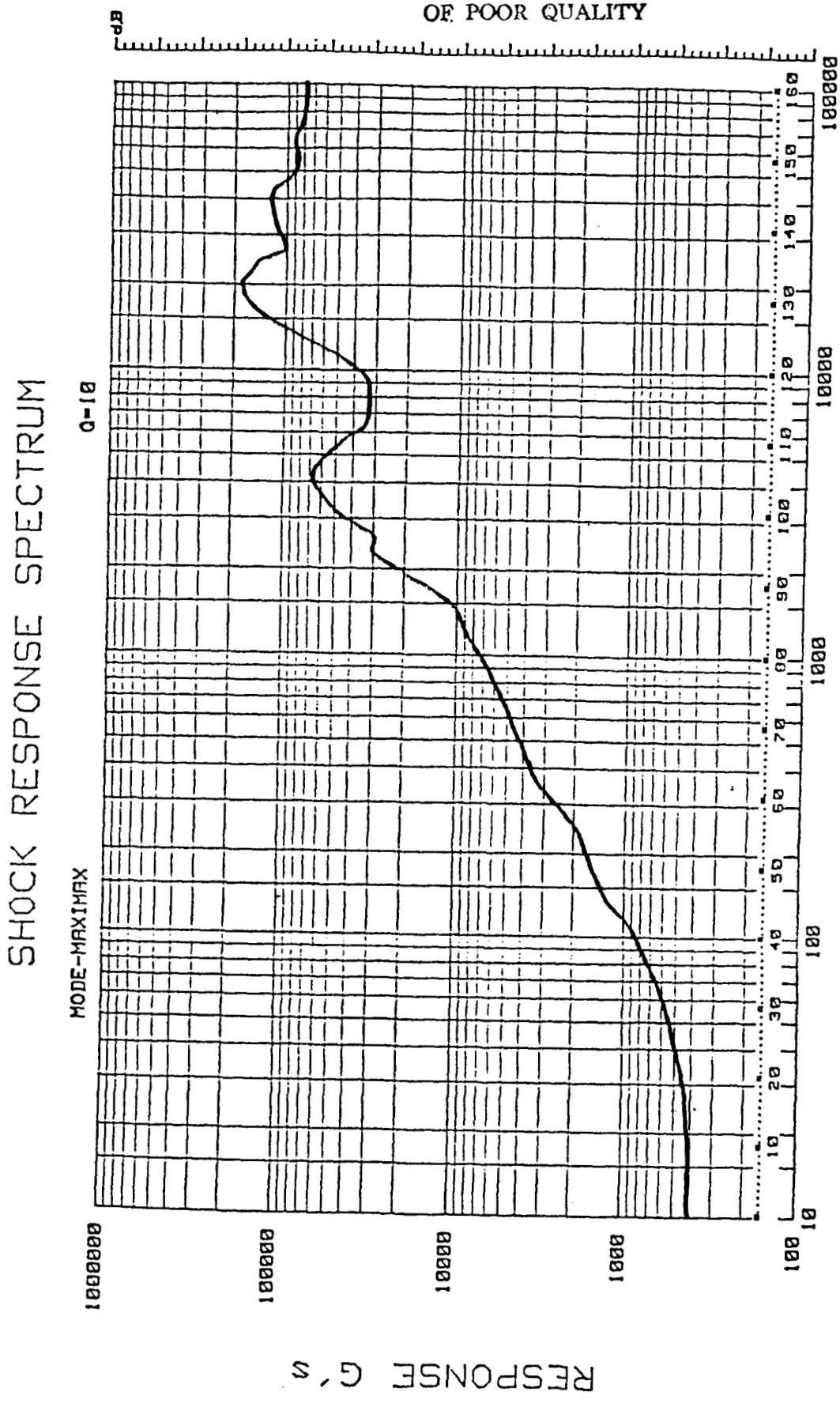

Figure 21. SRS: Old base reference mean.

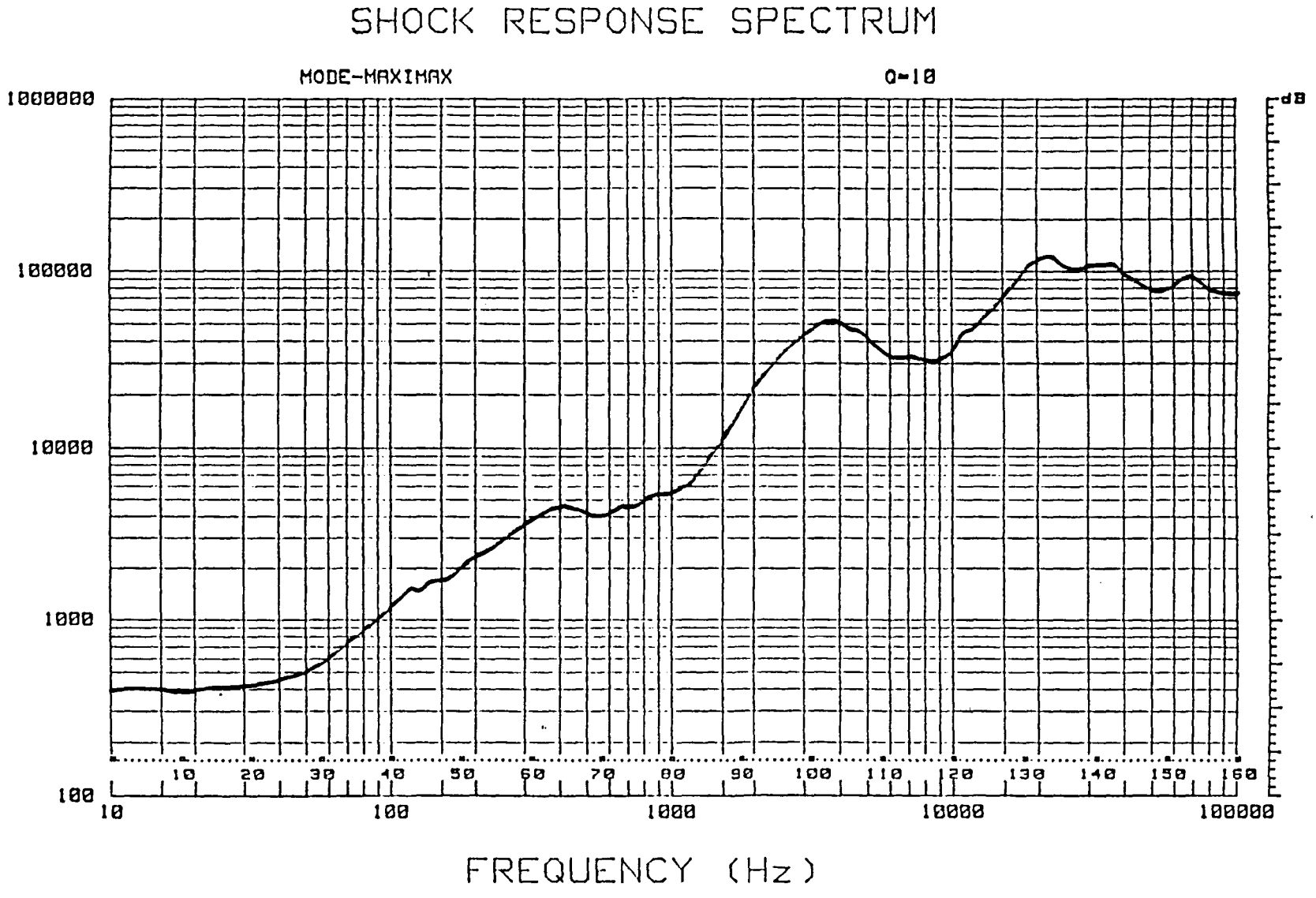

Figure 22. SRS: Old maximum combination.

ORIGINAL PAGE IS
OF POOR QUALITY

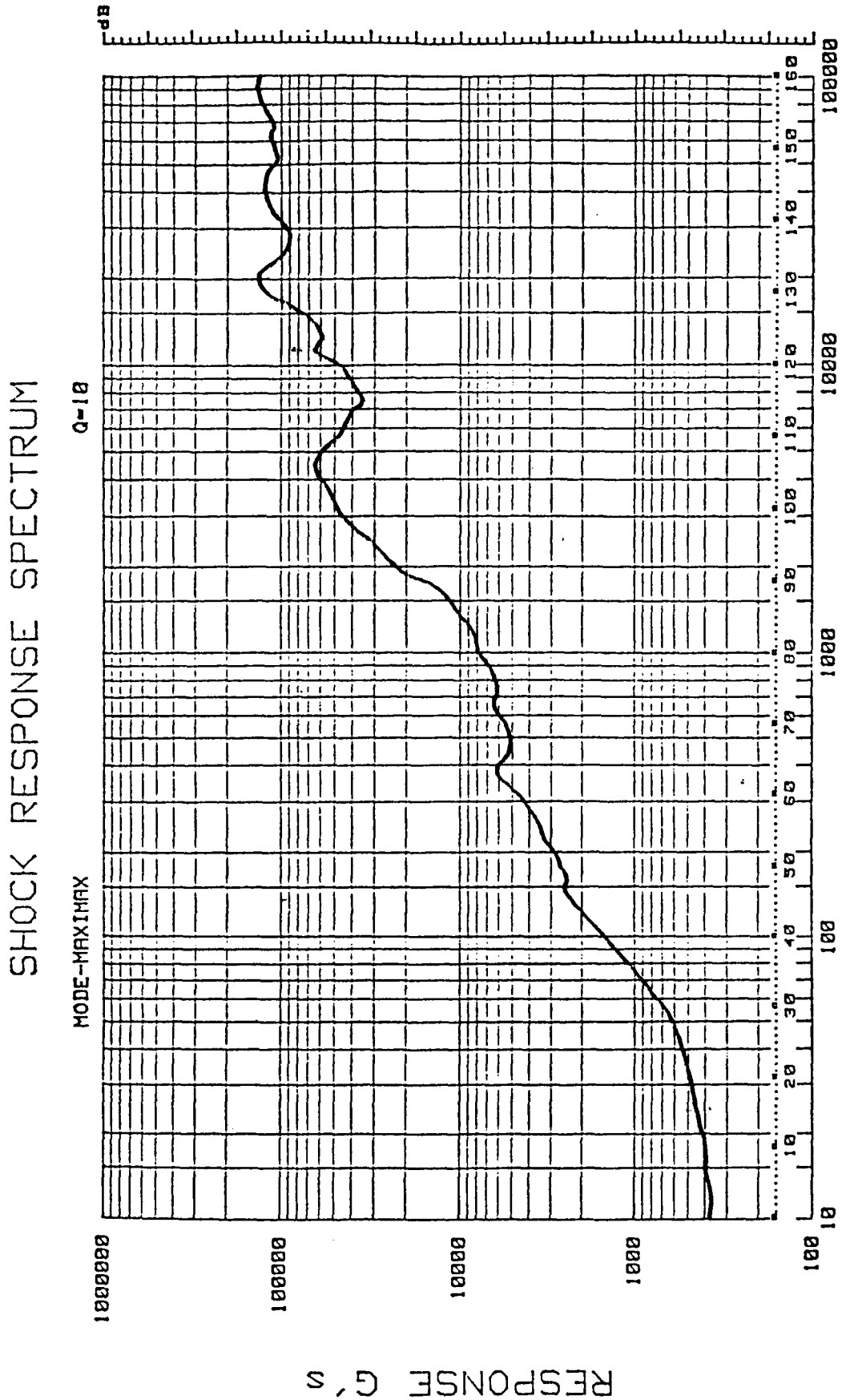

Figure 23. SRS: Old minimum combination.

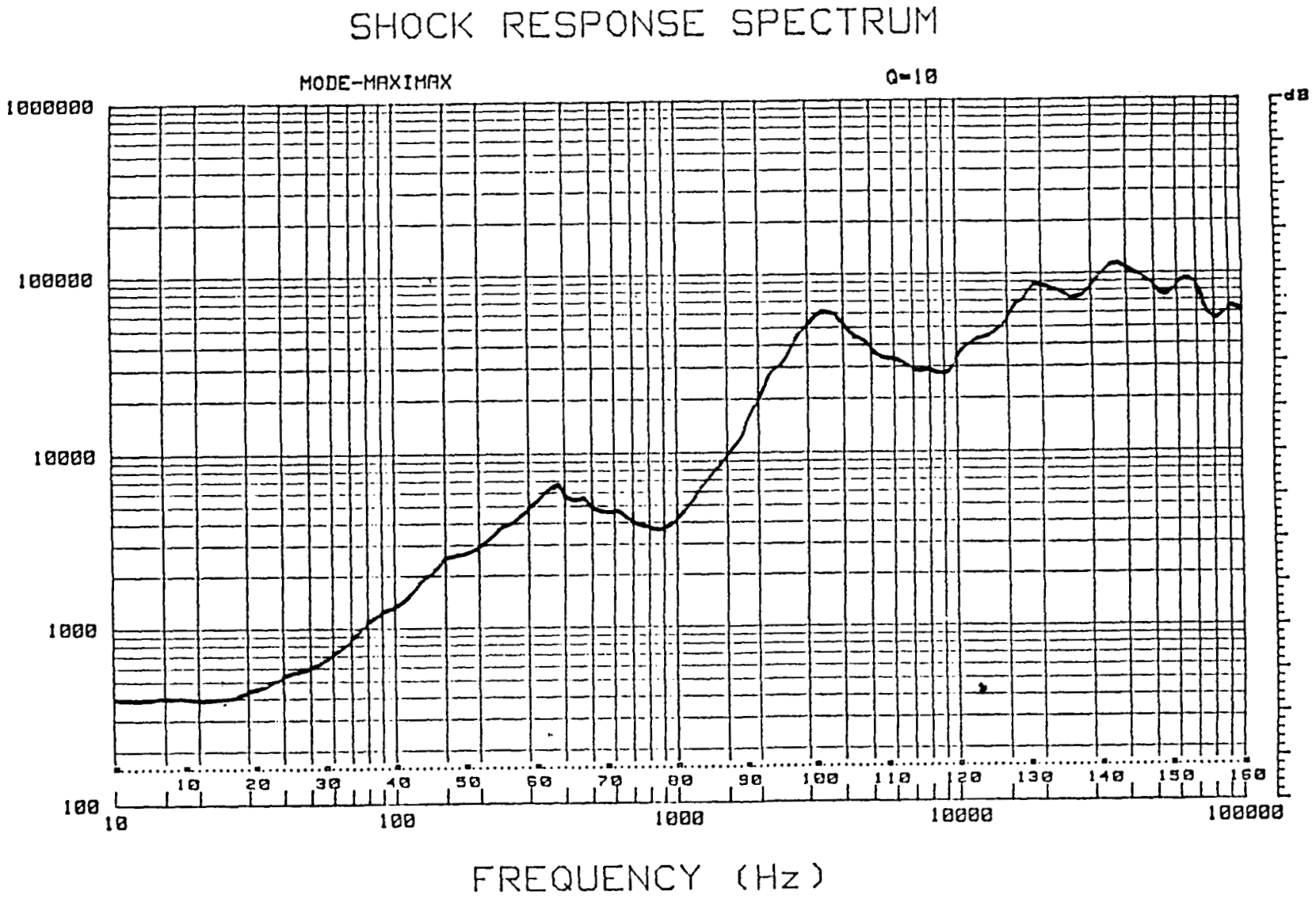

Figure 24. SRS: Old gross overload.

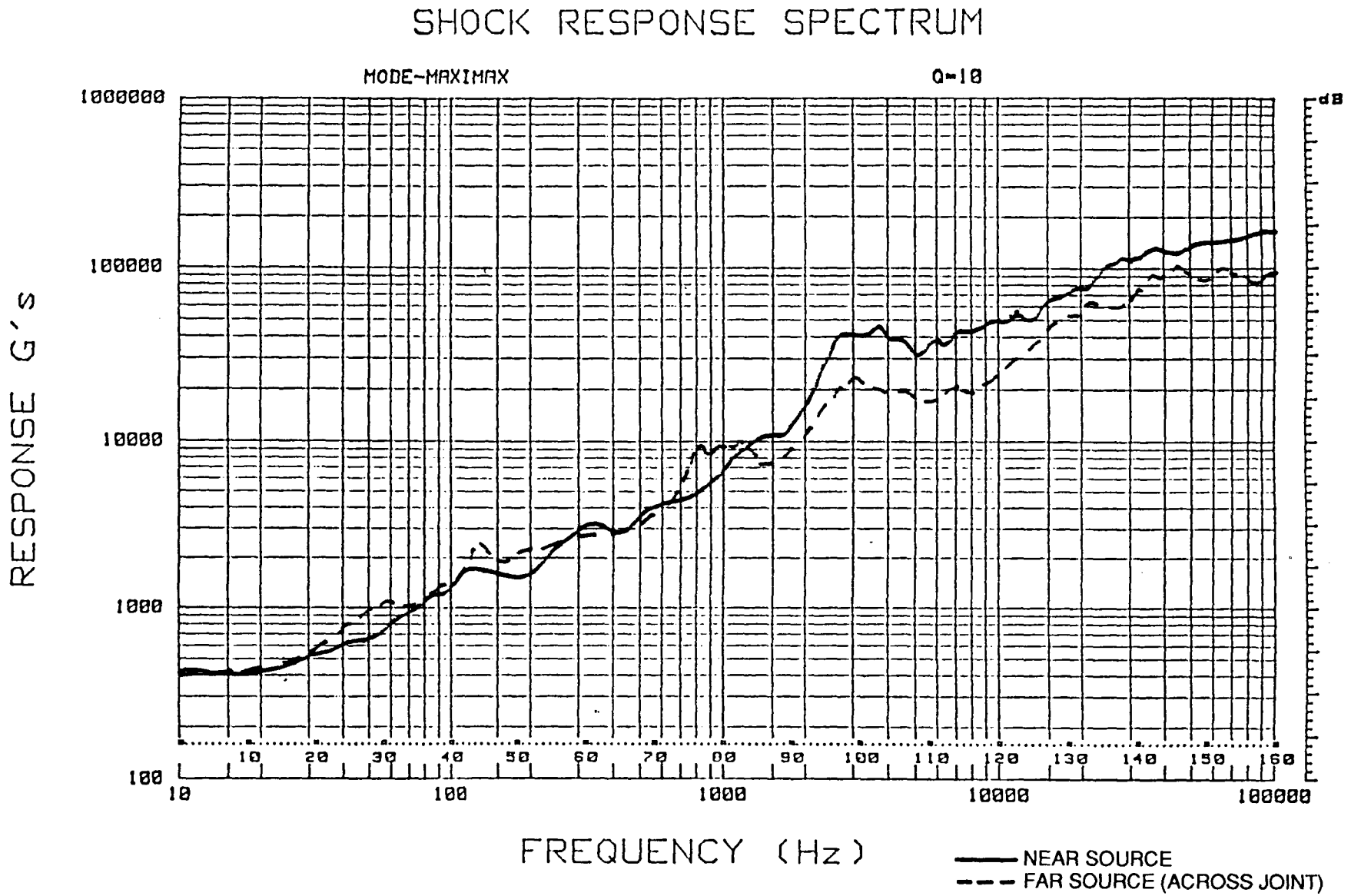

Figure 25. SRS: Old joint test.

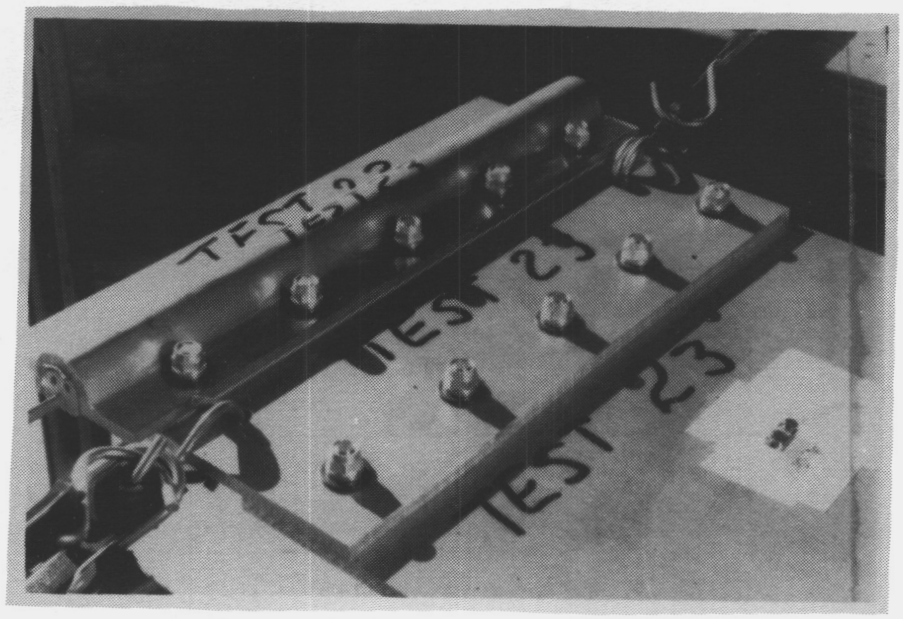

Figure 26. Old joint test plate – top view.

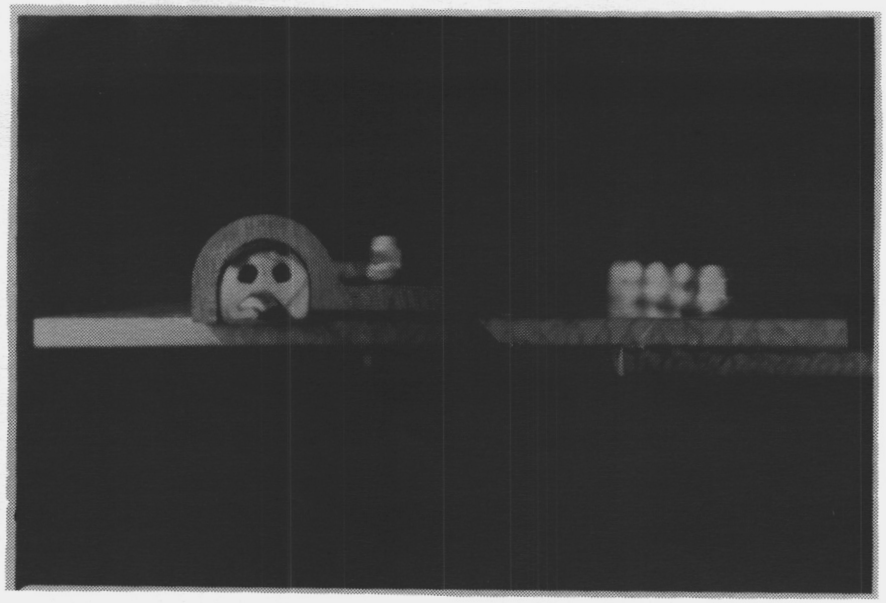

Figure 27. Old joint test plate – edge view.

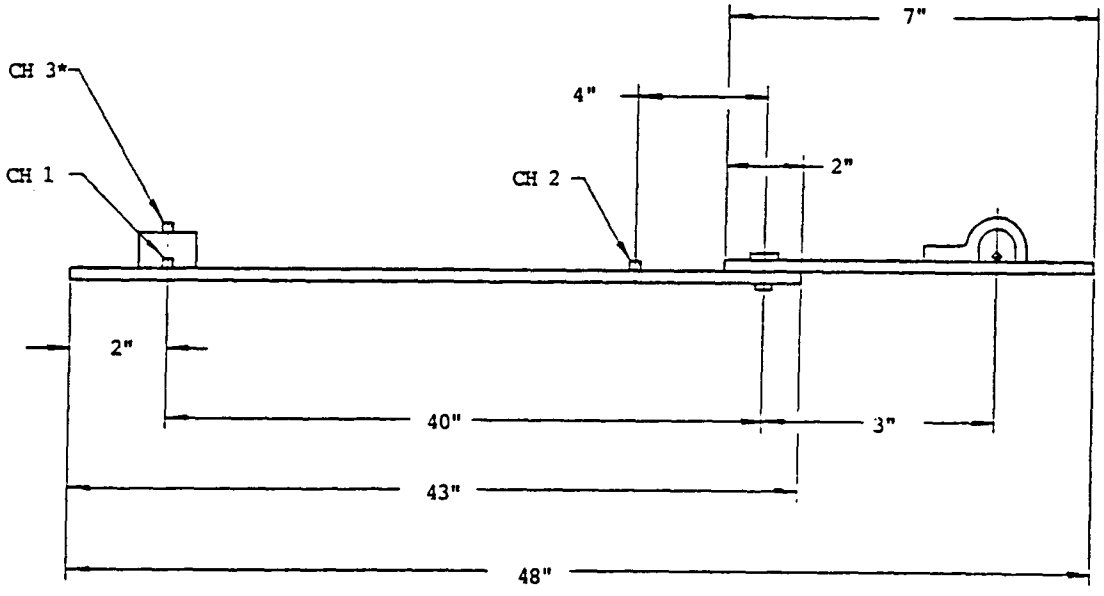

Figure 28. Old lap joint test configuration.

past. Only the new Endevco 7270 accelerometer yielded consistent, high-quality data throughout the study. All other accelerometers including other Endevco models yielded distorted data or failed altogether. One can conclude that instrumentation is just on the verge of being able to accurately measure pyroshock.

Variations in coreload, standoff, charge holder coupling, and LSC apex angle do not affect SRS as long as complete plate severance occurs. Manufacturing and assembly tolerances do not affect SRS. Also, the SRS is the same for all three axes when the shock is generated by LSC's.

Simple lap joints do not affect the SRS below 10,000 Hz. A slight decrease was noted above 10,000 Hz. Accelerometer mounting methodology is very critical. Most past studies used mounting blocks. Mounting blocks act as mechanical filters removing high frequency energy. Therefore, the true shock is not measured, but the mounting block response is actually measured. One can conclude from flat-mounted accelerometer data that mounting blocks should not be used in pyrotechnic tests because they remove high frequency energy that is capable of destroying flight hardware.

One may conclude that the 1970 NASA study [2,3] and the seven volume report associated with that study are accurate only for low frequency data.

Data analysis indicates that shock level is not a function of distance from the source for free-free pyrotechnic test plates. However, one should be careful to note that for this test fixture, free-free plate conditions existed and total energy is not dissipated very rapidly as a function of distance. If the long sides of the plate, perpendicular to the charge axis, has been clamped, the energy levels would have been dissipated rapidly with distance.

Recommendations from the previous study were to refrain from using mounting blocks, to investigate joint effects, and to repeat the same tests with the same variables except for using clamped or rigid mounted test plates. The remainder of this paper covers the present study which is a direct result of the recommendations of the previous study summarized above.

B. Joint Tests

All joint test plates were center severed and elastomerically restrained as previously noted. Test plates 1 and 2 were the experimental controls – these plates contained no joints. Figures 29 and 30 show typical time histories. Figures 31 and 32 show typical Fourier transforms. Both time histories and Fourier transforms were used in analyzing the data, but will be omitted from this paper because of the volume of the data. Figures 33 through 36 show the SRS for the four measurements made on each control plate. Figures 37 and 38 show all four SRS for each control plate. As in the previous study, little variation is noted, between plates, and as a function of distance along each particular plate. Without joints, measurements are the same all over the plate for free-free boundary conditions. Less than 2 dB difference was noted for either of the above comparisons. Figures 39, 40, and 41 show SRS envelopes for these tests.

A reference mean SRS was calculated for each plate and for both plates as shown in Figures 42 and 43. Even though the severance location for the previous study (end severed) was different than that for the joint tests above (center severed), the two means are comparable as shown in Figure 44.

Figures 45 through 48 illustrate all the SRS data for test plates 3, 4, 5, and 6 – the actual joint tests. On test plate 3, one channel was lost, probably due to a solder connection failing internal to the accelerometer. Figures 49 and 50 illustrate SRS from the charge side or near source measurements for tests 1 through 6 for both narrow and wide test joints. Figures 51 and 52 are envelopes of these measurements. Charge side or near source levels for all joint tests vary only slightly and are very comparable to the base reference means from this study and the previous study as shown in Figures 53 and 54.

The shock source is very repeatable for test plates with free-free boundary conditions. In addition, added plate mass due to test joints seems to be insignificant for charge side measurements on test plates that have free-free boundary conditions.

Figures 55 through 62 are the SRS plots for the eight test joints on plates 3 through 6.

Test plate number three consisted of a 3-in. and a 6-in. simple lap joint as previously shown. Figures 55 and 56 are the SRS data for plate 3. Both near source measurements were comparable to the base reference mean. No decrease in energy levels below 1500 Hz was observed for the narrow joint. However, a 2 to 3 dB decrease above 1500 Hz was noted. The exact same results were noted for the wide joint. Energy levels decreased 2 to 3 dB above 1500 Hz and remained the same below 1500 Hz for measurements made across the wide joint.

Figures 57 and 58 are SRS plots from plate number 4. Plate 4 consisted of a 3-in. and 6-in. double lap joint. Near source measurements compared directly with the base reference mean. Across the joints, once again the narrow joint showed no energy decrease below 1500 Hz, and a 2 to 3 dB decrease above 1500 Hz. The SRS across the wide joint was 3 to 4 dB lower above 1500 Hz, with no decrease below 1500 Hz. This one decibel difference between joints could be due to increased surface contact area or the increased mass of the wide joint. However, it is more likely, the difference is due to the "Sandwich Theory." This theory states regardless of the mass, more energy is dissipated through a multi-layered plate than through a solid plate of the same size. The more layers, the greater the energy decrease.

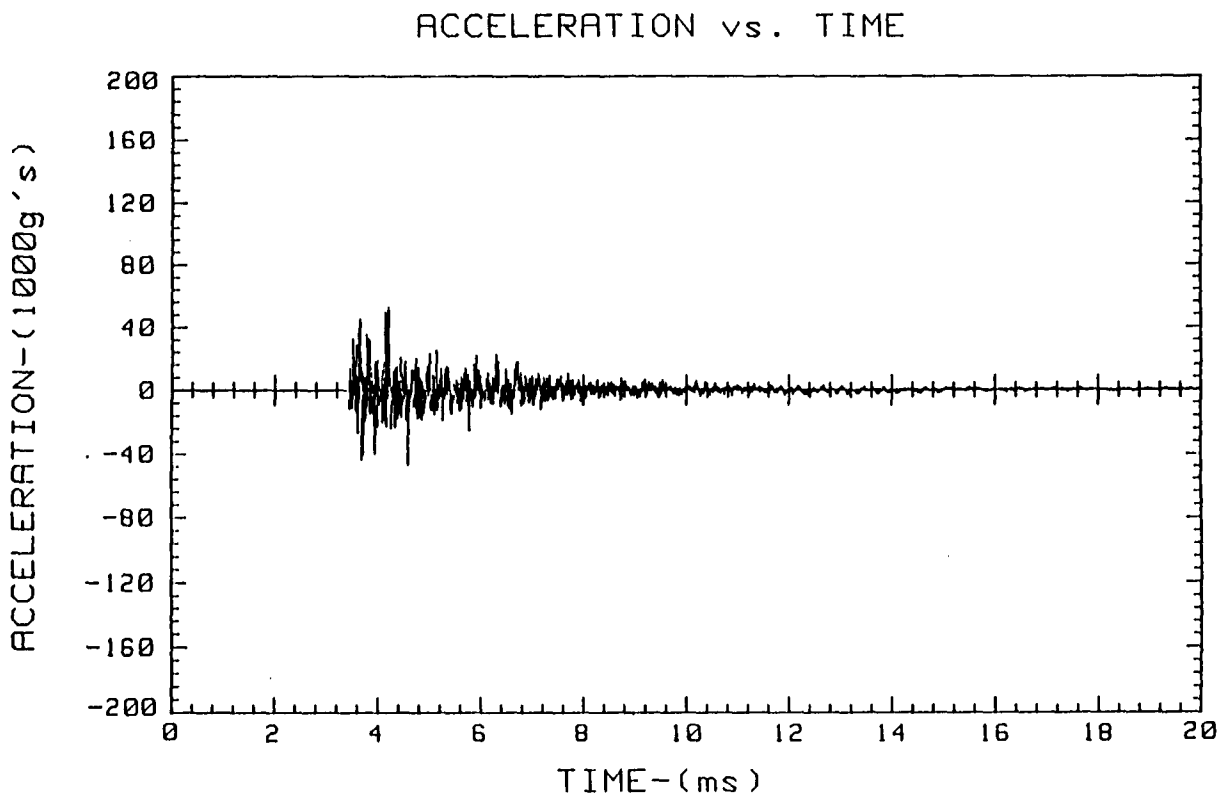

Figure 29. Typical time history (20-ms window).

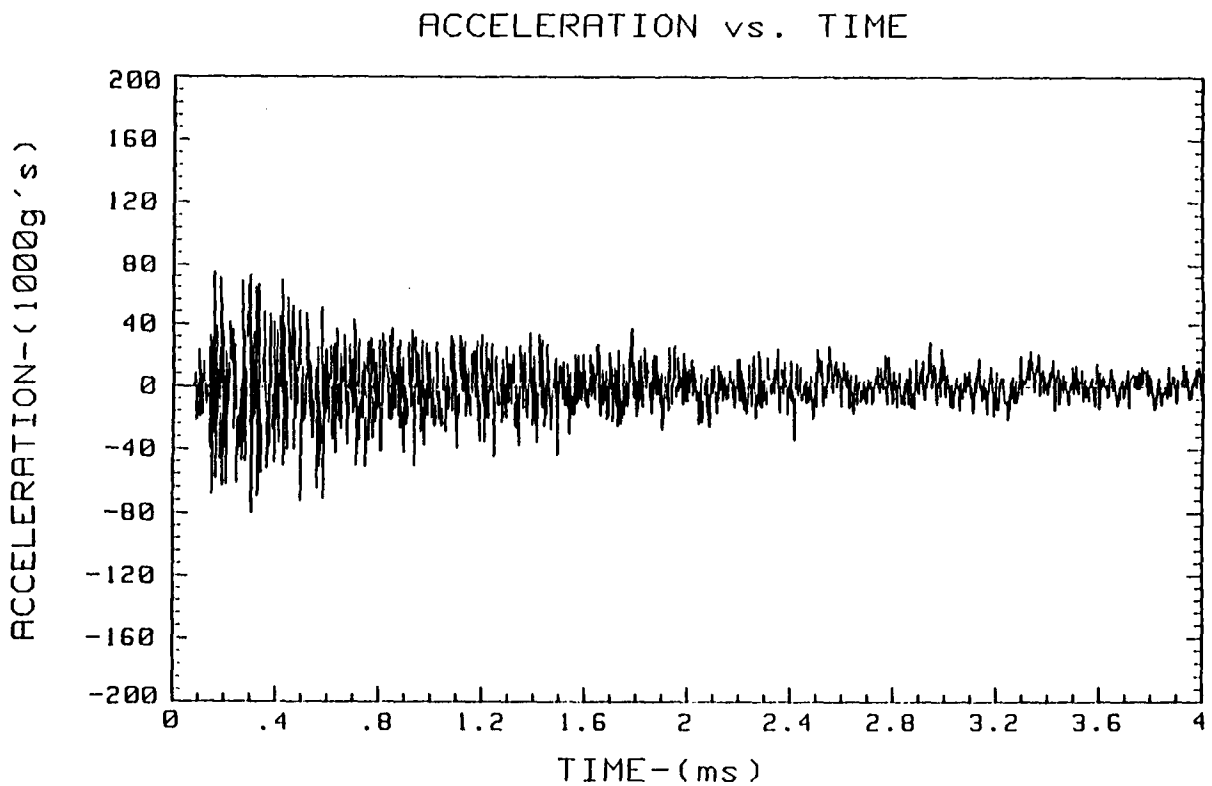

Figure 30. Typical time history (4-ms window).

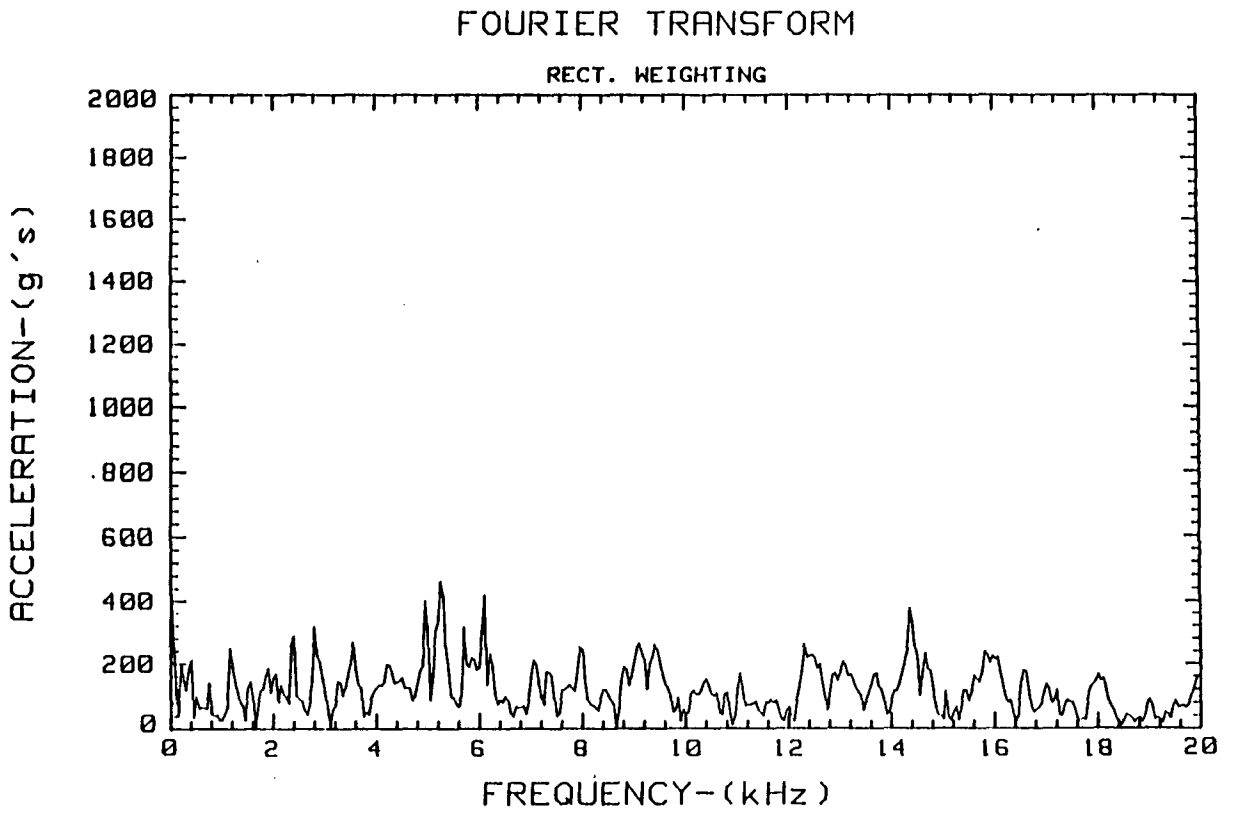

Figure 31. Typical Fourier transform (0 to 20,000 Hz).

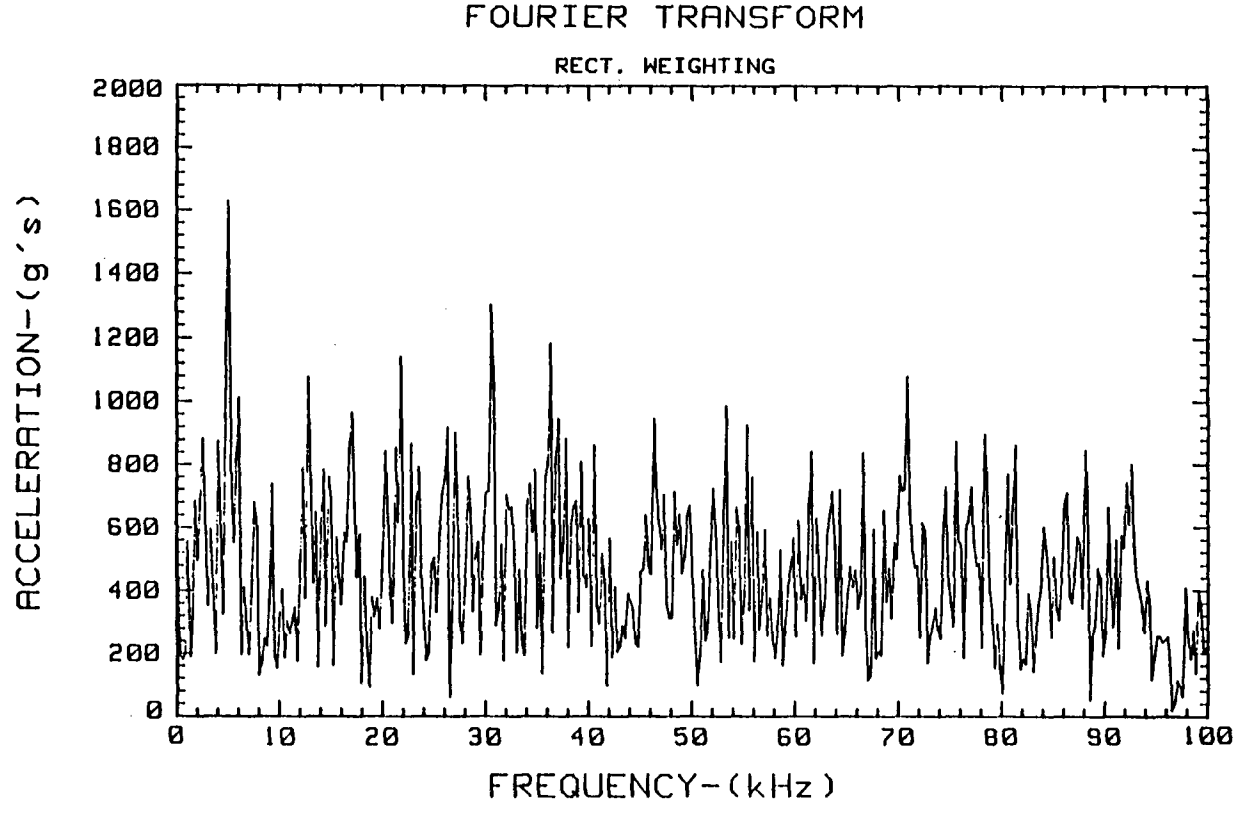

Figure 32. Typical Fourier transform (0 to 100,000 Hz).

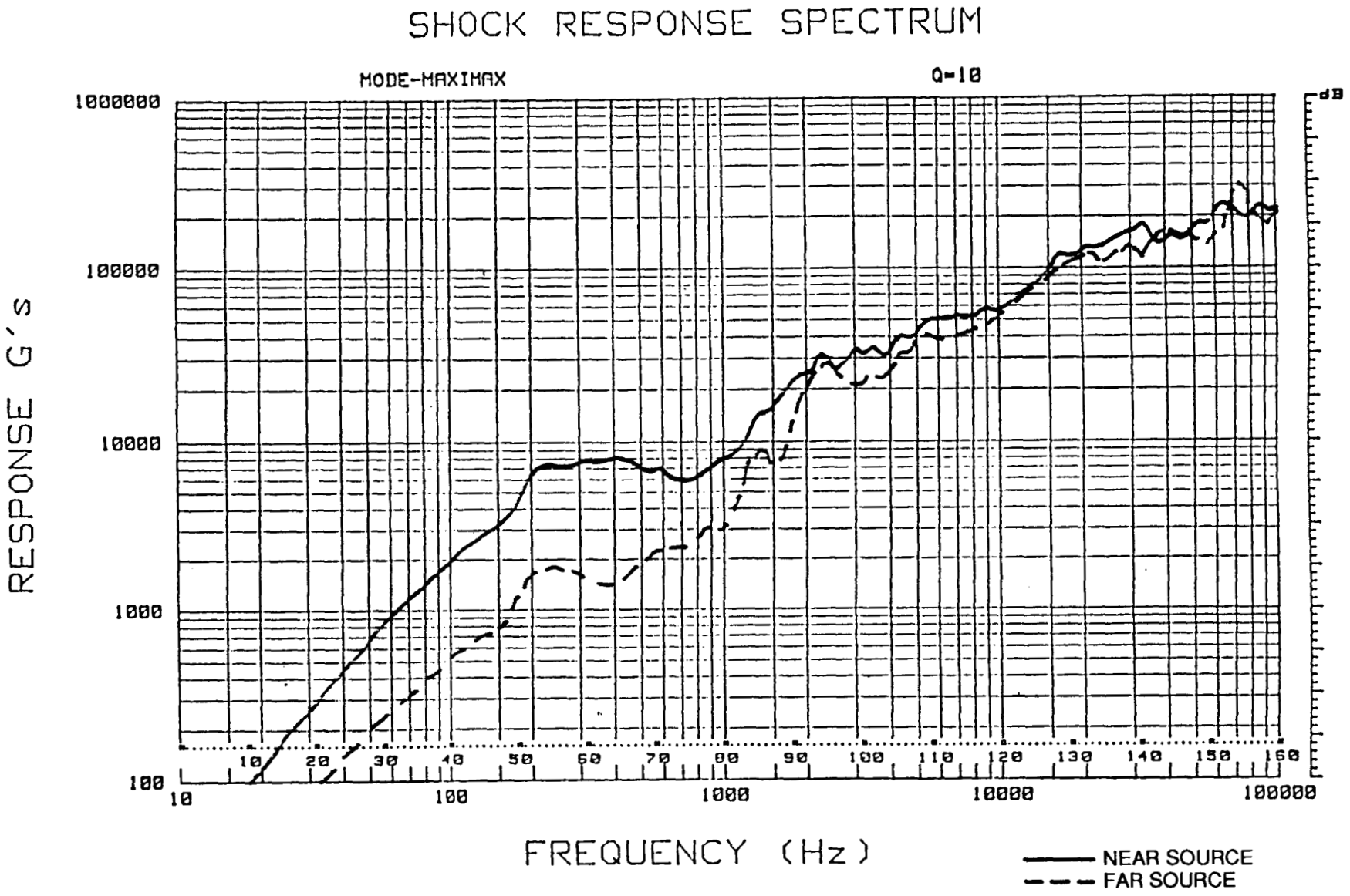

Figure 33. SRS: Joint test control – plate No. 1, narrow joint side.

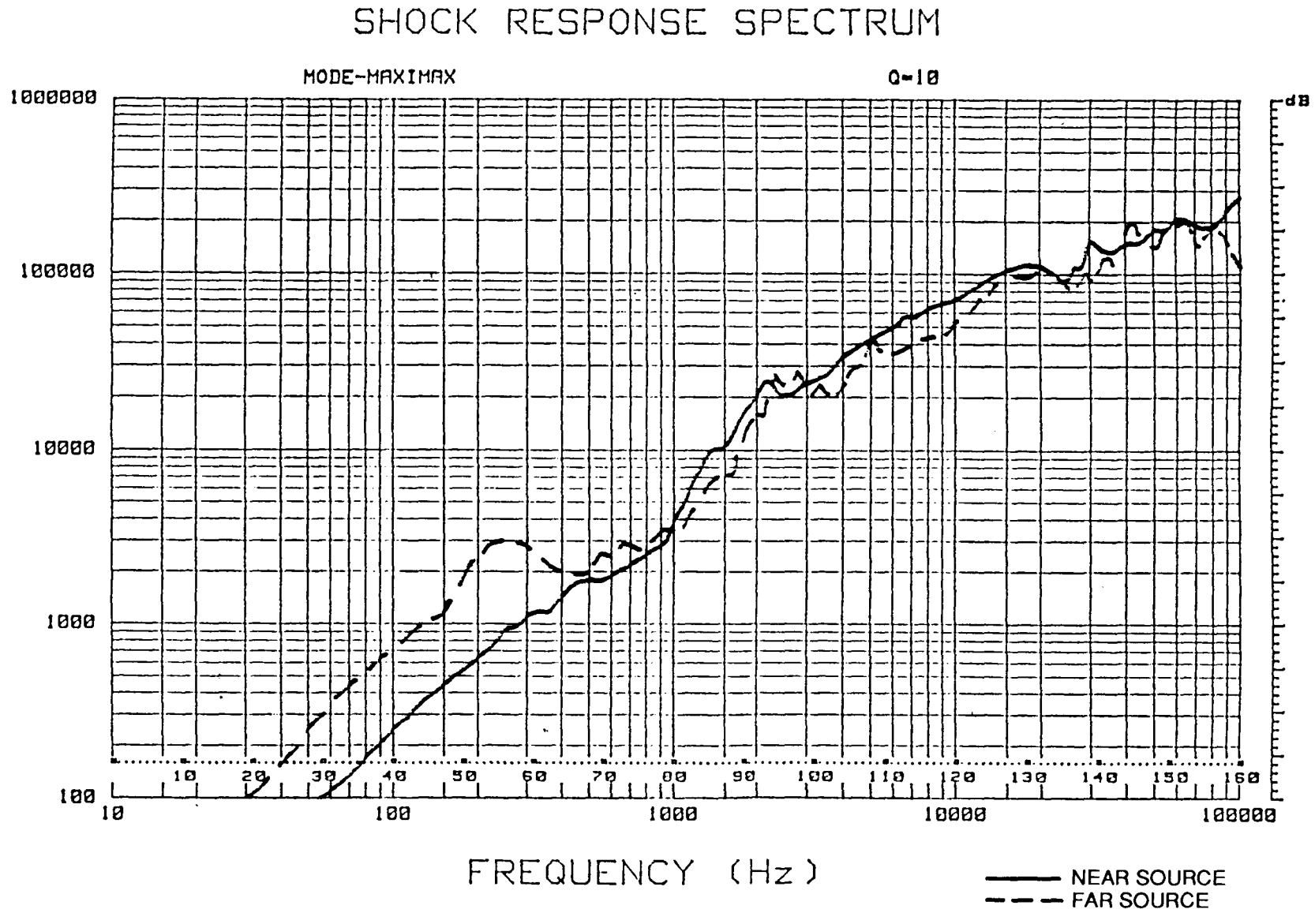

Figure 34. SRS: Joint test control – plate No. 1, wide joint side.

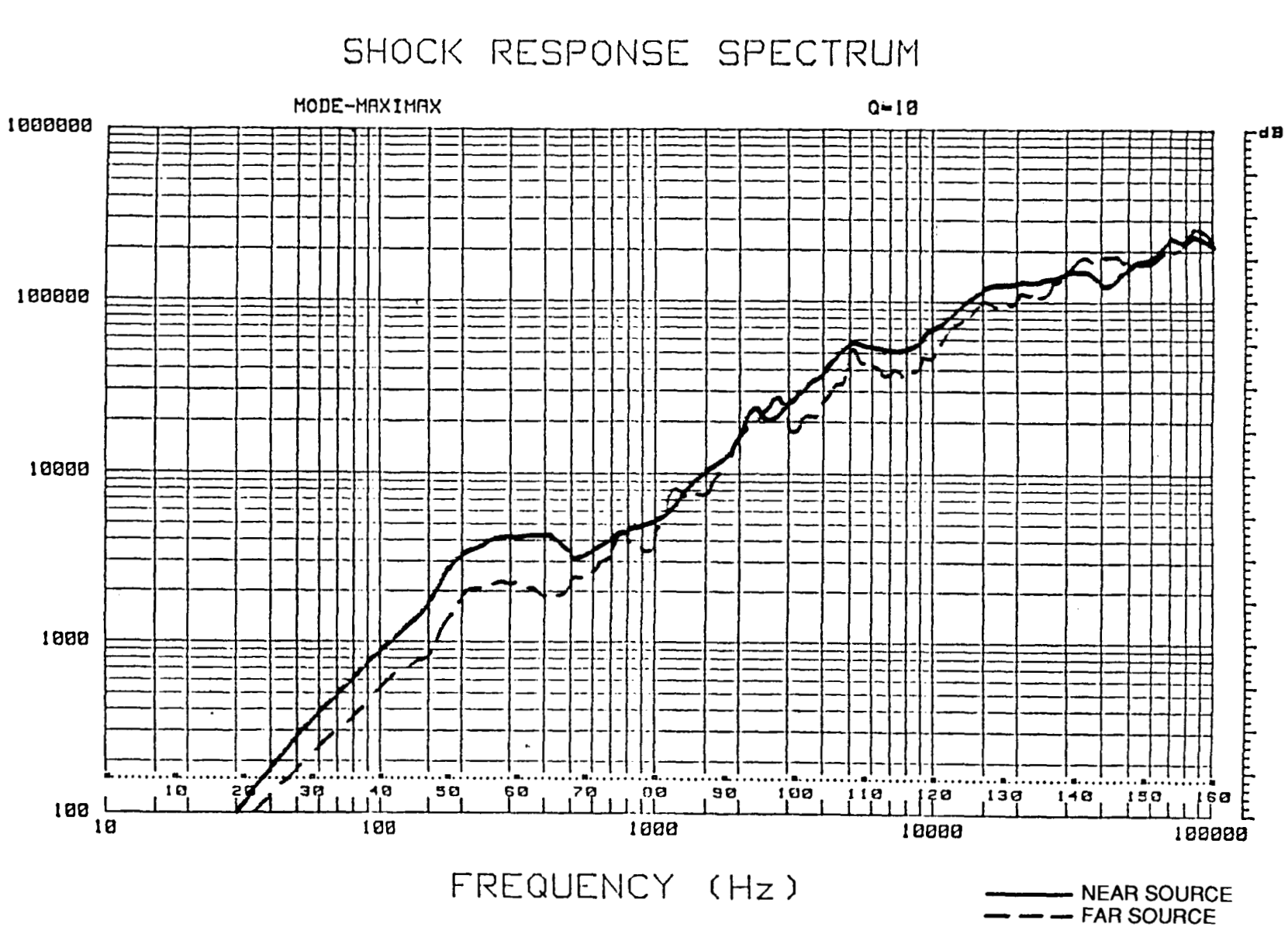

Figure 35. SRS: Joint test control – plate No. 2, narrow joint side.

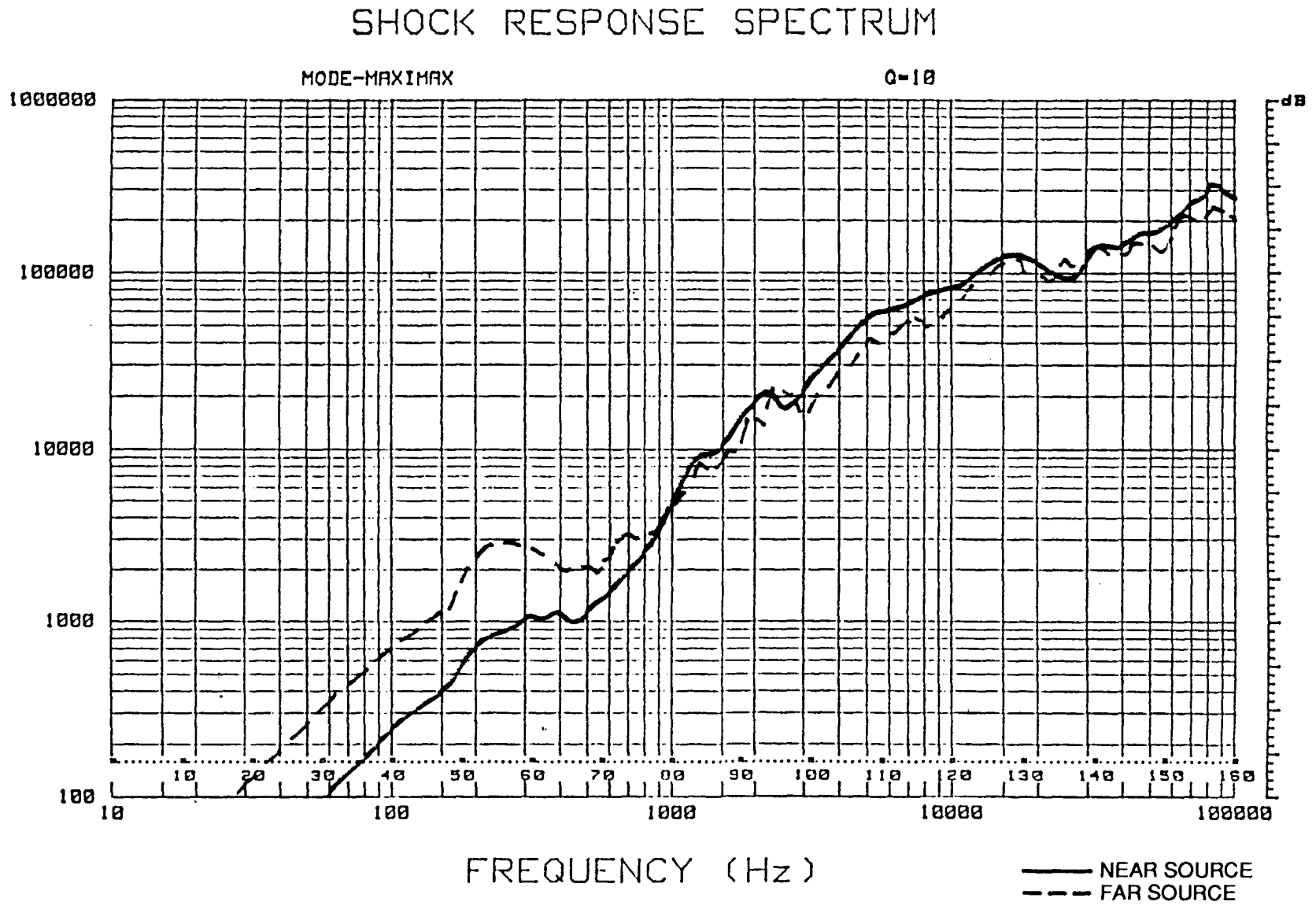

Figure 36. SRS: Joint test control – plate No. 2, wide joint side.

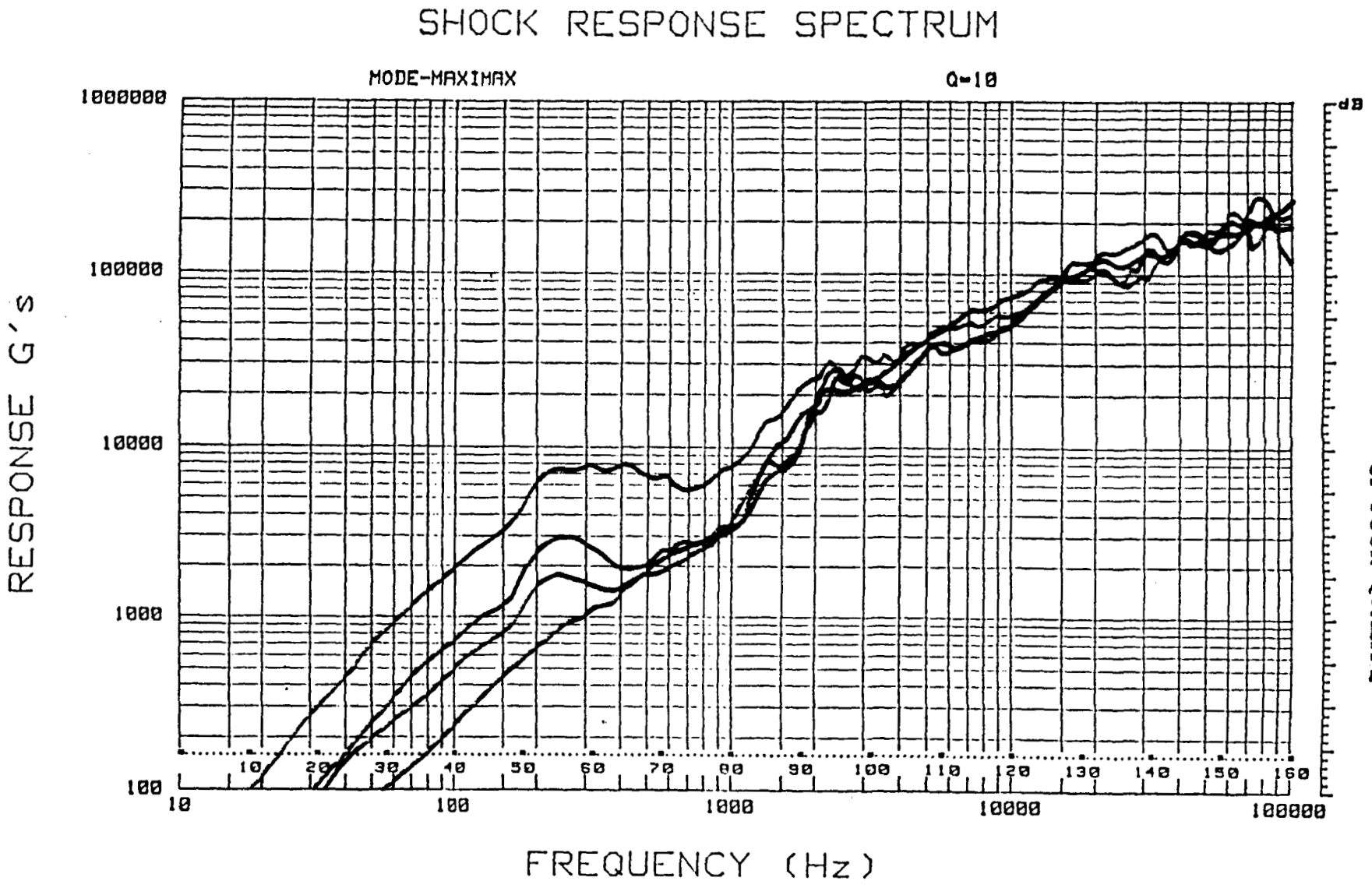

Figure 37. SRS: Joint test control – plate No. 1, all four channels.

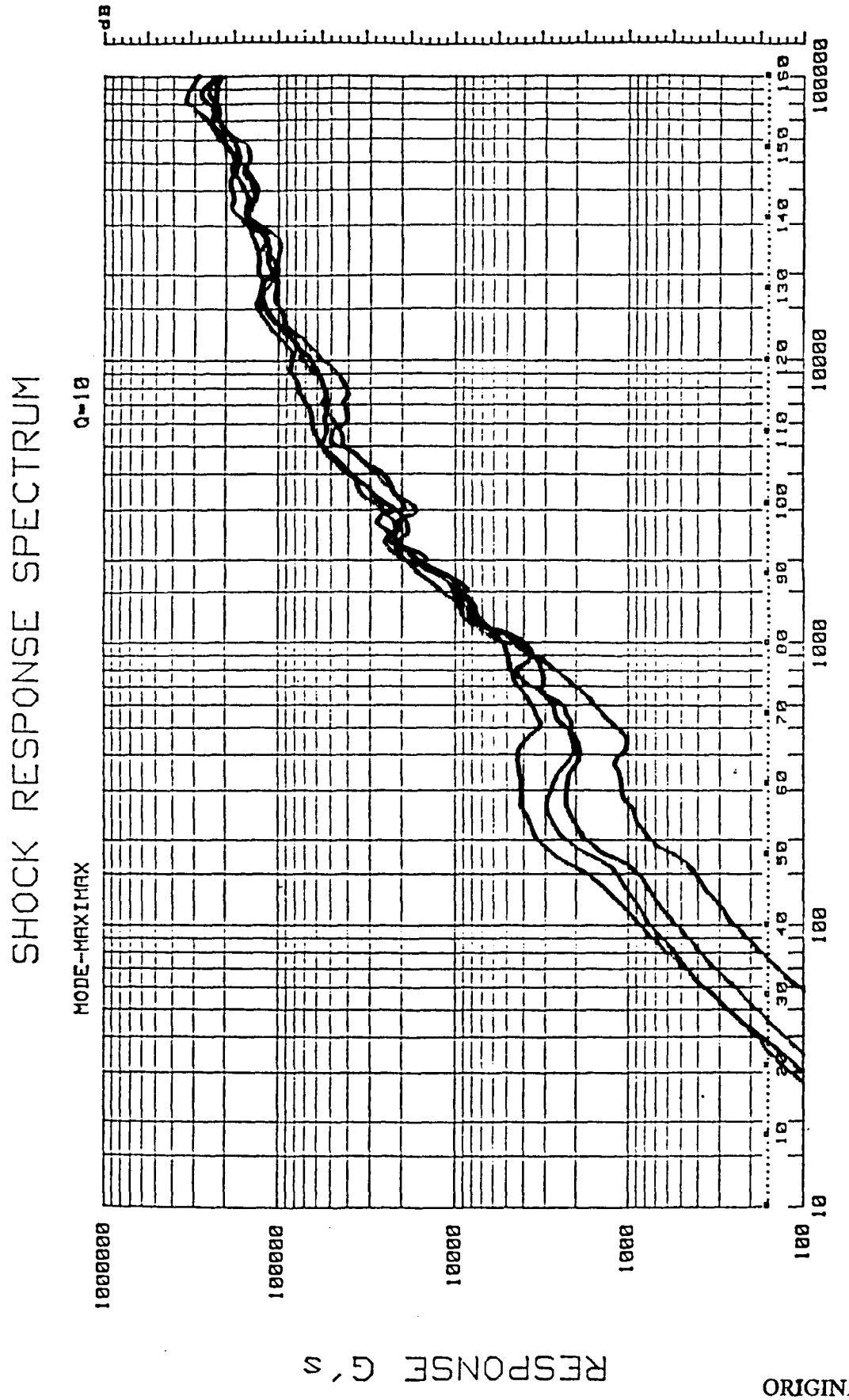

Figure 38. SRS: Joint test control – plate No. 2, all four channels.

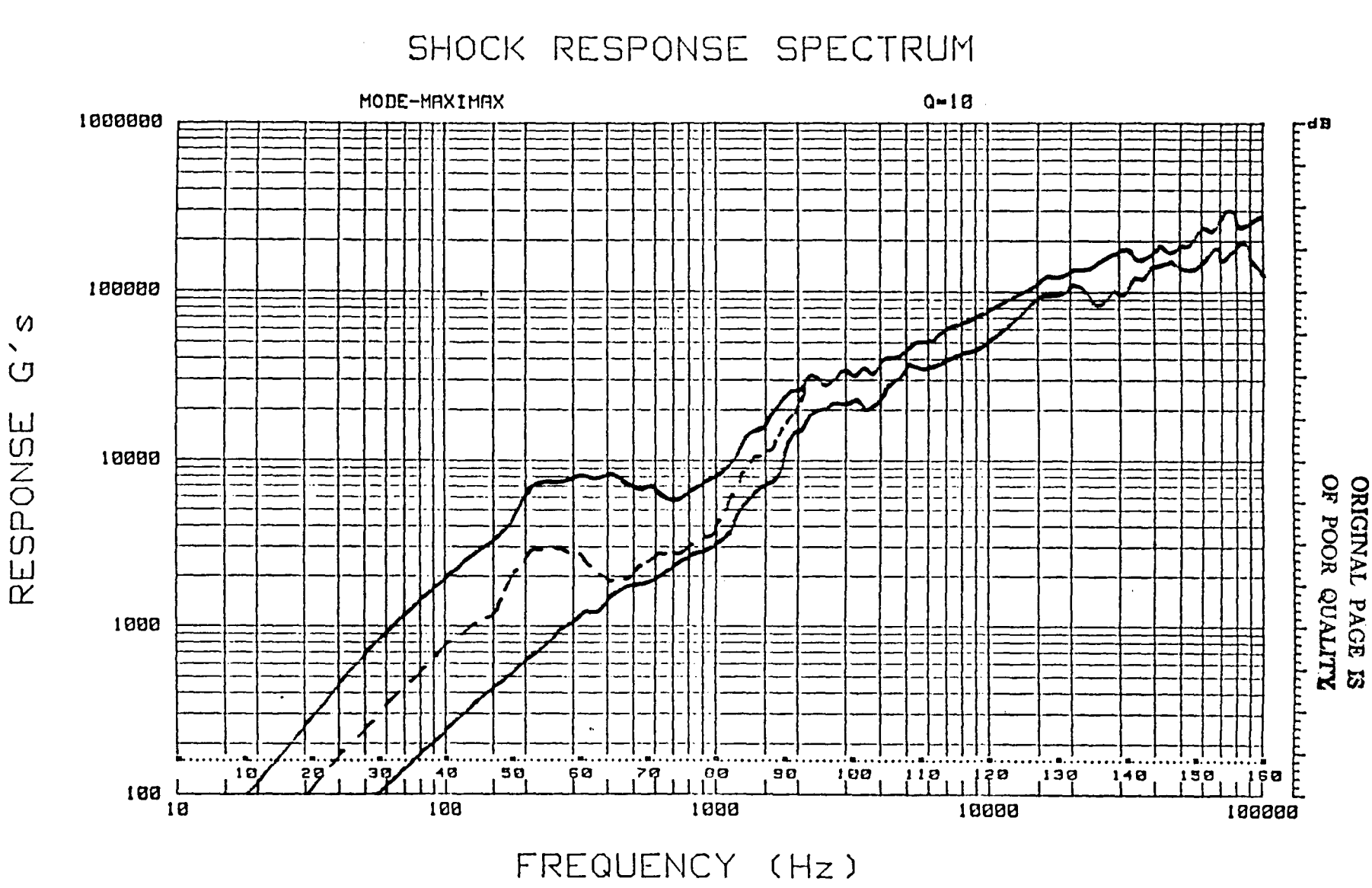

Figure 39. SRS: Joint test control – plate No. 1, data envelope.

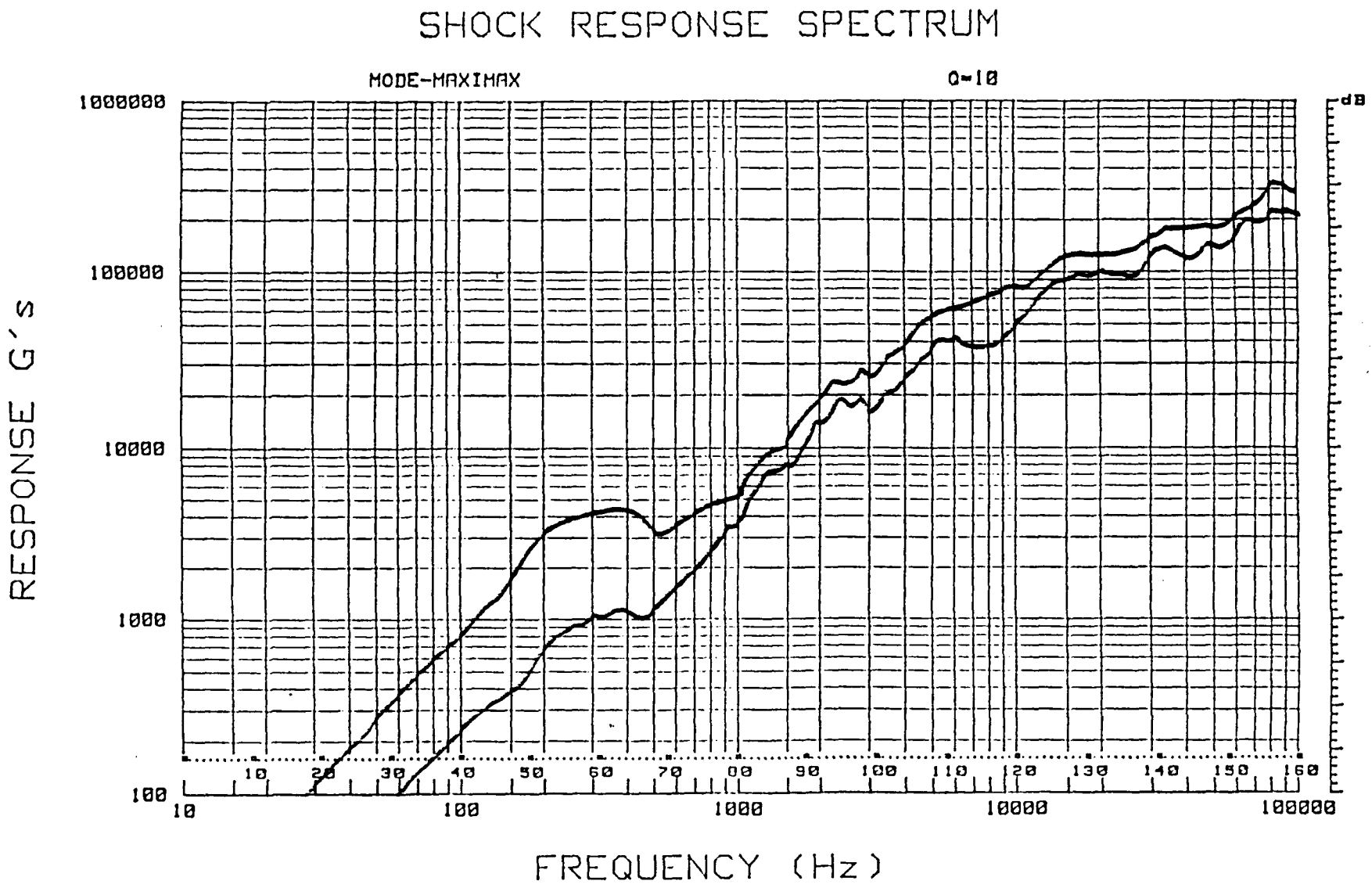

Figure 40. SRS: Joint test control – plate No. 2, data envelope.

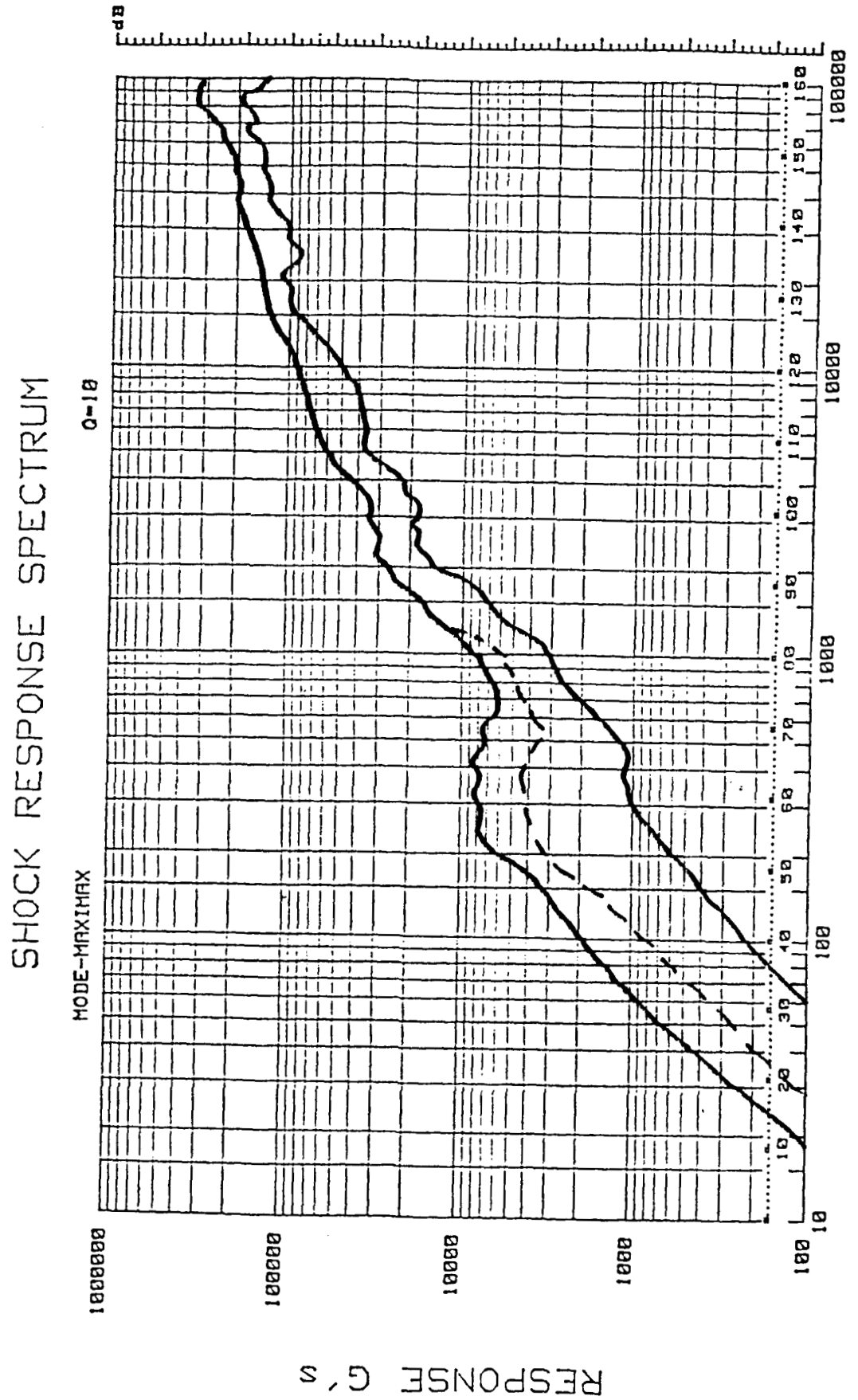

Figure 41. SRS: Joint test control – plate Nos. 1 and 2, data envelope.

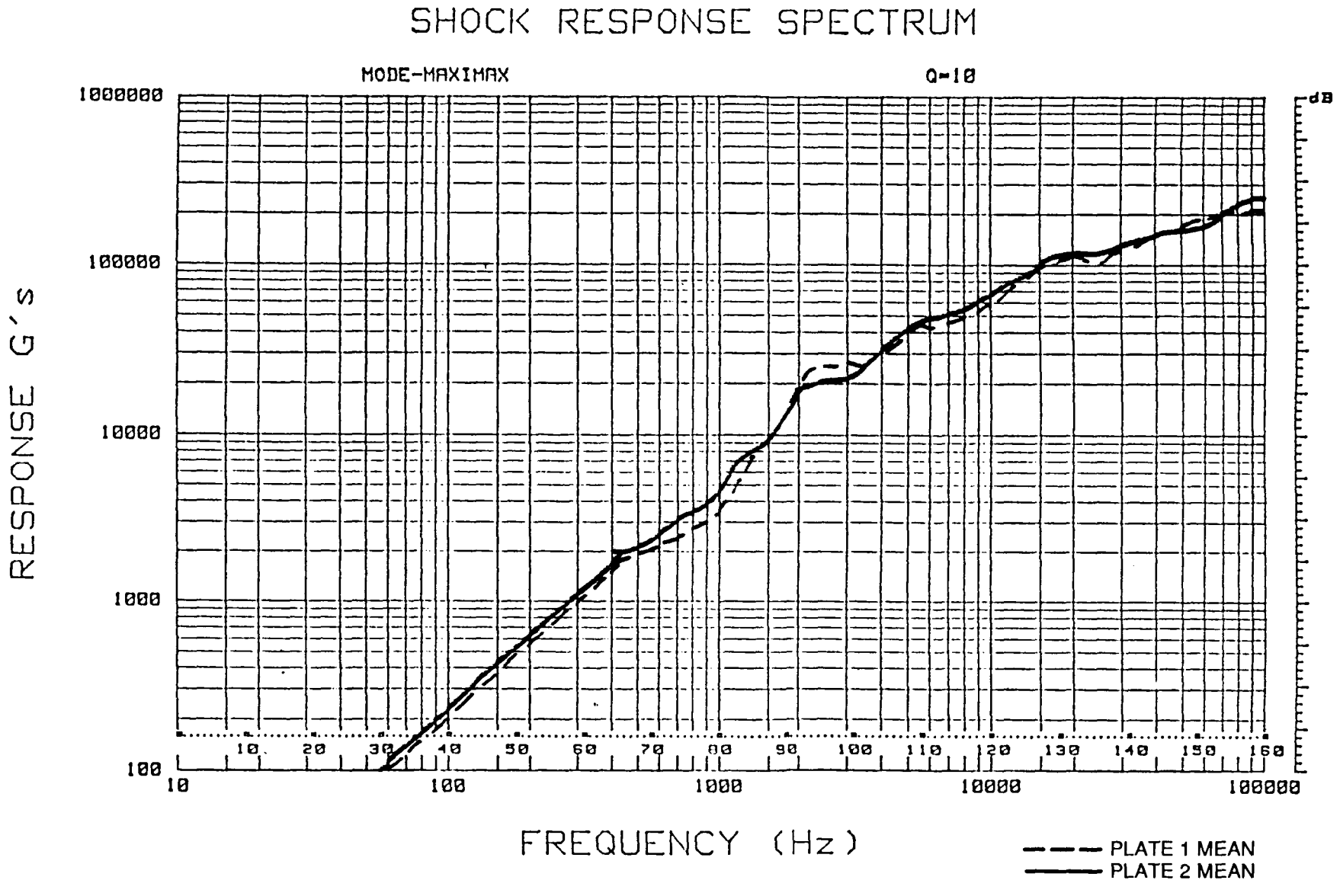

Figure 42. SRS: Joint test control – plate Nos. 1 and 2, means.

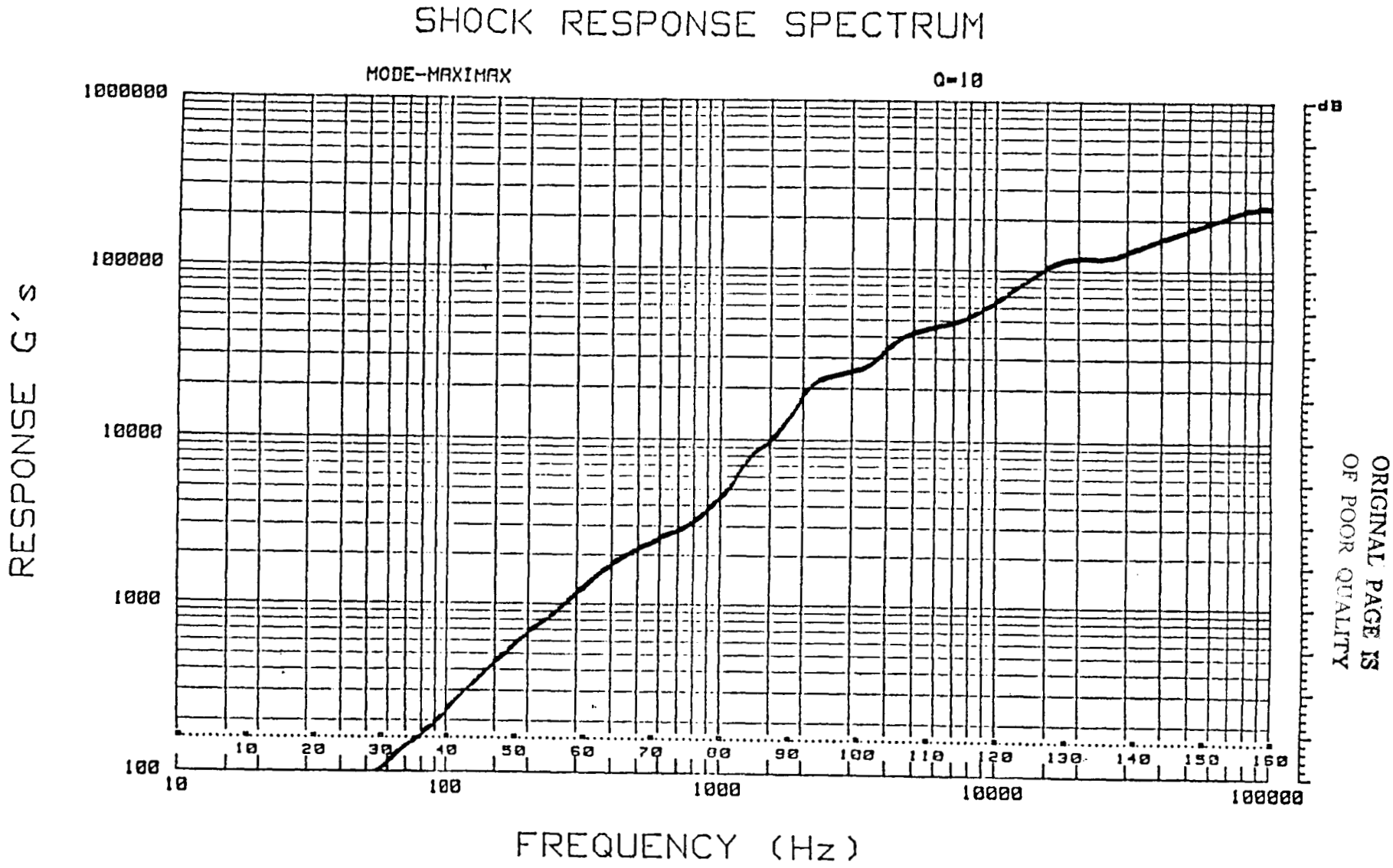

Figure 43. SRS: Joint test base reference mean.

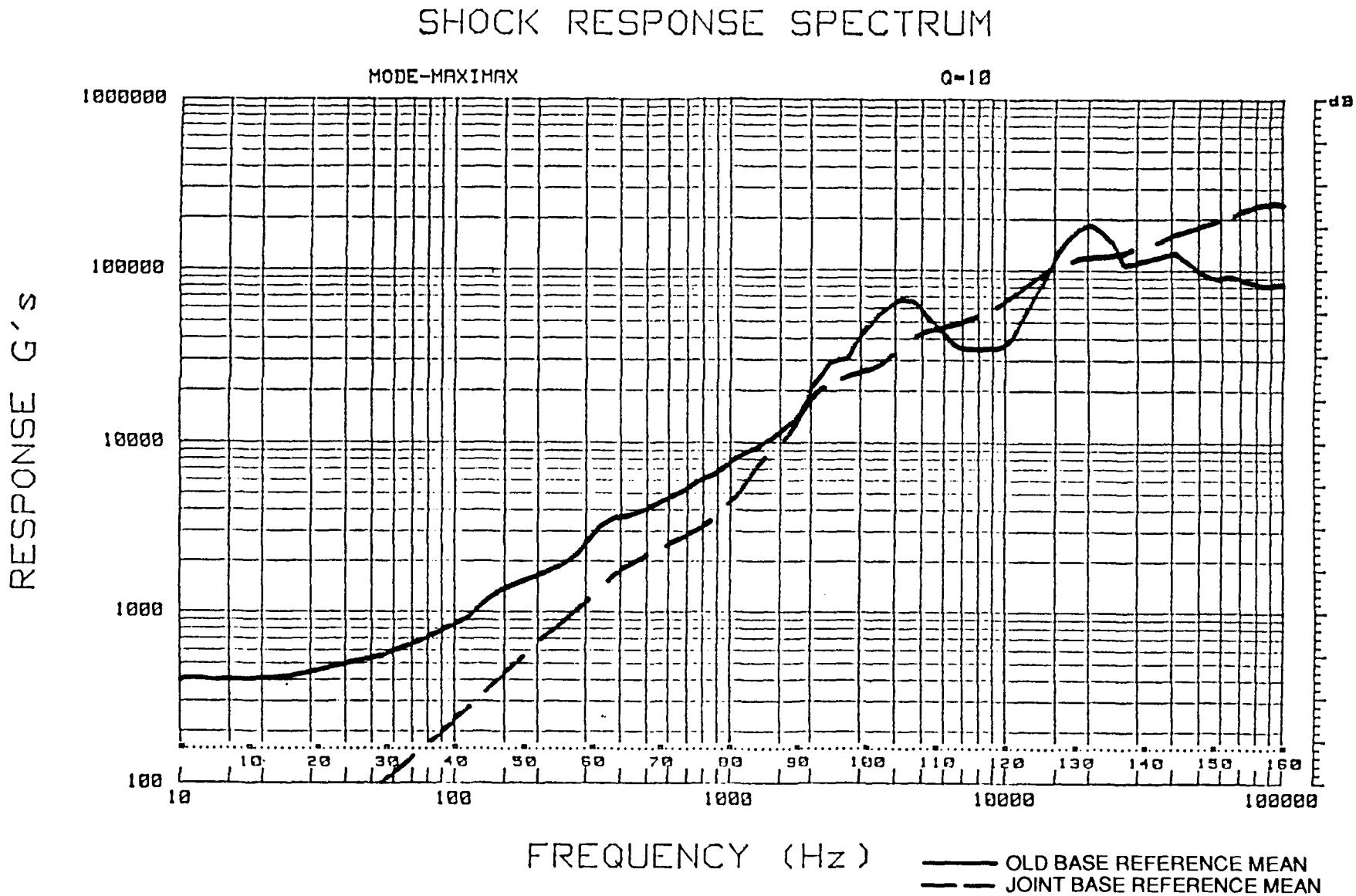

Figure 44. SRS: Joint test versus old base reference means.

ORIGINAL PAGE IS
OF POOR QUALITY

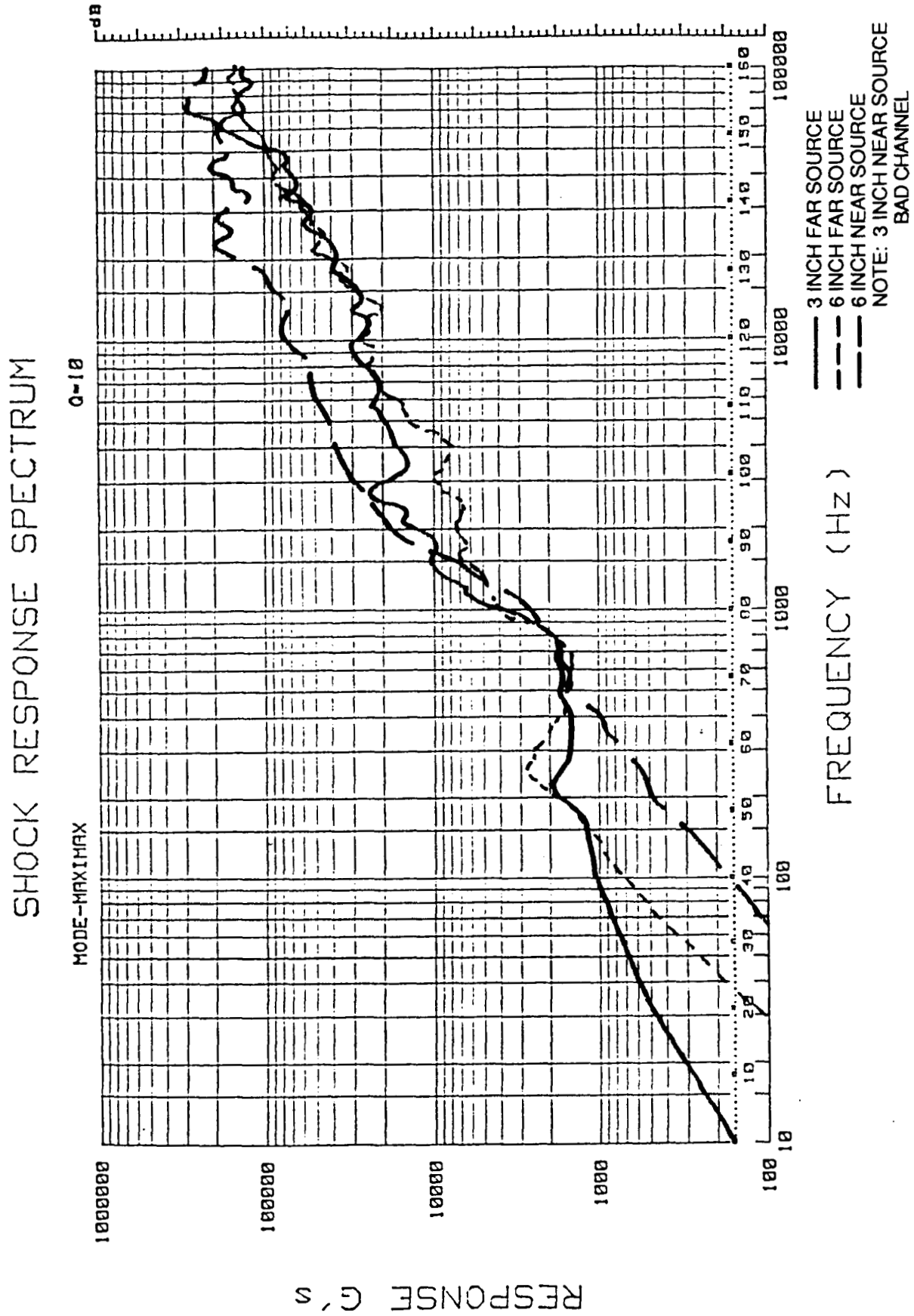

Figure 45. SRS: Joint test – plate No. 3.

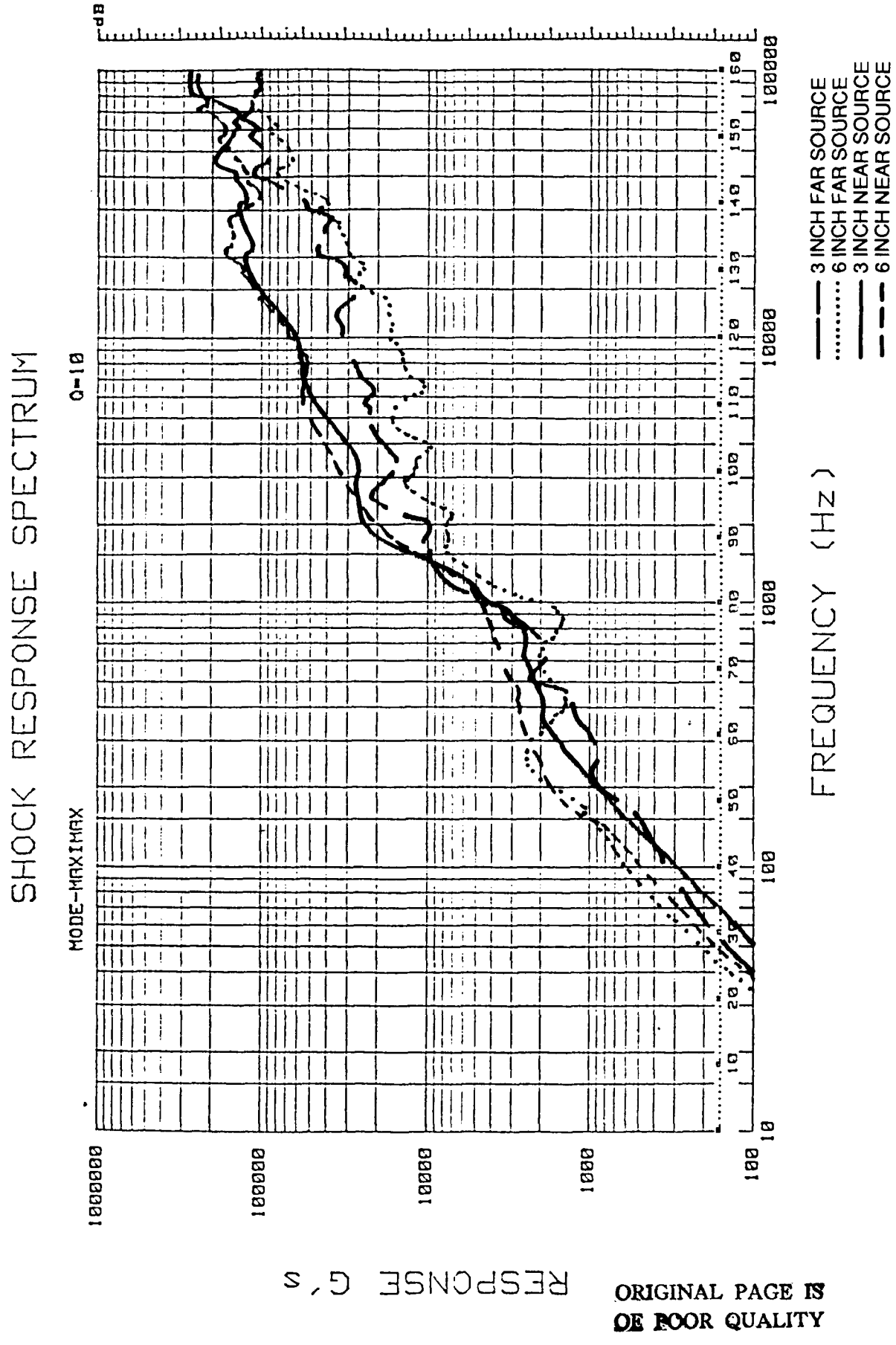

Figure 46. SRS: Joint test – plate No. 4.

ORIGINAL PAGE IS
OF POOR QUALITY

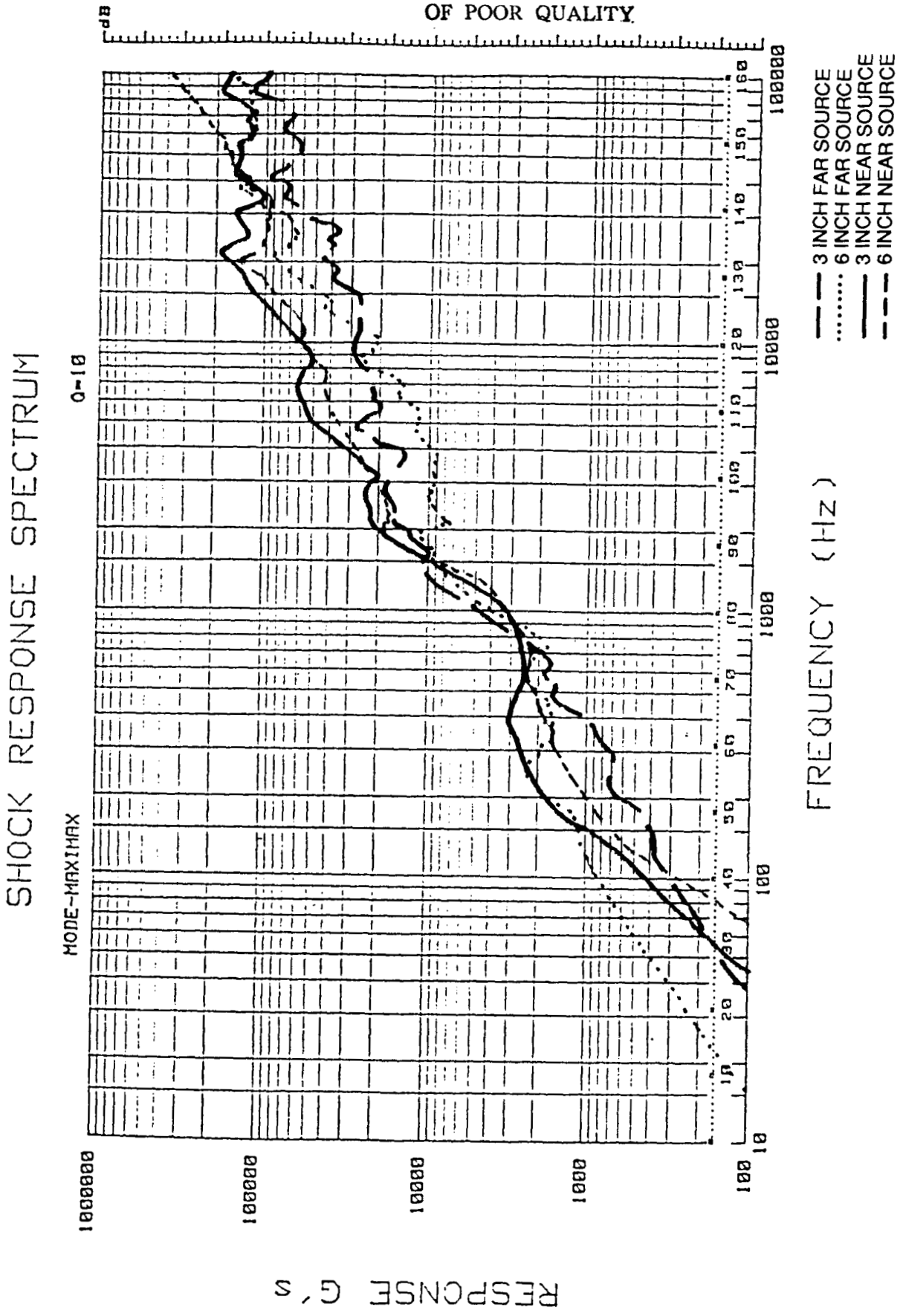

Figure 47. SRS: Joint test – plate No. 5.

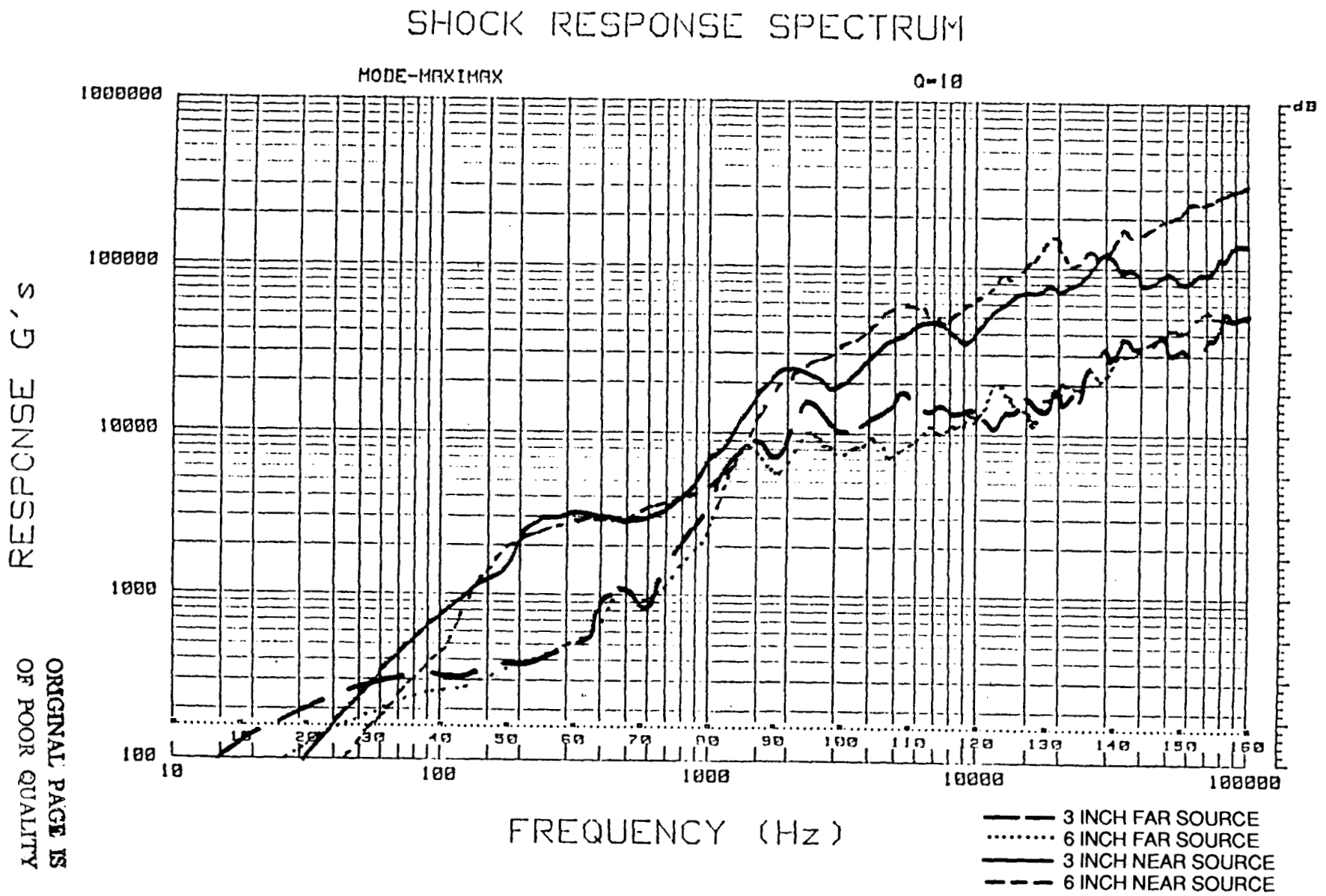

Figure 48. SRS: Joint test – plate No. 6.

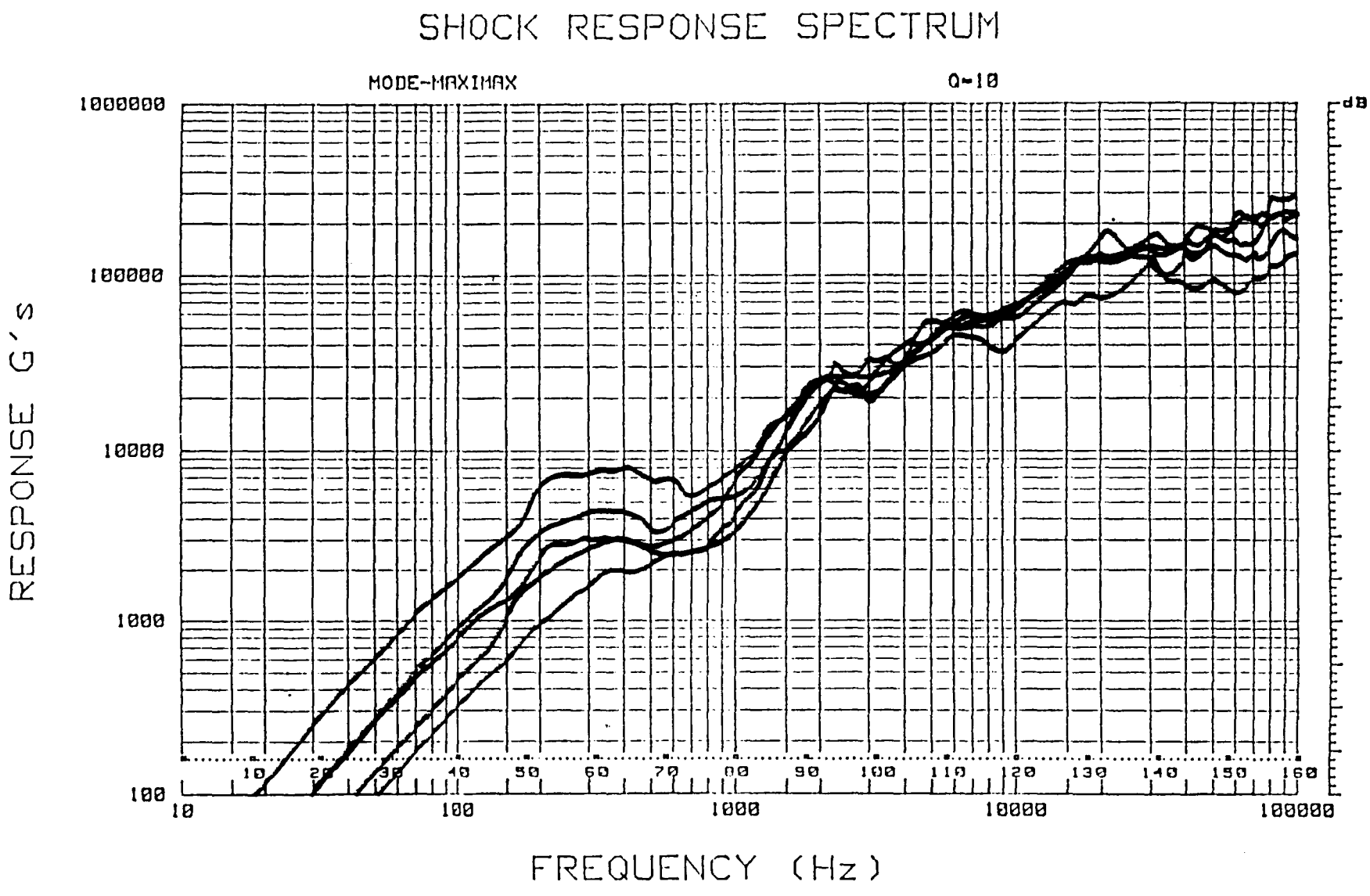

Figure 49. SRS: 3-in. joint near source – plate Nos. 1, 2, 4, 5, and 6.

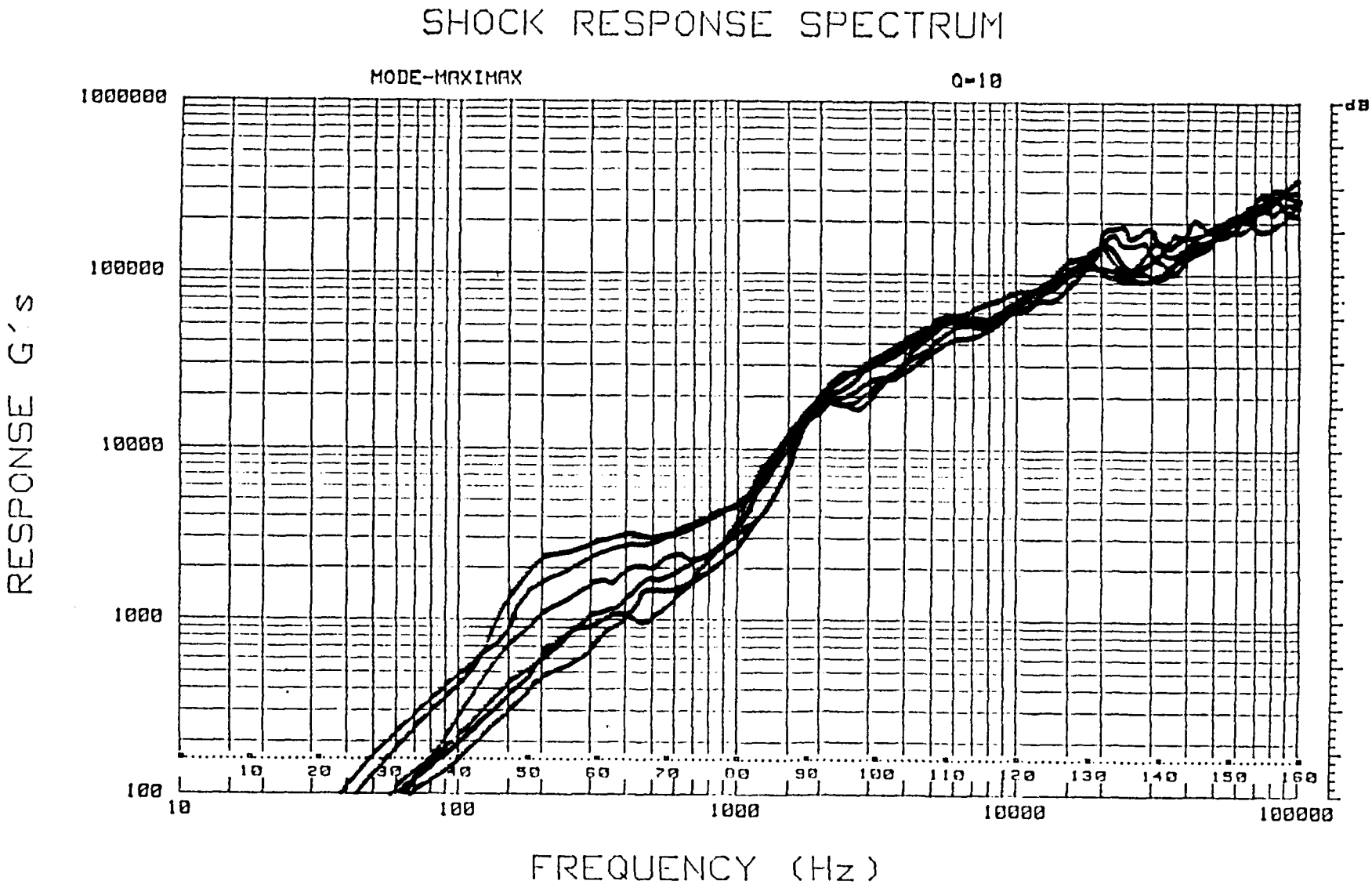

Figure 50. SRS: 6-in. joint near source – plate Nos. 1, 2, 3, 4, 5, and 6.

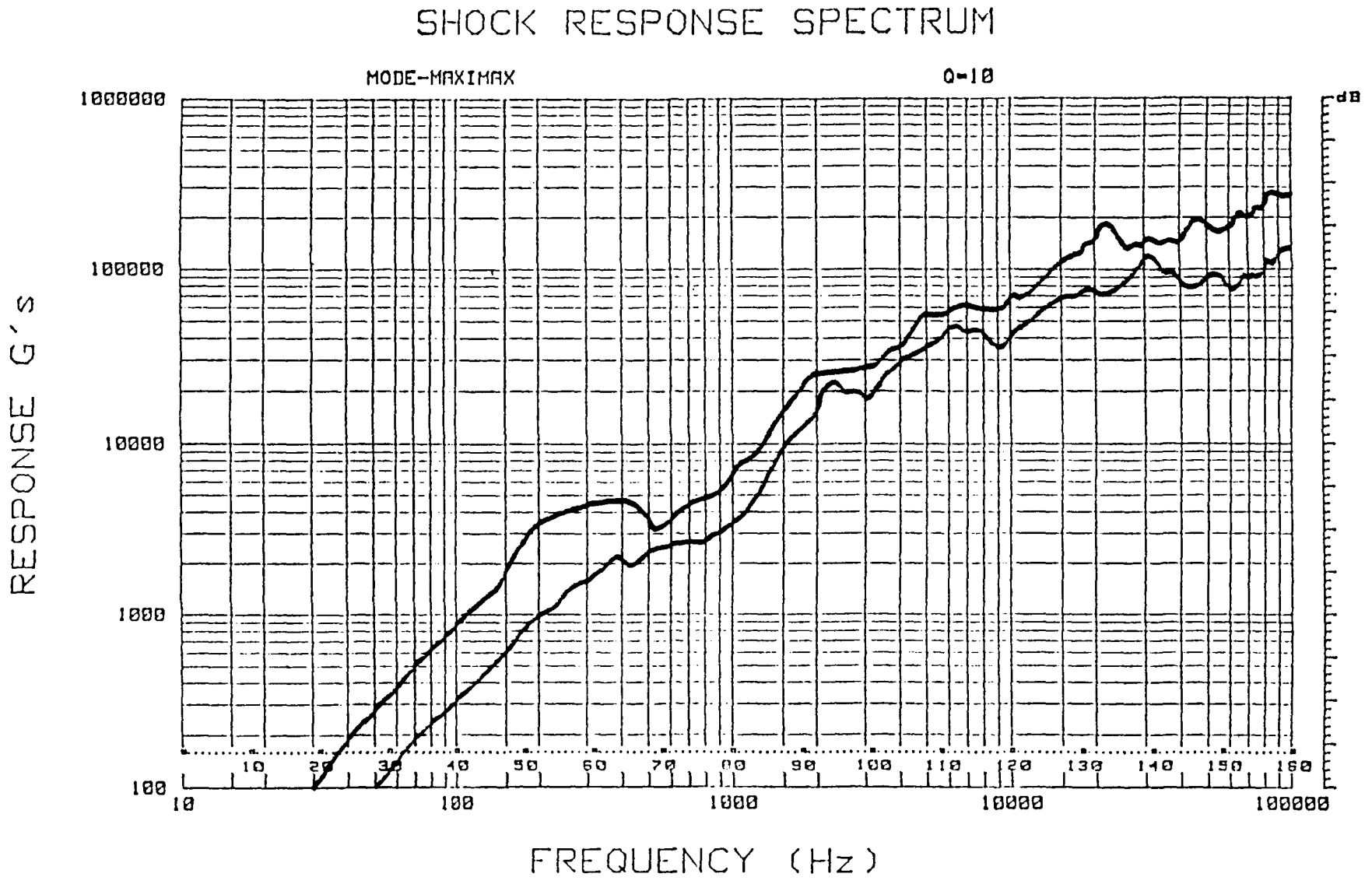

Figure 51. SRS: 3-in. joint near source envelope.

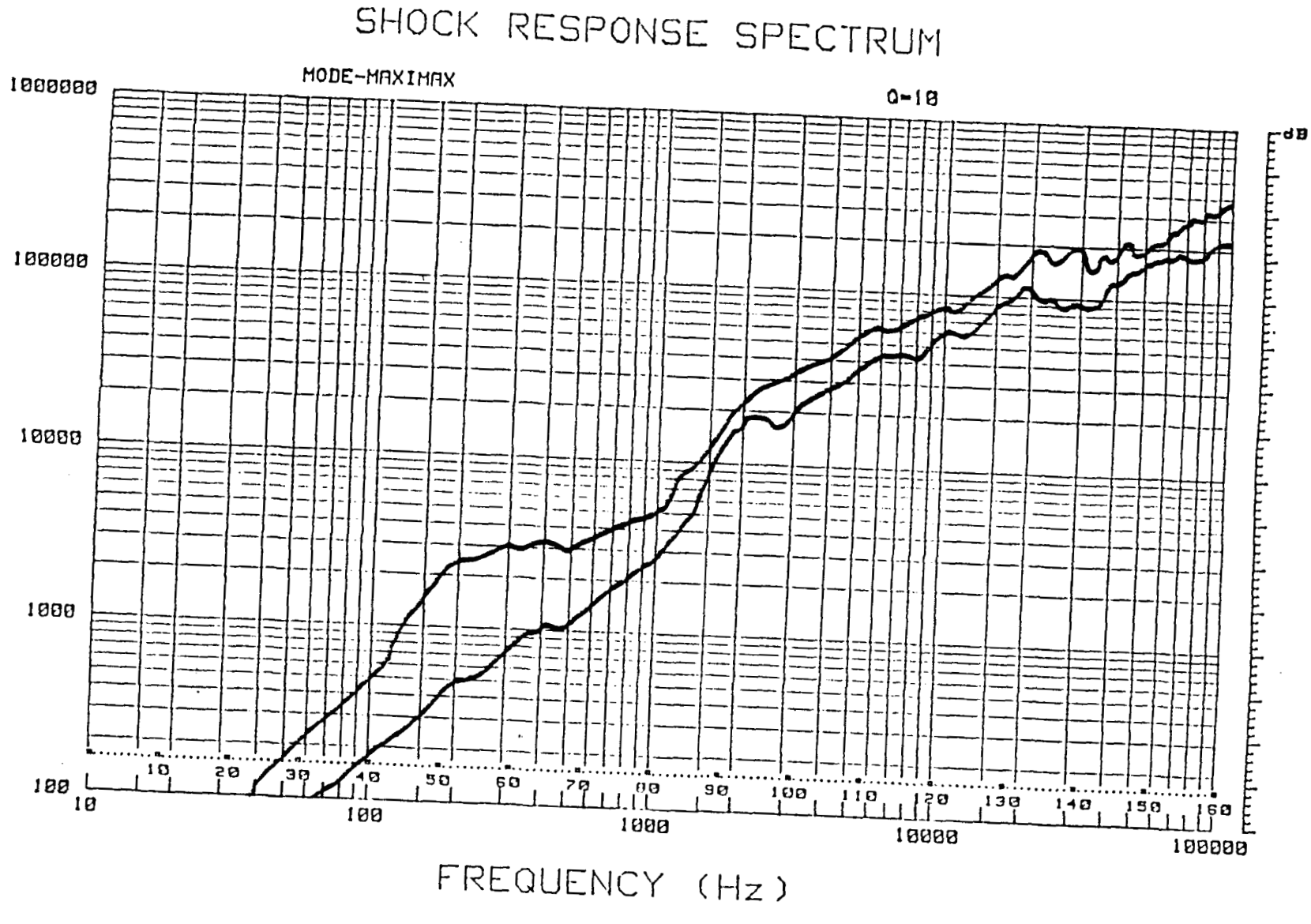

Figure 52. SRS: 6-in. joint near source envelope.

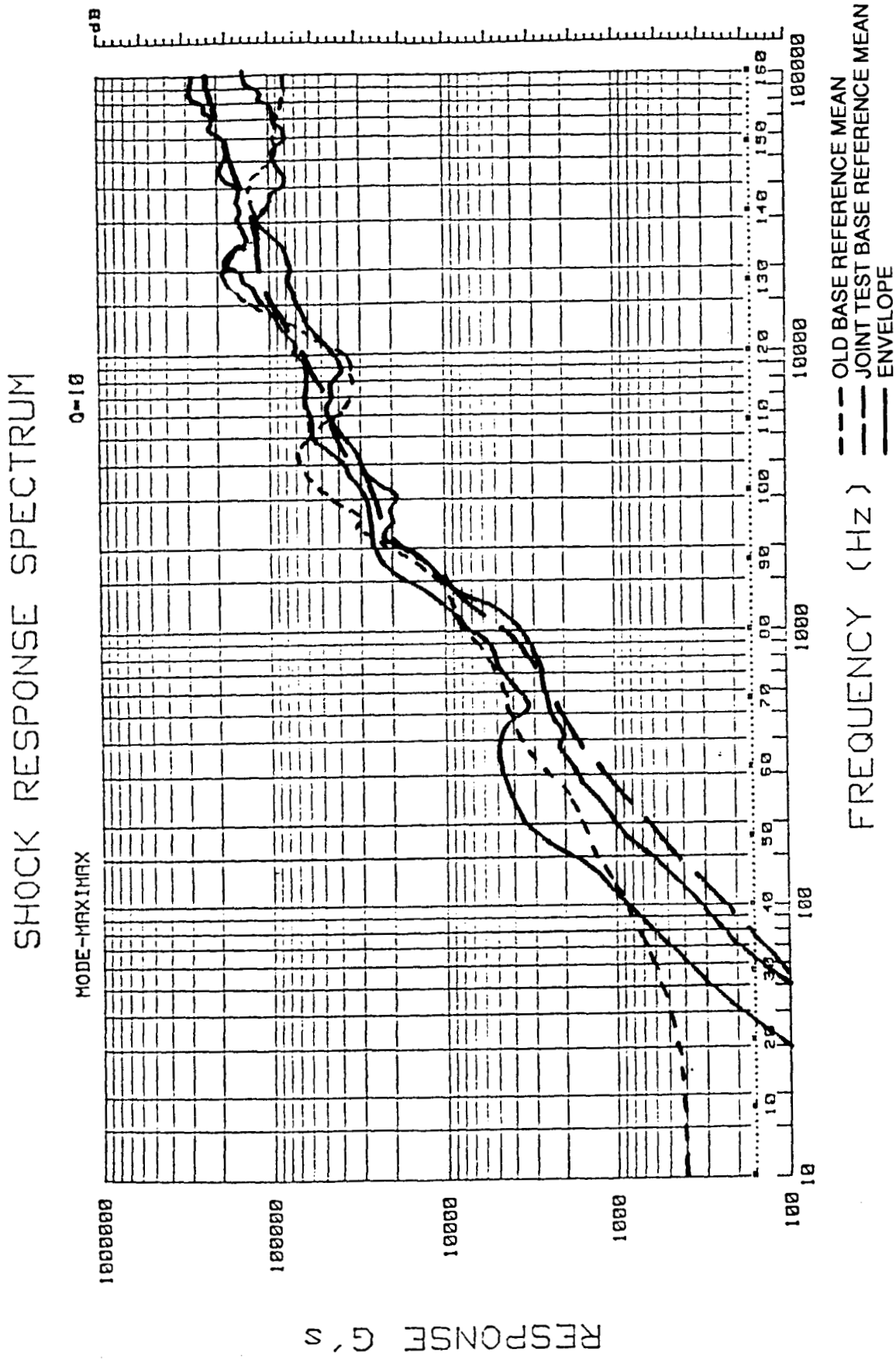

Figure 53. SRS: 3-in. joint near source envelope versus joint test base reference mean and old base reference mean.

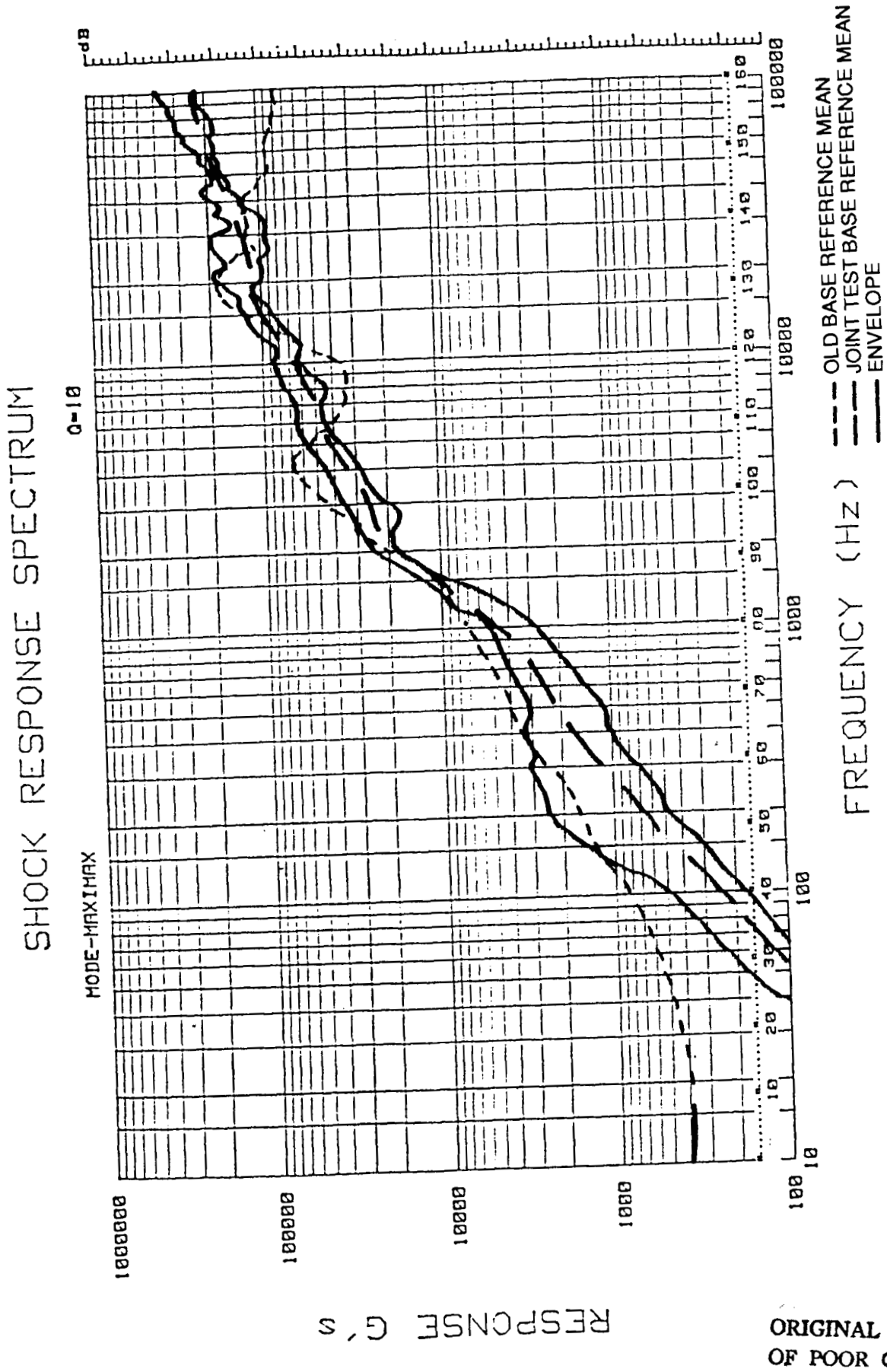

Figure 54. SRS: 6-in. joint near source envelope versus joint test base reference mean and old base reference mean.

ORIGINAL PAGE IS
OF POOR QUALITY

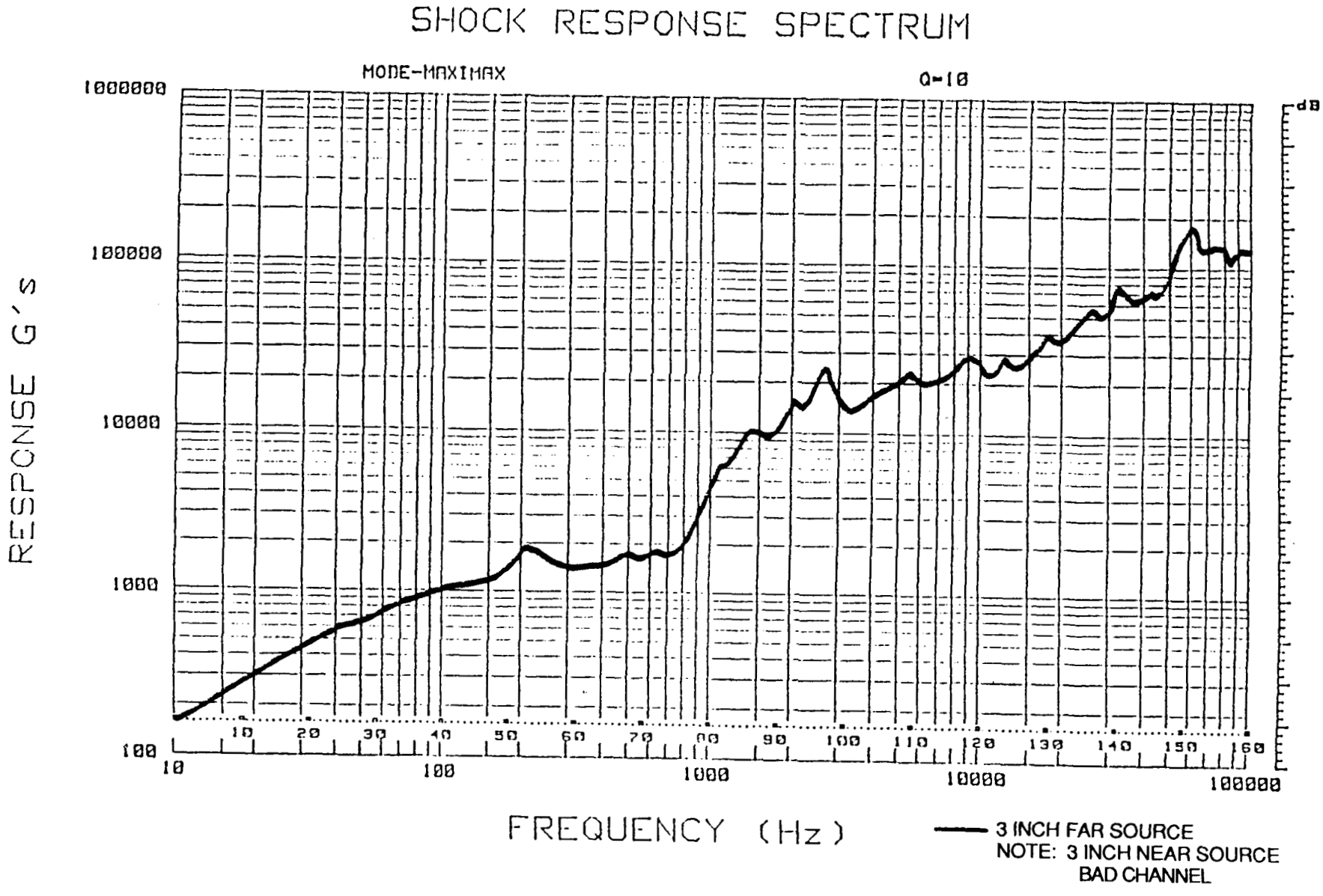

Figure 55. SRS: Joint test – plate No. 3.

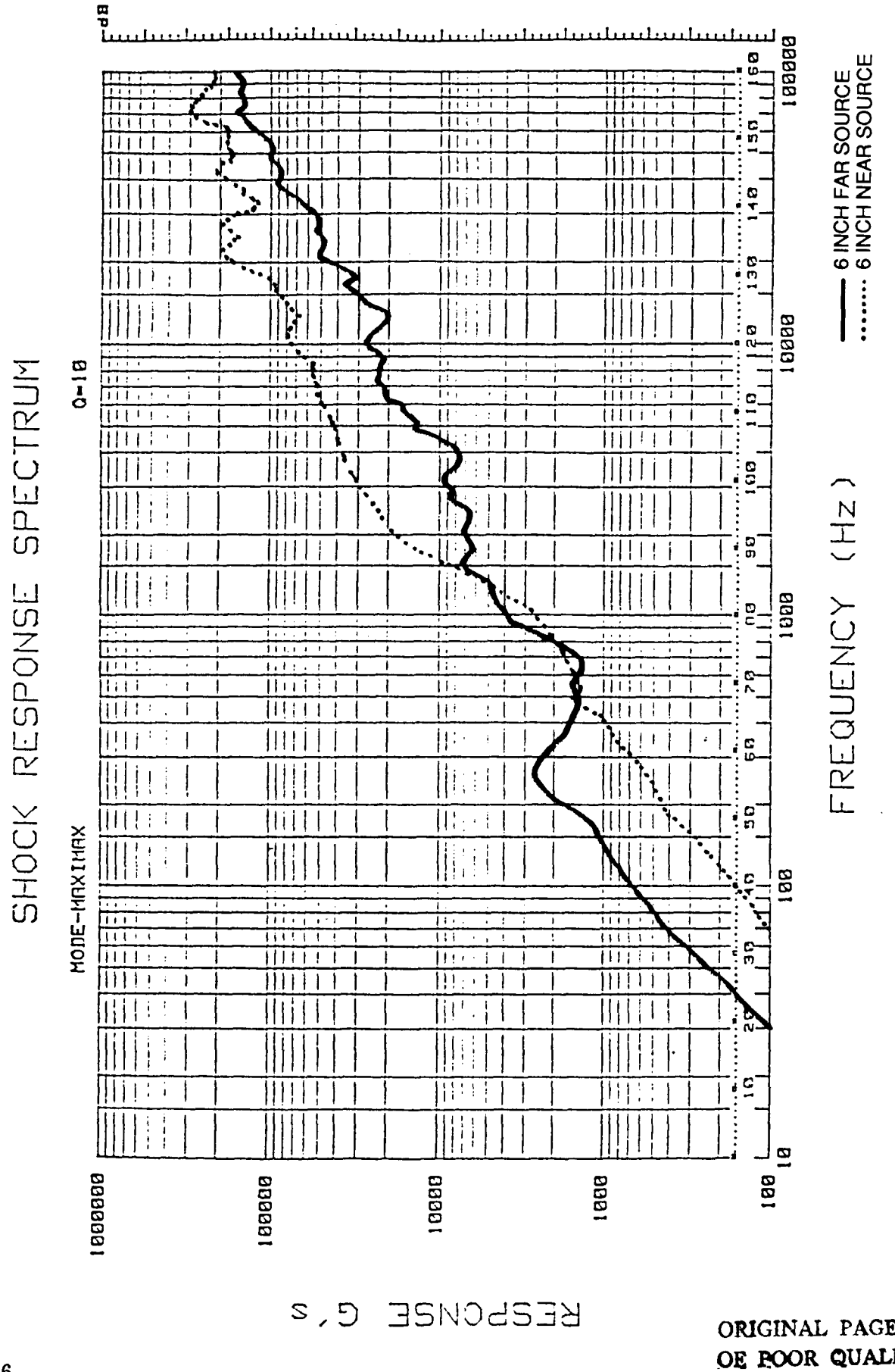

Figure 56. SRS: Joint test – plate No. 3.

ORIGINAL PAGE IS
OE POOR QUALITY

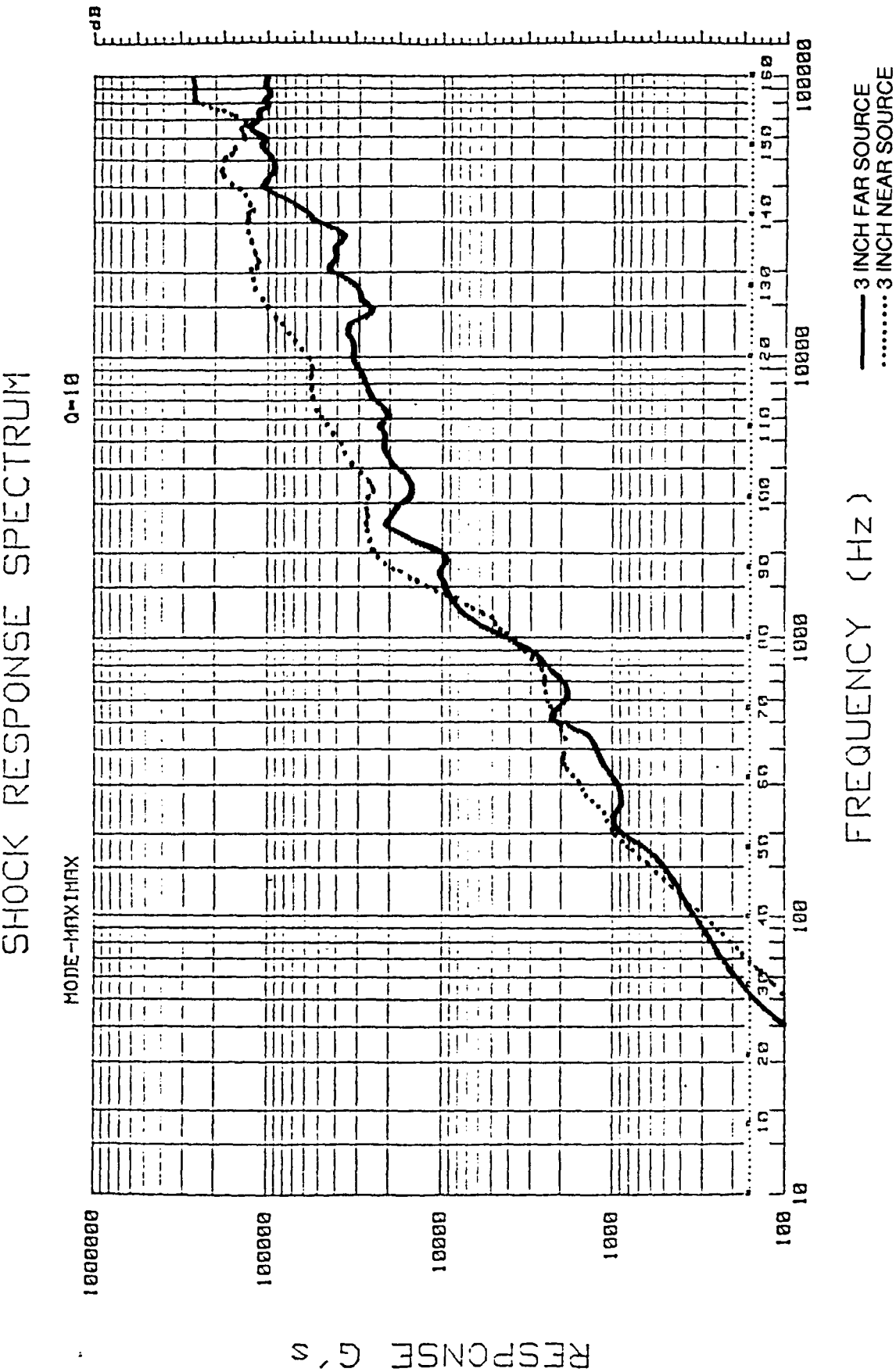

Figure 57. SRS: Joint test – plate No. 4.

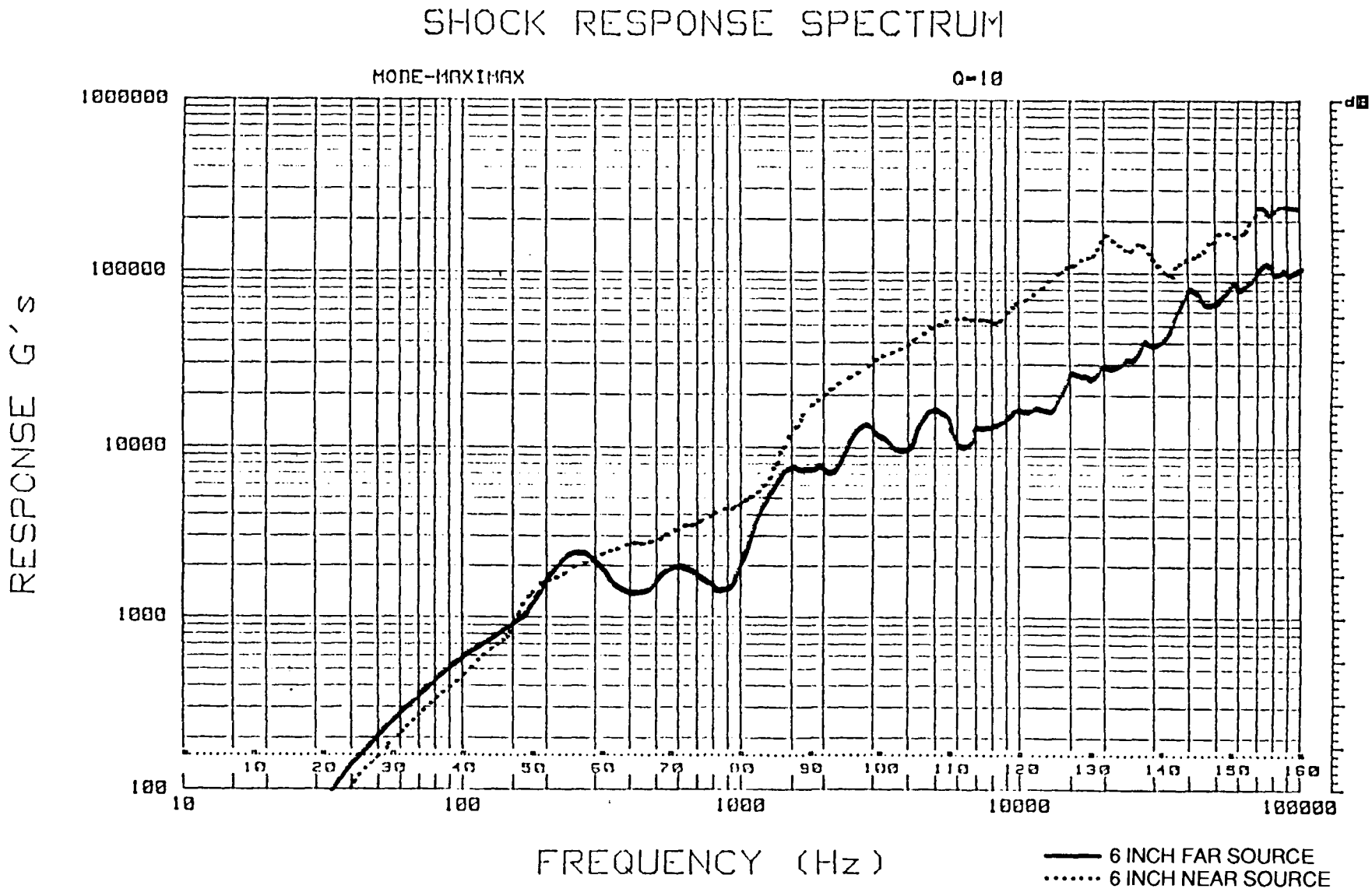

Figure 58. SRS: Joint test – plate No. 4.

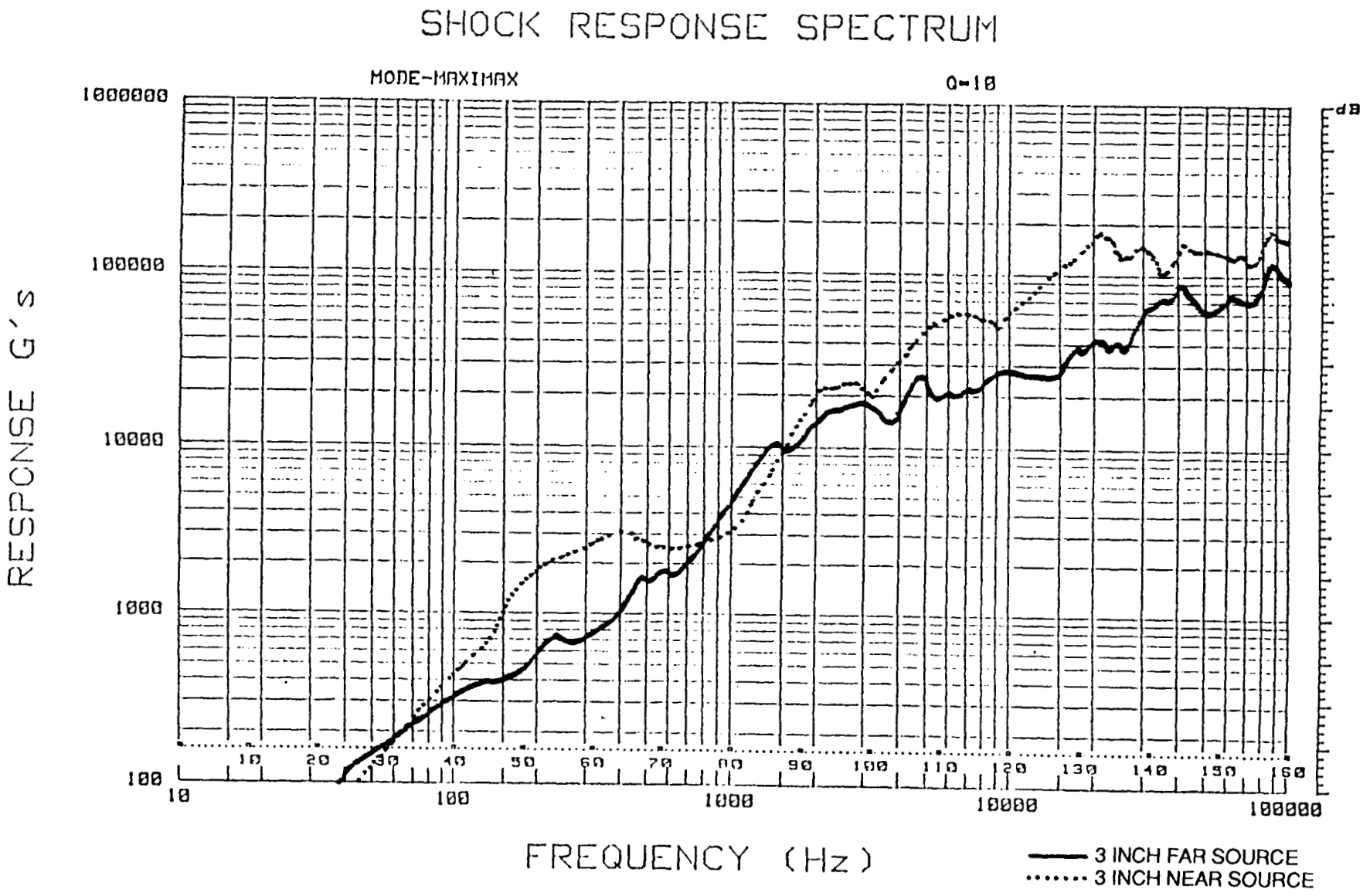

Figure 59. SRS: Joint test – plate No. 5.

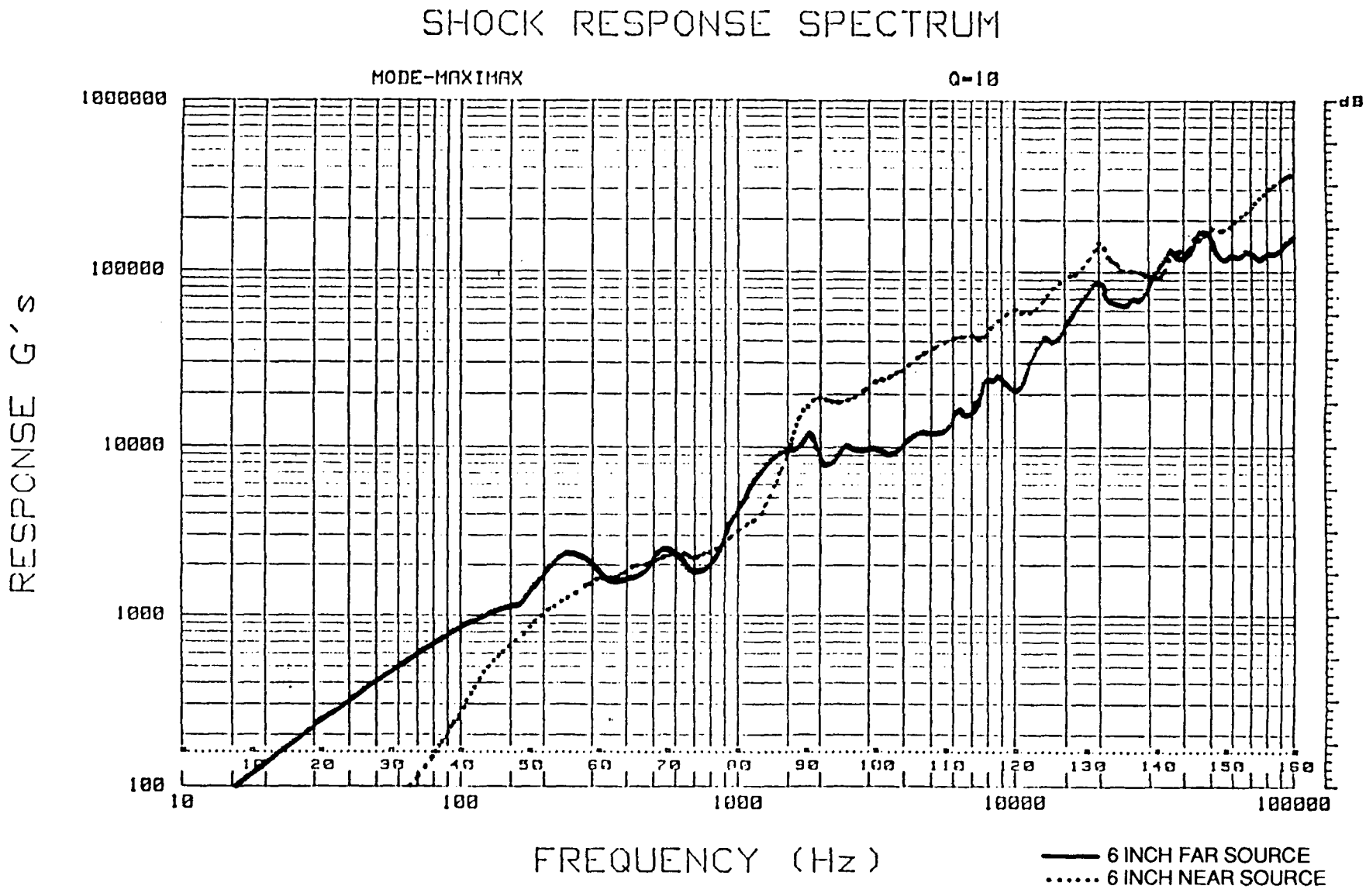

Figure 60. SRS: Joint test – plate No. 5.

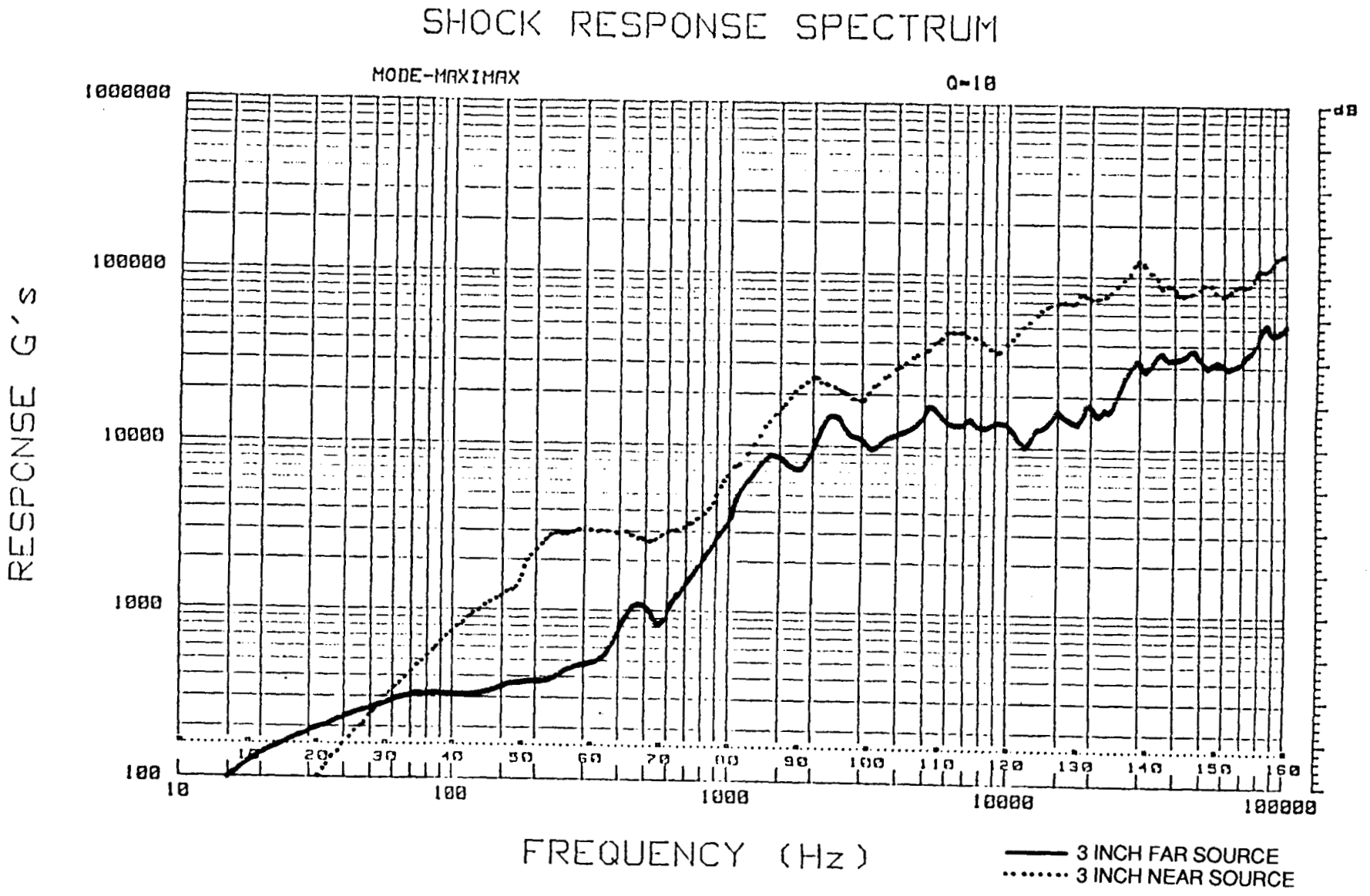

Figure 61. SRS: Joint test – plate No. 6.

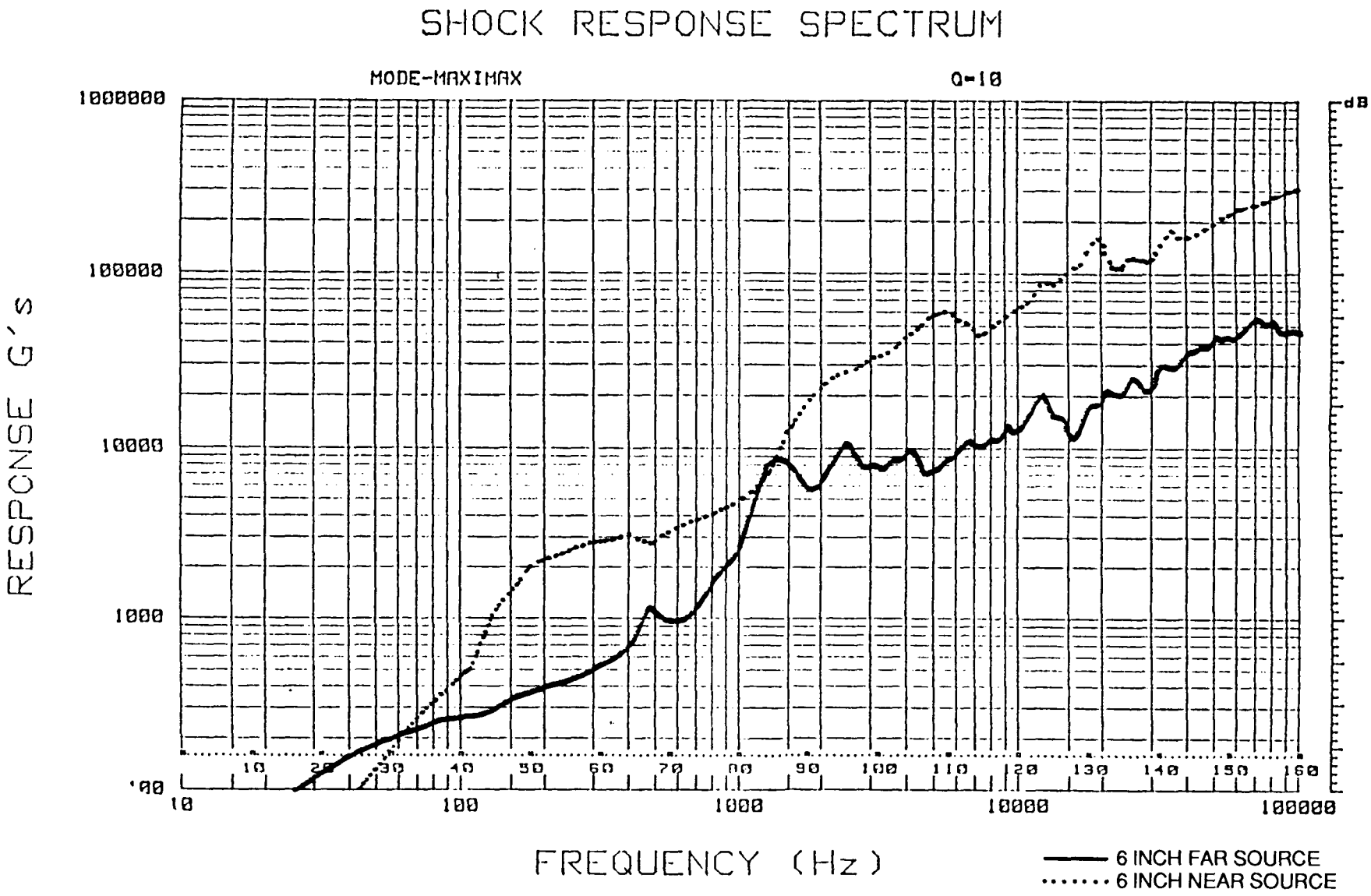

Figure 62. SRS: Joint test – plate No. 6.

Test plate number 5 consisted of a 3-in. and a 6-in. simple lap joint, just as in plate 3, with an added 1-in. gap. Test 5 SRS plots are shown in Figures 59 and 60. Near source measurements were consistent with the base reference mean. Across the narrow joint, energy levels were the same below 3000 Hz and 2 to 3 dB lower above 3000 Hz. Across the wide joint, energy levels were the same below 1500 Hz, and 2 to 3 dB lower above 1500 Hz.

Test plate number 6 SRS plots are shown in Figures 61 and 62. A 3-in. and a 6-in. double lap joint were used. A 1-in. gap and shims (3-in. and 6-in.) were used. Near source levels were comparable to the base reference mean. Across the narrow joint, a 3 to 4 dB decrease was observed above 1500 Hz, with no decrease below 1500 Hz. Across the wide joint, energy levels dropped 3 to 5 dB above 1500 Hz, and remained the same below 1500 Hz. The increased change across the narrow joint and wide joint as compared to tests 3, 4, and 5 could be due to increased mass, but is more likely due to the "Sandwich Theory."

Figures 63 through 70 compare the joint test SRS from the previous 1984-1986 study to the data from tests 3 through 6 above. The old test consisted of an end-severed plate. The plate was cut in half and the halves bolted together with a 3-in. lap. This form of lap joint is even simpler than that employed in test 3 above. This joint was illustrated earlier in this section. Near source levels are comparable. Across the joint very little decrease is noted in the old test data due to the joint design. It is clear the more complex the joint the greater the energy decrease.

C. Rigid Mount Tests

The rigid mount tests utilized the end-severed plate configuration that was used in the previous 1984-1986 study. This test program repeats many of the previous plate tests with the difference being the boundary conditions. As noted previously in the equipment section of this paper, the rigid mount plates are bolted to the test fixture. One would expect overall levels to be lower and energy levels to decrease as a function of distance from the source.

Tests 7 and 8 were the experimental controls, designed to provide a base reference mean for comparison with the 1984-1986 data. A mass loading experiment was conducted on test 8. This will be discussed later under a separate heading.

Test 9 consisted of a combination of variables designed to produce the maximum SRS for this plate. Variables included maximum coreload, minimum LSC standoff, and maximum coupling, all within tolerance, but at the extremes.

Test 10 included the combination of minimum coreload, maximum LSC standoff, and minimum coupling, all at the tolerance extremes. This should produce the minimum SRS for this plate.

Test 11 used a 40 grain/foot LSC, a gross LSC overload, designed to produce an increased SRS due to an increase in the source. An extra unamplified accelerometer was included on this test as an additional side study. This side study will be covered later under a separate heading.

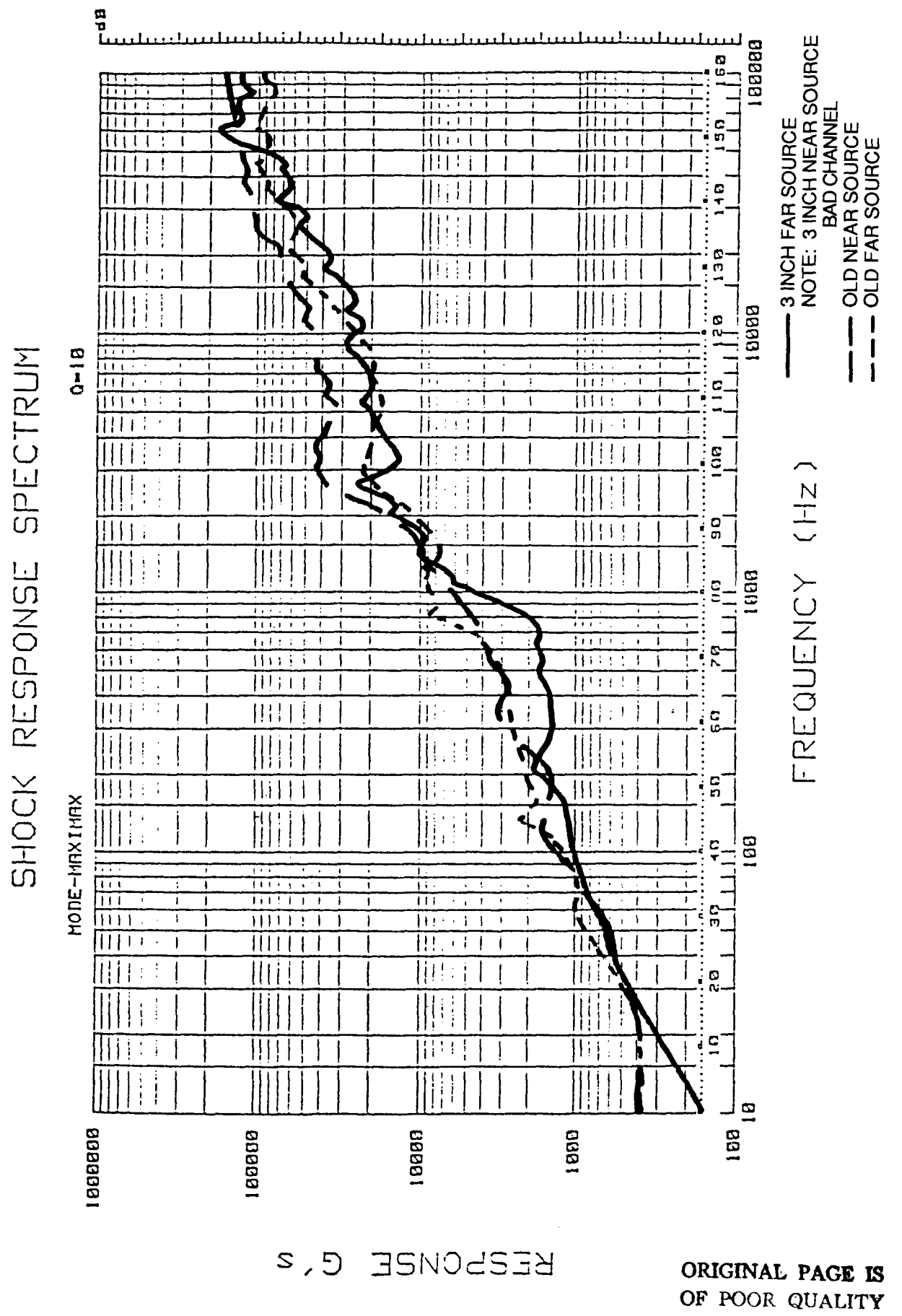

Figure 63. SRS: Joint test – plate No. 3, 6-in joint versus old joint near and far source.

ORIGINAL PAGE IS
OF POOR QUALITY

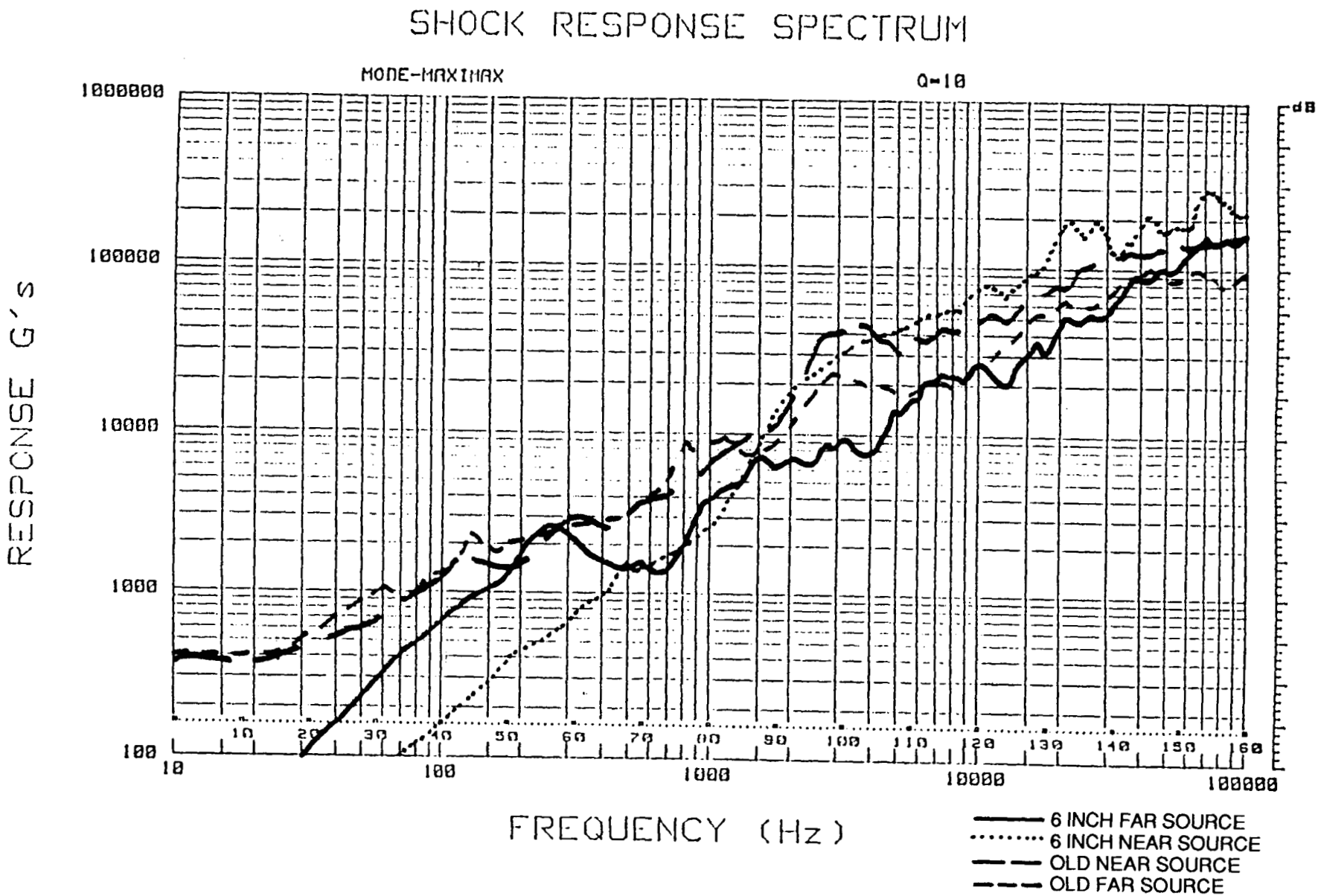

Figure 64. SRS: Joint test – plate No. 3, 6-in. joint versus old joint near and far source.

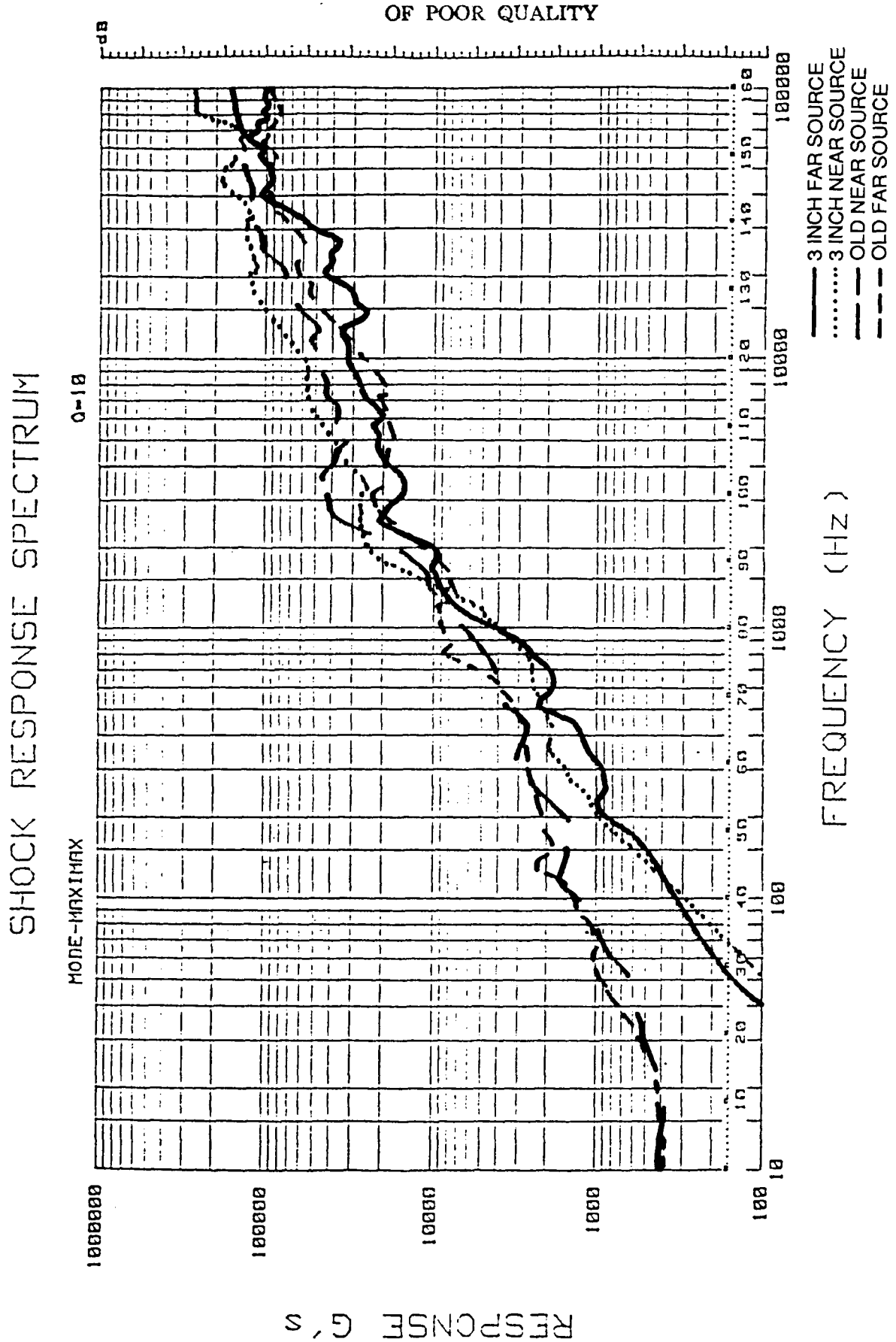

Figure 65. SRS: Joint test – plate No. 4, 3-in. joint versus old joint near and far source.

ORIGINAL PAGE IS
OF POOR QUALITY

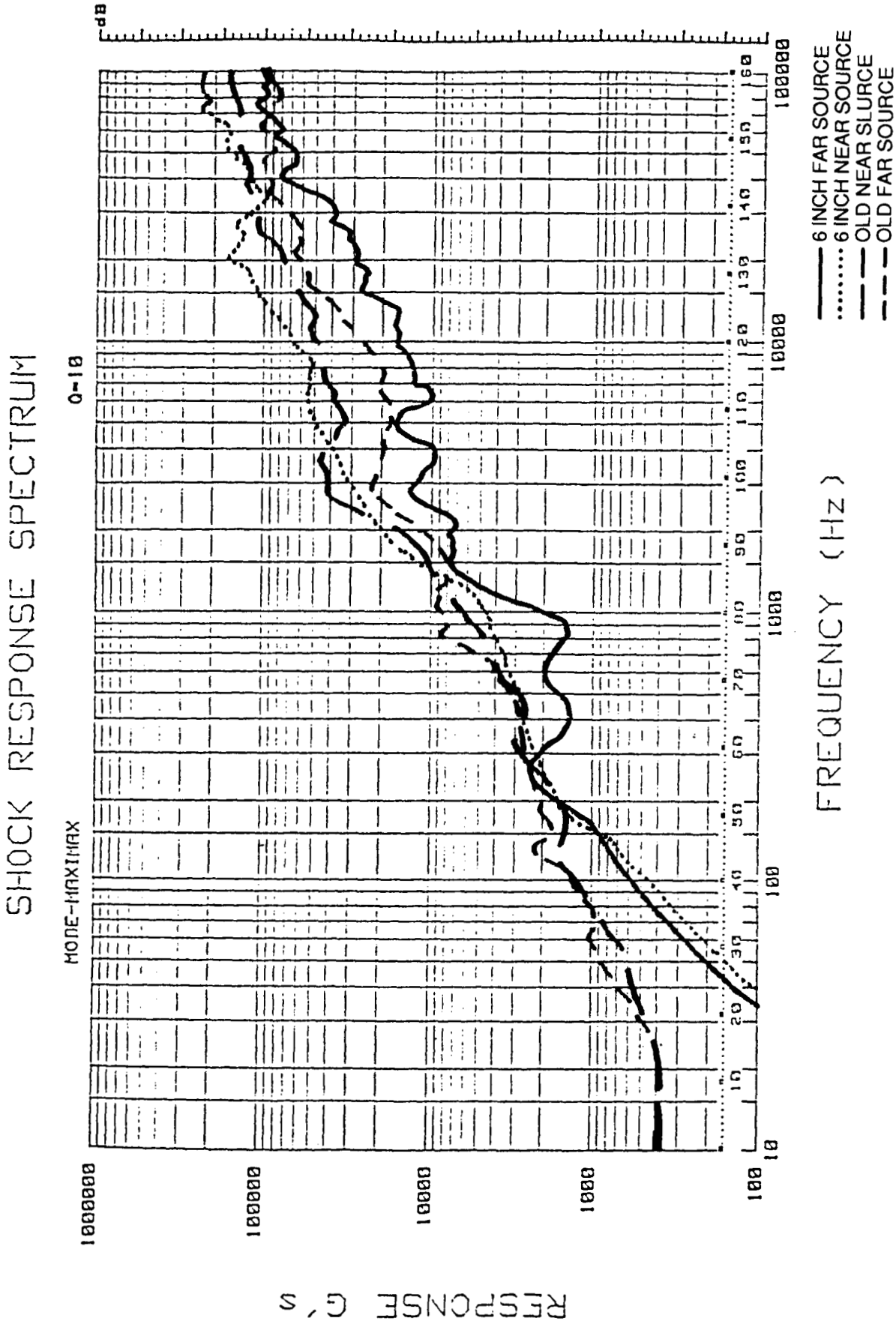

Figure 66. SRS: Joint test – plate No. 4, 6-in. joint versus old joint near and far source.

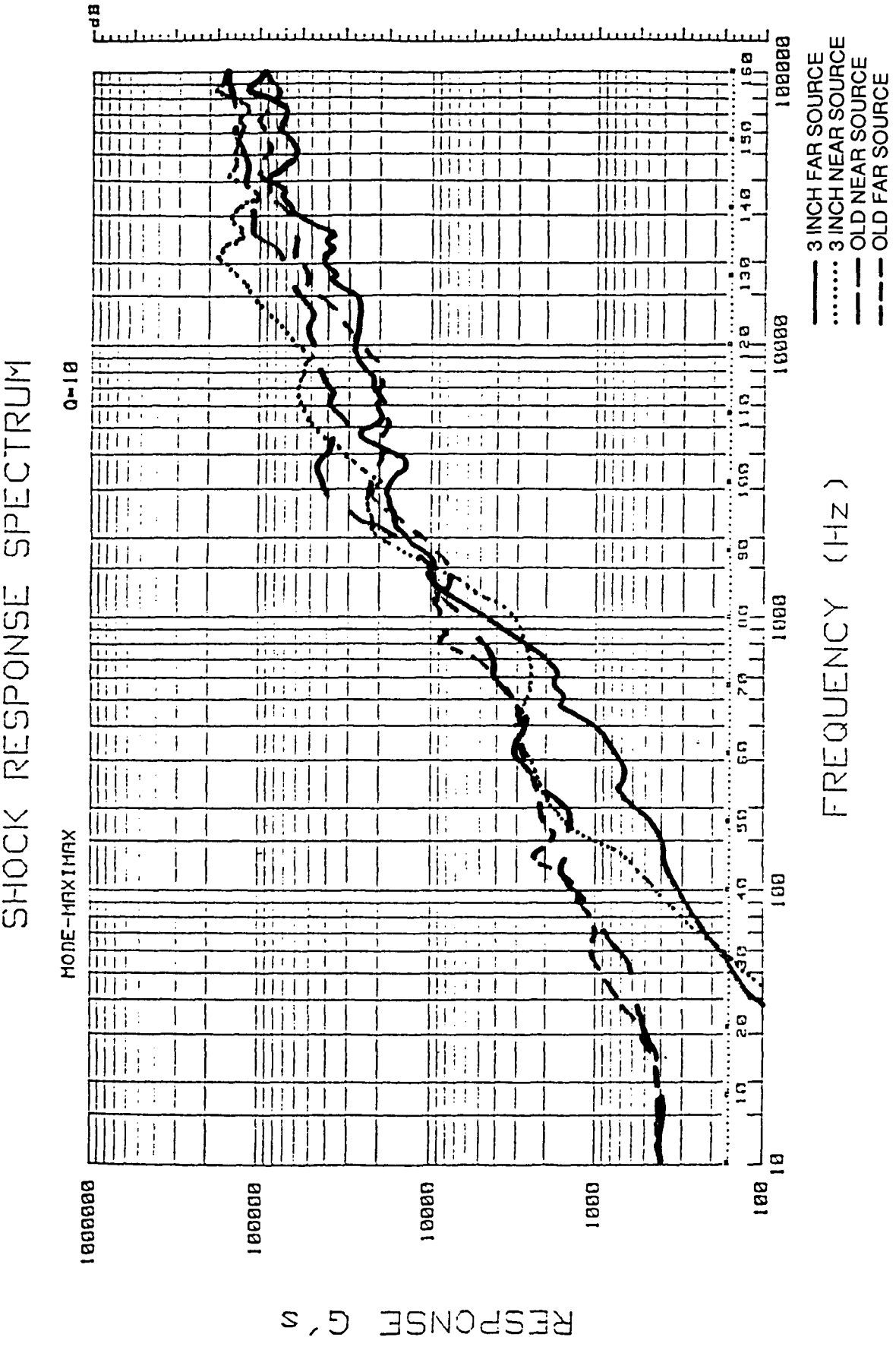

Figure 67. SRS: Joint test – plate No. 5, 3-in. joint versus old joint near and far source.

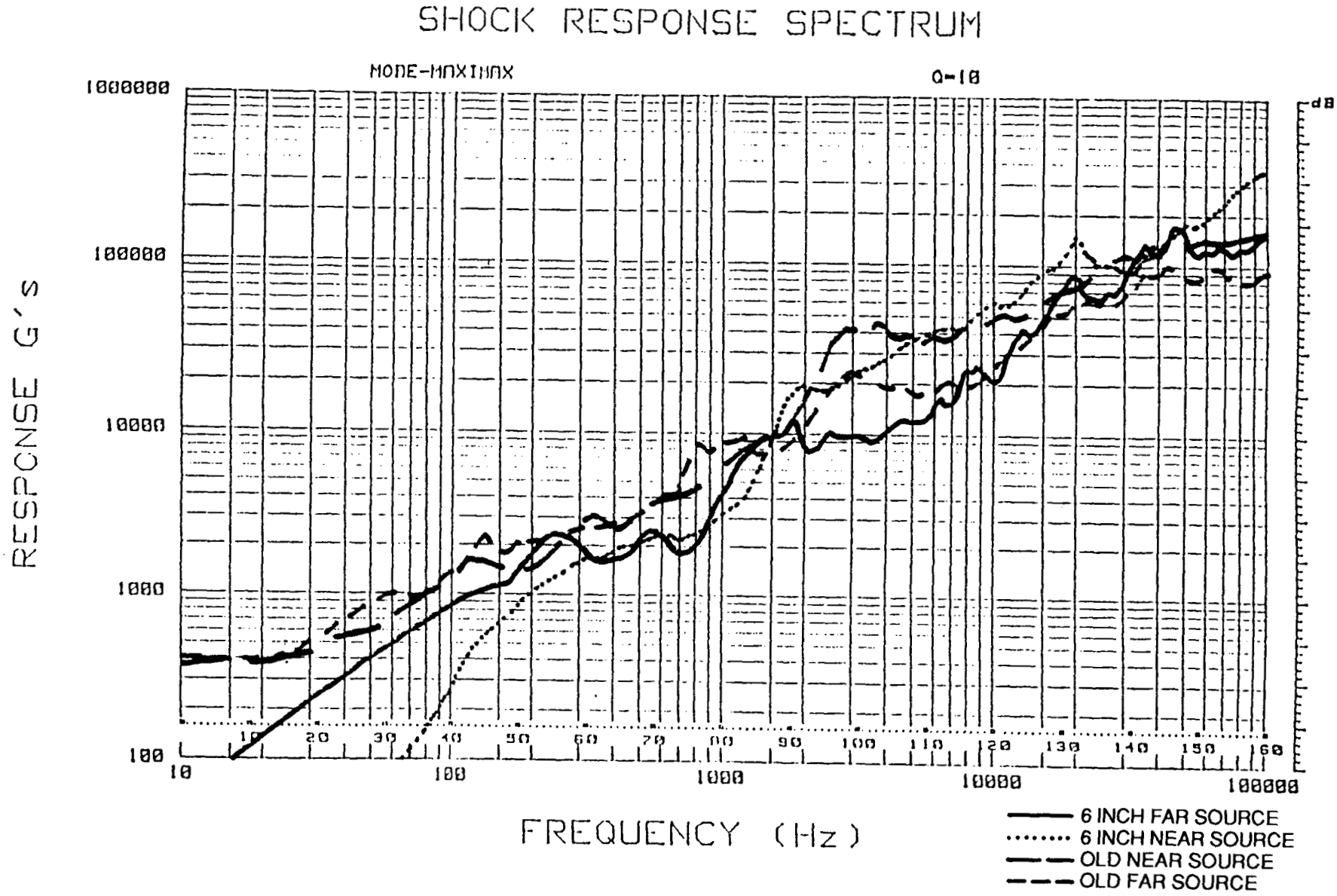

Figure 68. SRS: Joint test – plate No. 5, 6-in. joint versus old joint near and far source.

ORIGINAL PAGE IS
OF POOR QUALITY

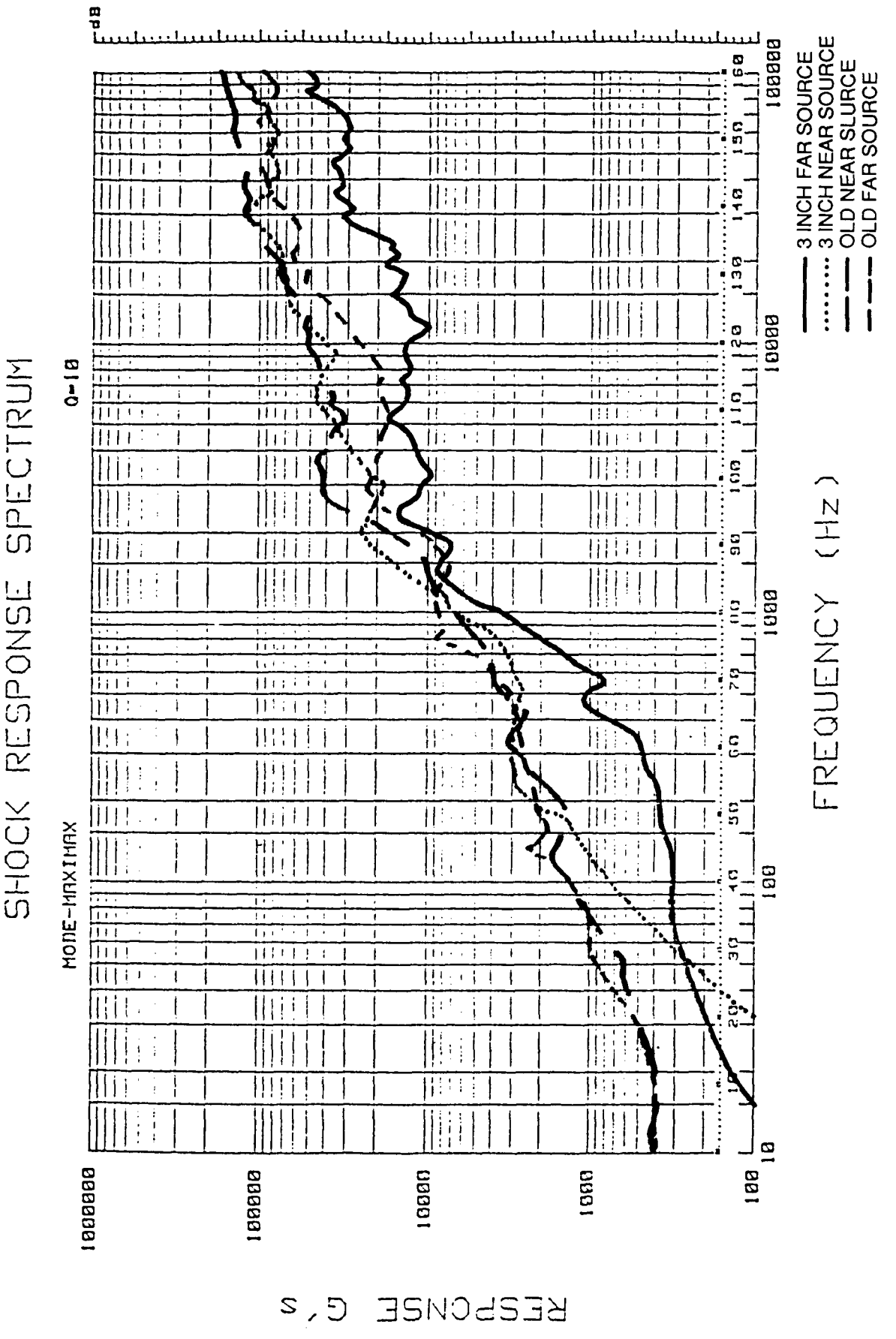

Figure 69. SRS: Joint test – plate No. 6, 3-in. joint versus old joint near and far source.

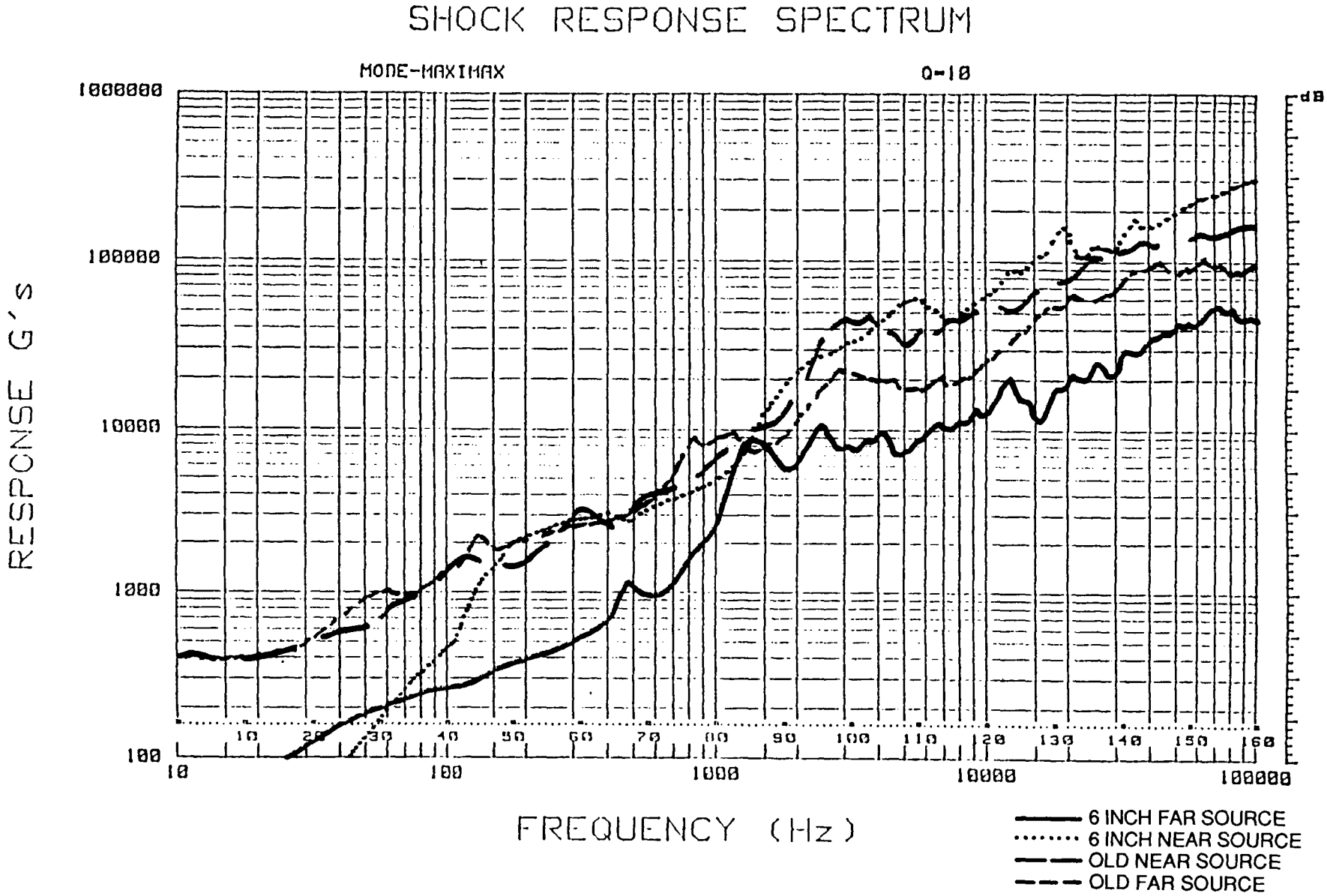

Figure 70. SRS: Joint test – plate No. 6, 6-in. joint versus old joint near and far source.

Figures 71 and 72 are the SRS for the control plates 7 and 8. Figure 73 shows the combined SRS for both plates. Review of the data showed that mass loading does affect SRS for clamped boundary plates. Data from test 8 was, therefore, not used to calculate a base reference mean. This resulted in test 7 data being the sole source for the reference SRS. Test 7 near source data is greater than far source data, but only by one decibel at the most. However, a distinct, clear, difference is noted. On test 8 only a slight difference is noted with no distinct pattern being evident. Both SRS from test 7 become the near and far source base reference SRS for the remaining tests. Figure 74 compares the SRS levels from test 7 with the old base reference mean from the free-free end-severed tests. The rigid mount data near source is 2 to 3 dB lower below 6000 Hz than the free-free data. It is evident that the charge source highly influences the high frequency portion of the SRS, while the characteristics of the plate determine the low frequency portion of the SRS. As suspected, energy levels decrease as a function of distance with energy leaving the plate through the hard mount.

Figures 75 through 77 are the SRS for tests 9, 10, and 11. Figures 78 through 83 compare the base reference means from the 1984-1986 study and from test 7 to the data from tests 9, 10, and 11. None of the variables in tests 9, 10, or 11 affect the near or far source SRS. However, overall levels are 1 to 4 dB lower than the free-free tests at all frequencies with the greatest decreases at 6000 Hz and below.

D. Mass Loaded Test

Figure 84 shows the mass loaded near source SRS, near source base reference SRS, and the old base reference mean SRS. Figure 85 shows the mass loaded far source SRS, far source base reference SRS, and the old base reference mean SRS. There is a 2 to 3 dB decrease in some frequency regions, due to mass loading between, when the mass loaded plate number 8 is compared with the control plate number 7. The energy decrease does not appear to be a clear-cut function of frequency. The mass loaded SRS is an average of 3 dB lower than the old base reference mean SRS. It should be noted that the decrease in SRS due to mass loading appears to be significant only very near to the mass.

E. Unamplified Accelerometer Test

Test number 11 had three accelerometers instead of the two used on the other rigid mount tests. Two of the accelerometers were mounted side-by-side as shown in Figure 86. Figure 87 compares the SRS from the unamplified accelerometer to the SRS from the side-by-side mounted amplified accelerometer. The unamplified channel is much "cleaner" with less noise than the other channel. The unamplified channel is equivalent to the amplified channel except that the unamplified channel contains less noise in the low frequency region and is slightly lower in level, about 2 dB down between 15,000 Hz and 90,000 Hz.

V. SUMMARY, CONCLUSIONS, AND RECOMMENDATIONS

This section summarizes the research effort, lists all the conclusions that may be drawn about the study, and interjects several recommendations to NASA and the scientific community in general concerning pyrotechnic shock testing.

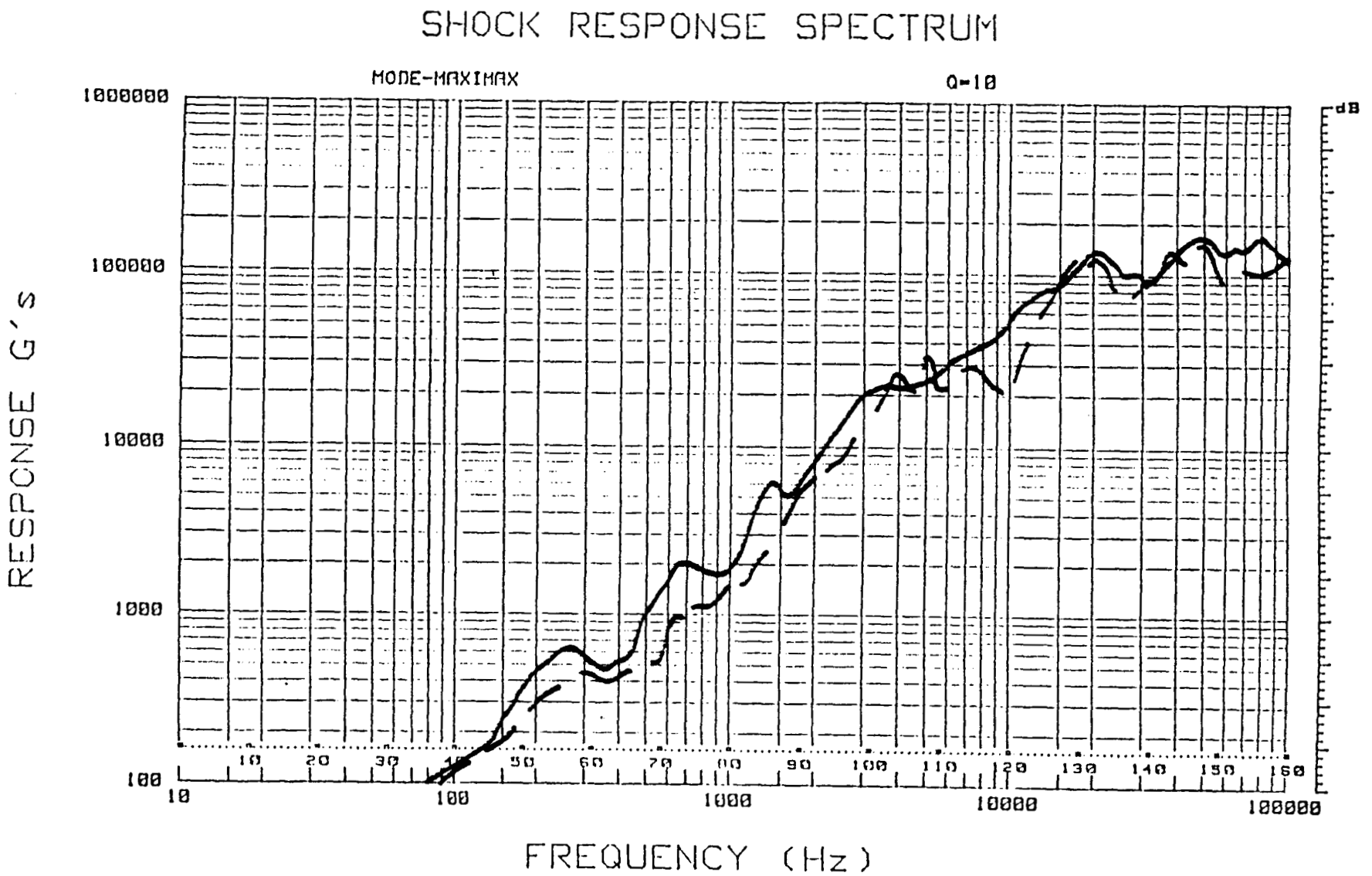

Figure 71. SRS: Rigid test – plate No. 7, experimental control.

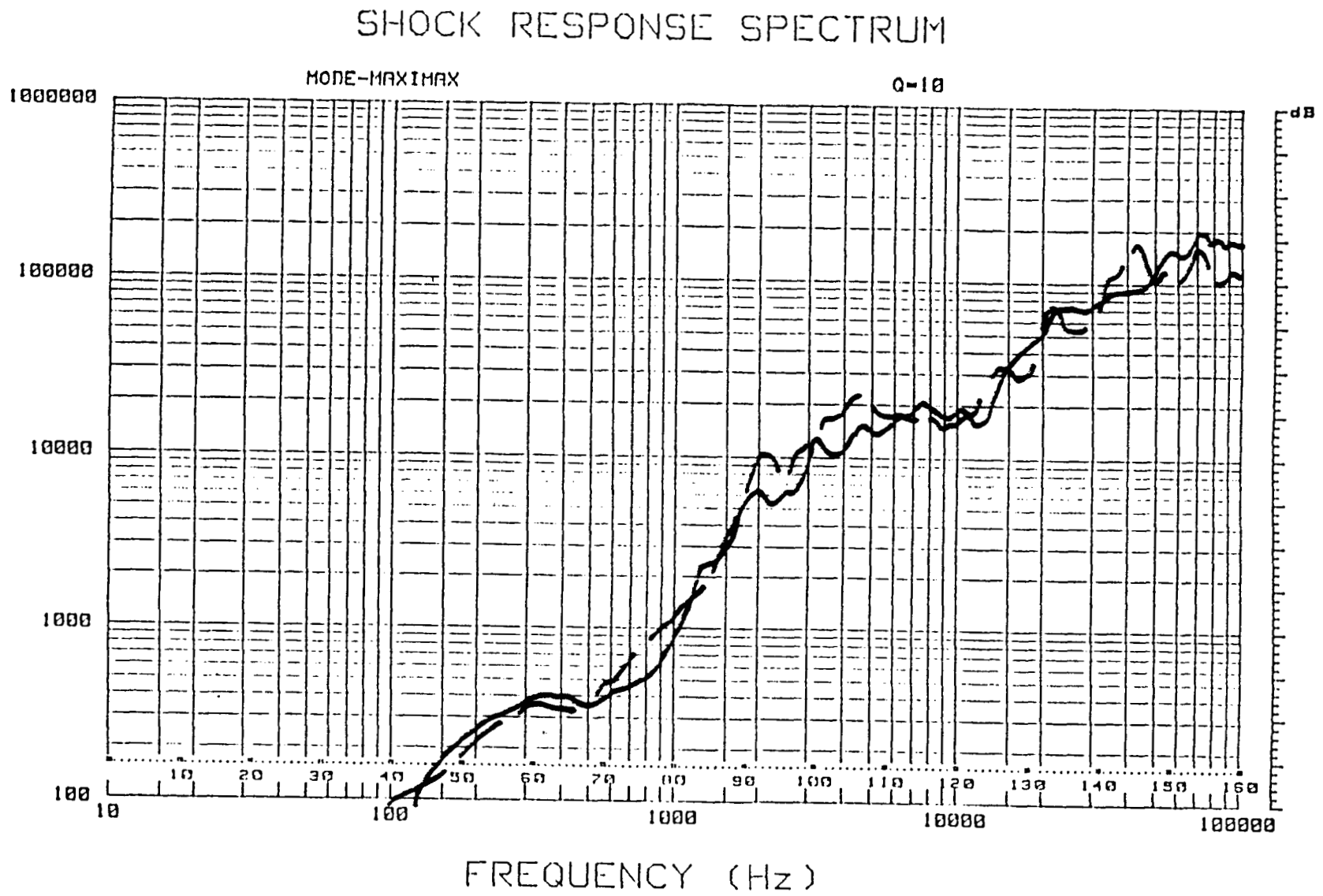

Figure 72. SRS: Rigid test – plate No. 8, experimental control.

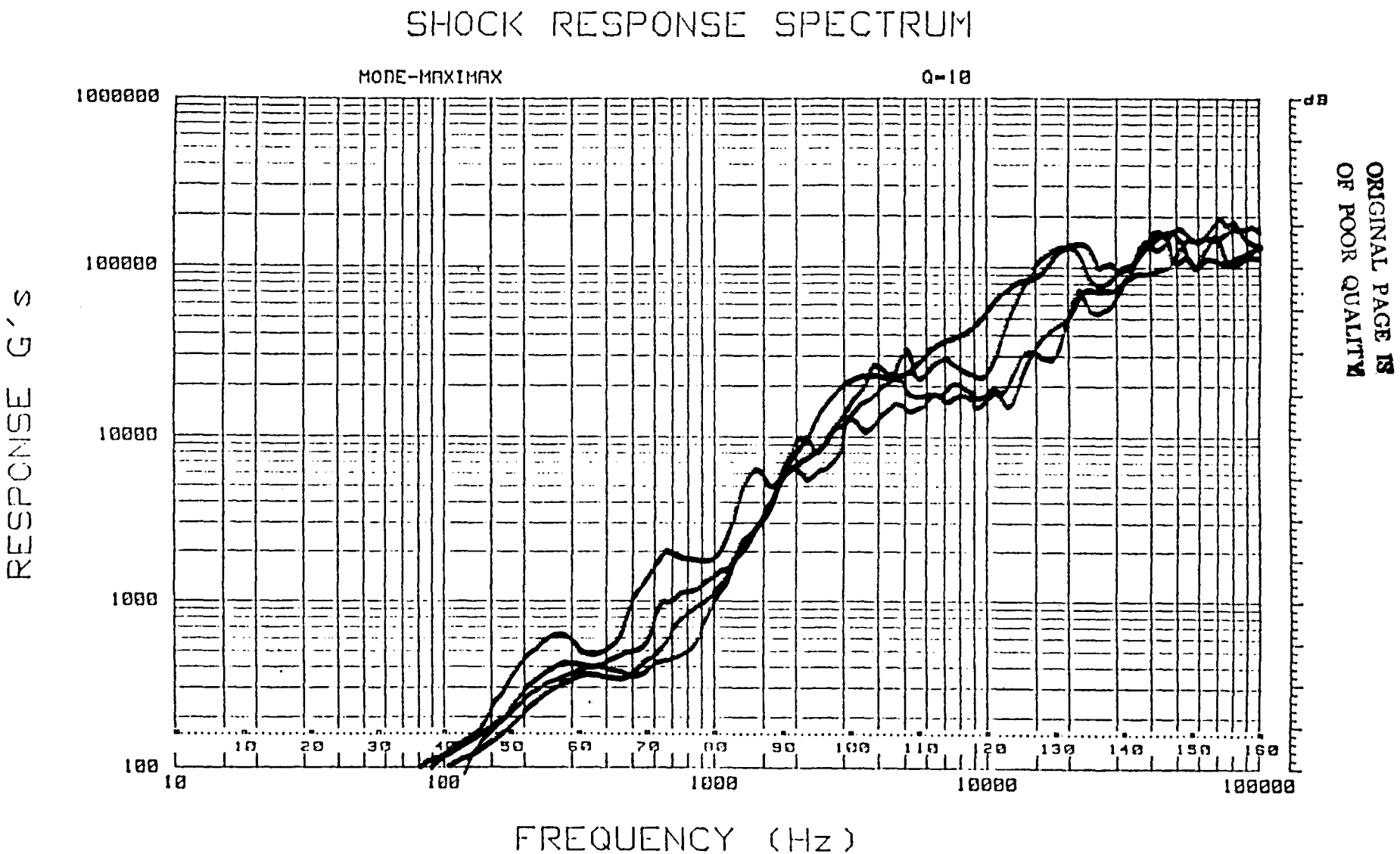

Figure 73. SRS: rigid test – plate Nos. 7 and 8, experimental control.

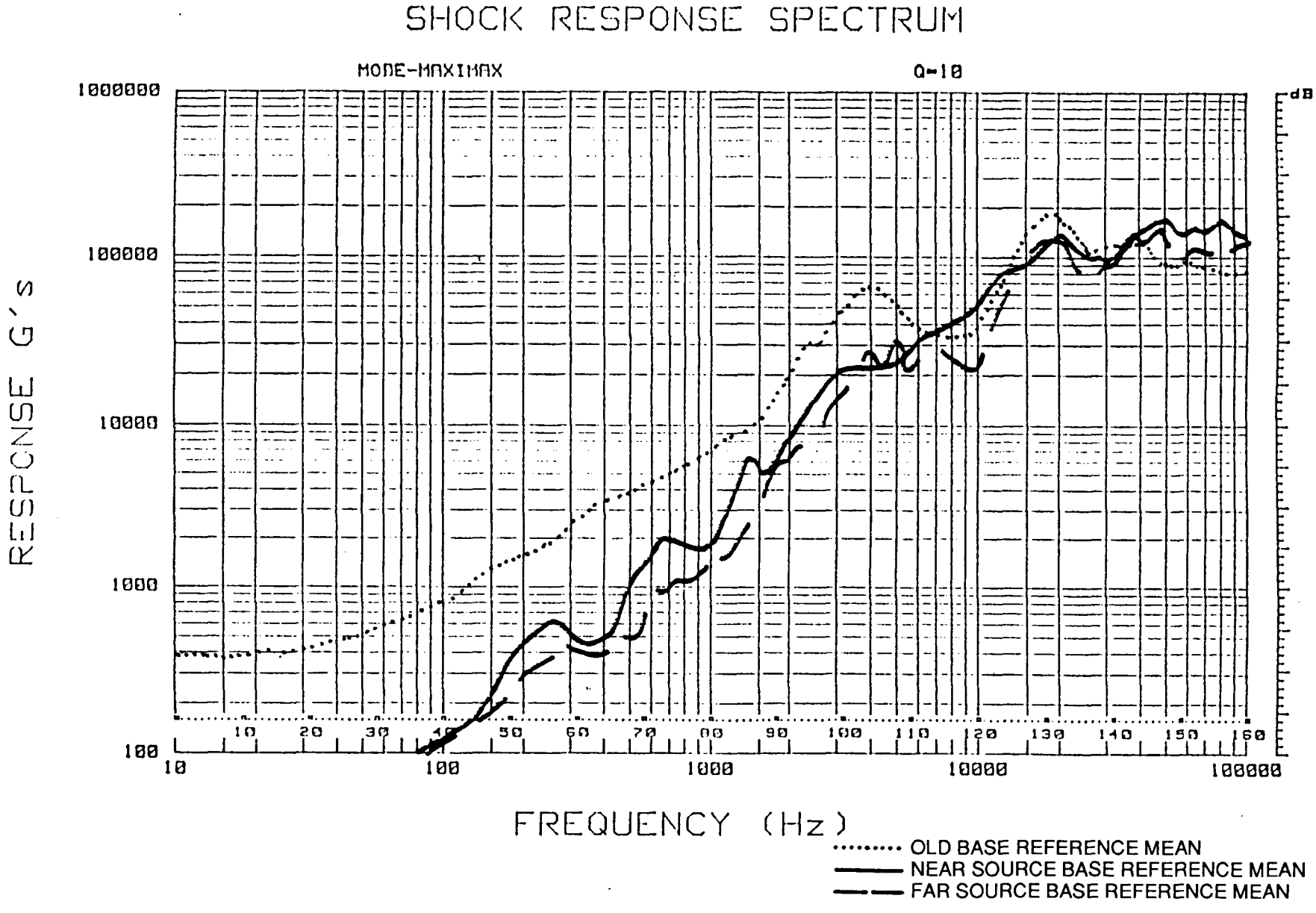

Figure 74. SRS: Rigid test near and far source versus old base reference means.

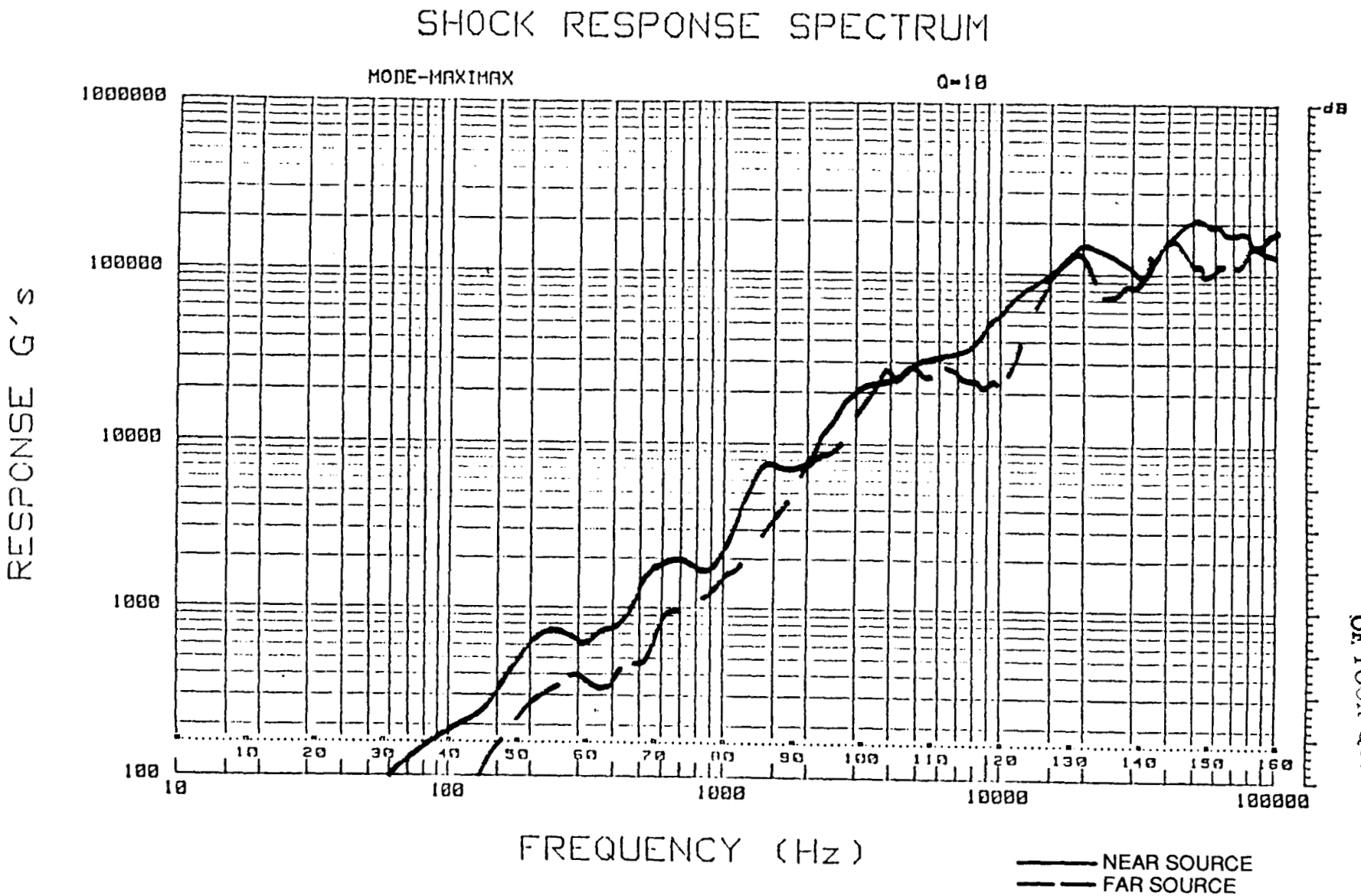

Figure 75. SRS: Rigid test – plate No. 9.

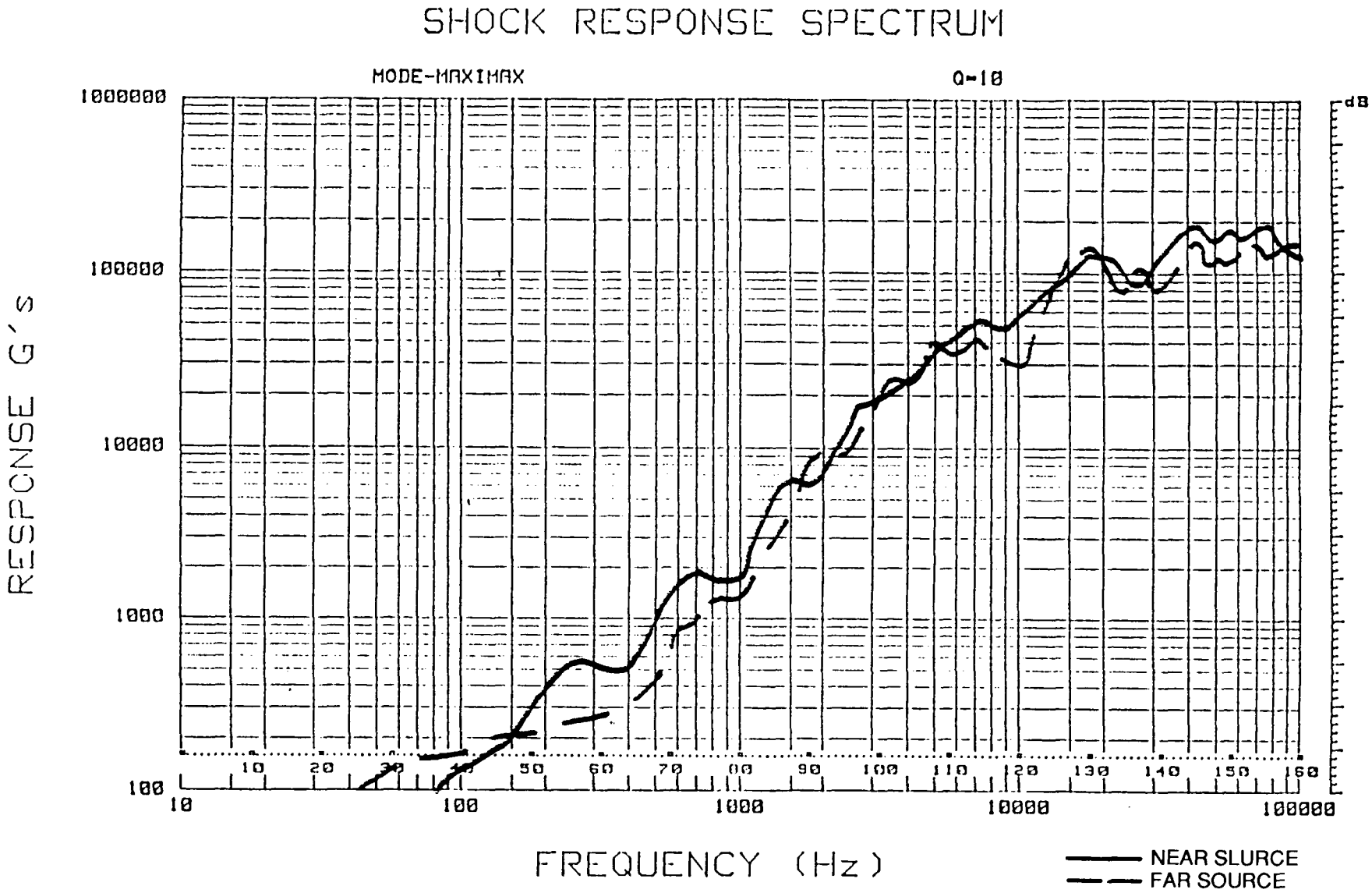

Figure 76. SRS: Rigid test – plate No. 10.

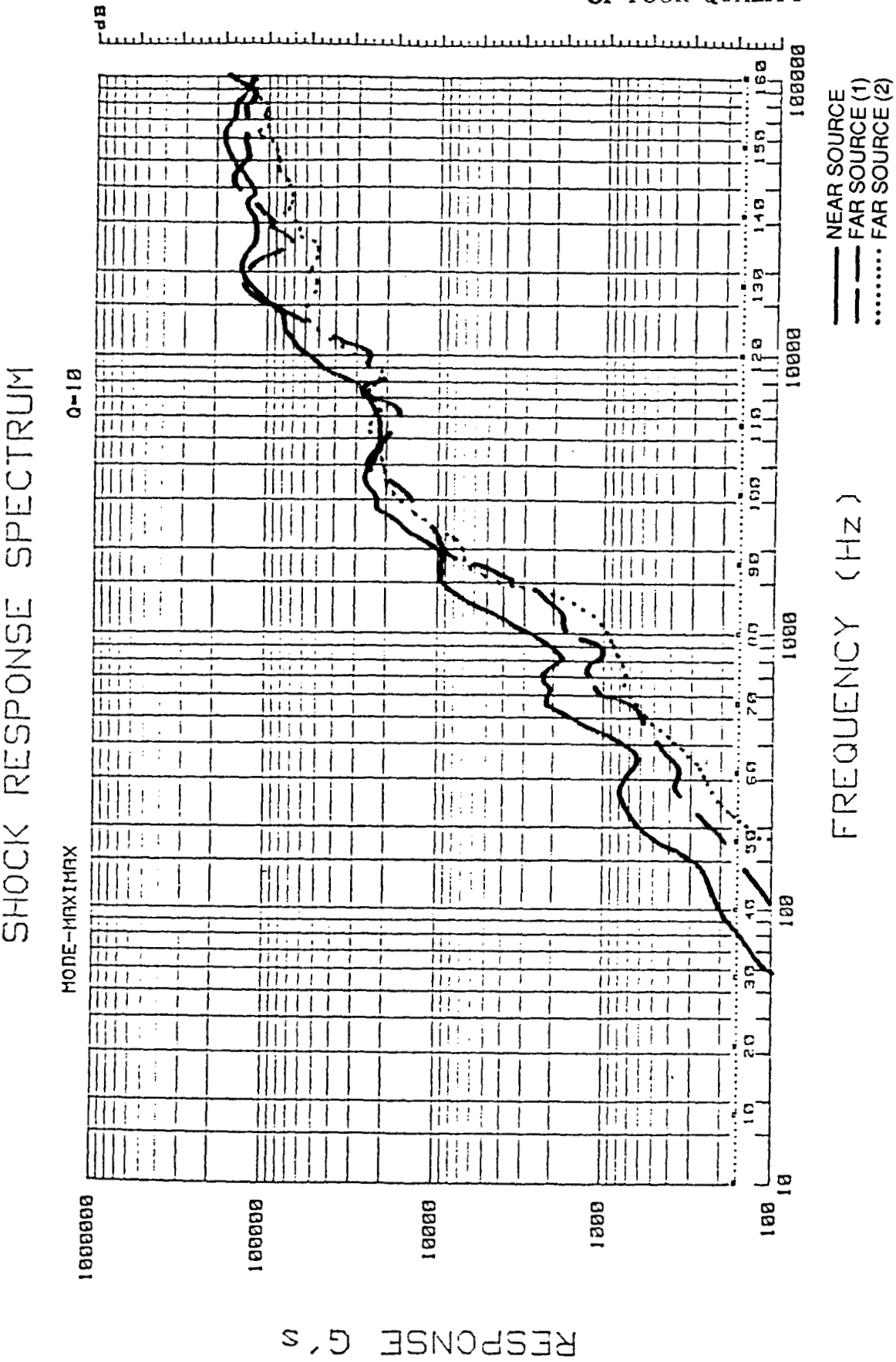

Figure 77. SRS: Rigid test – plate No. 11.

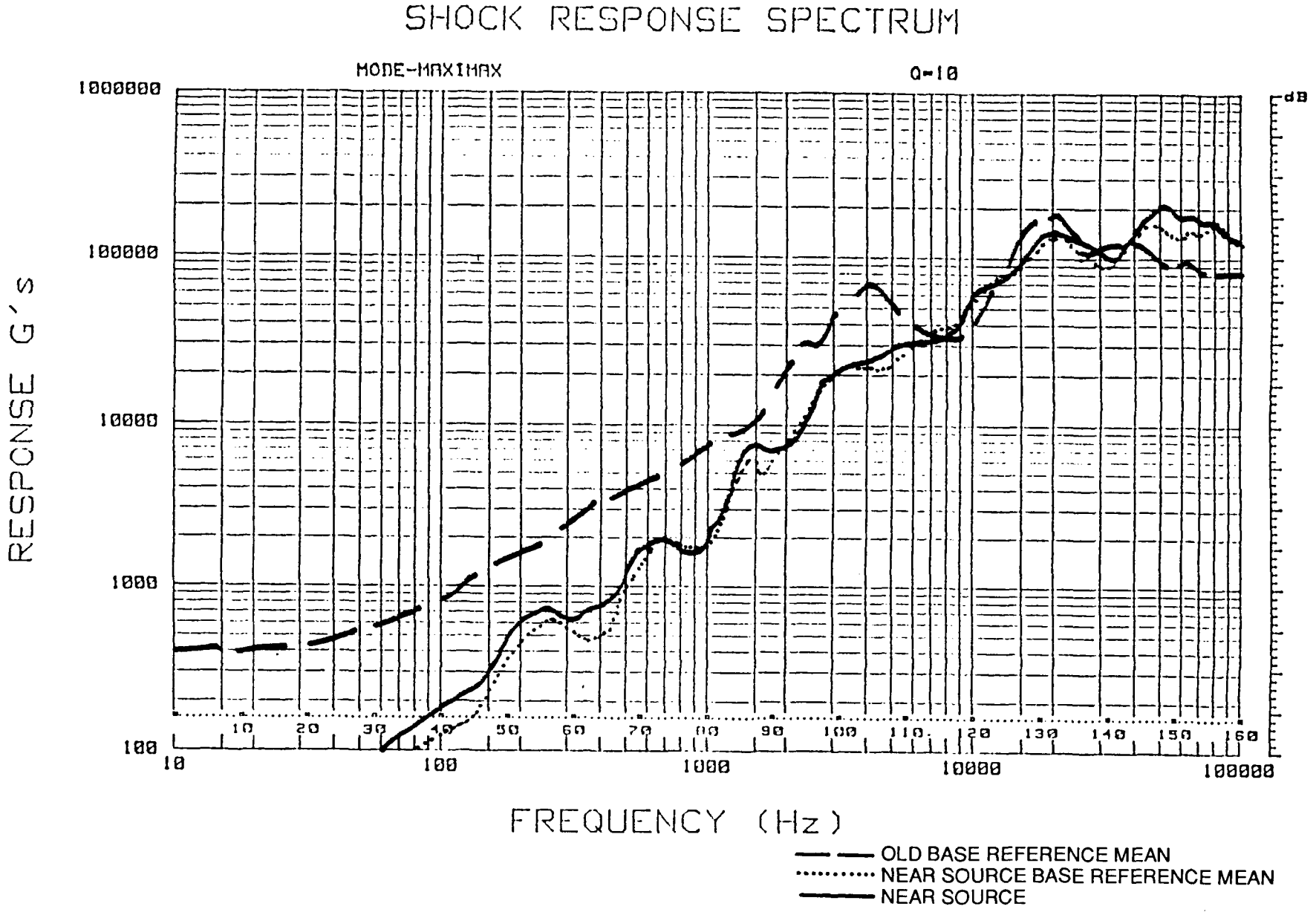

Figure 78. SRS: Rigid test – plate No. 9, near source versus near source and old base reference means.

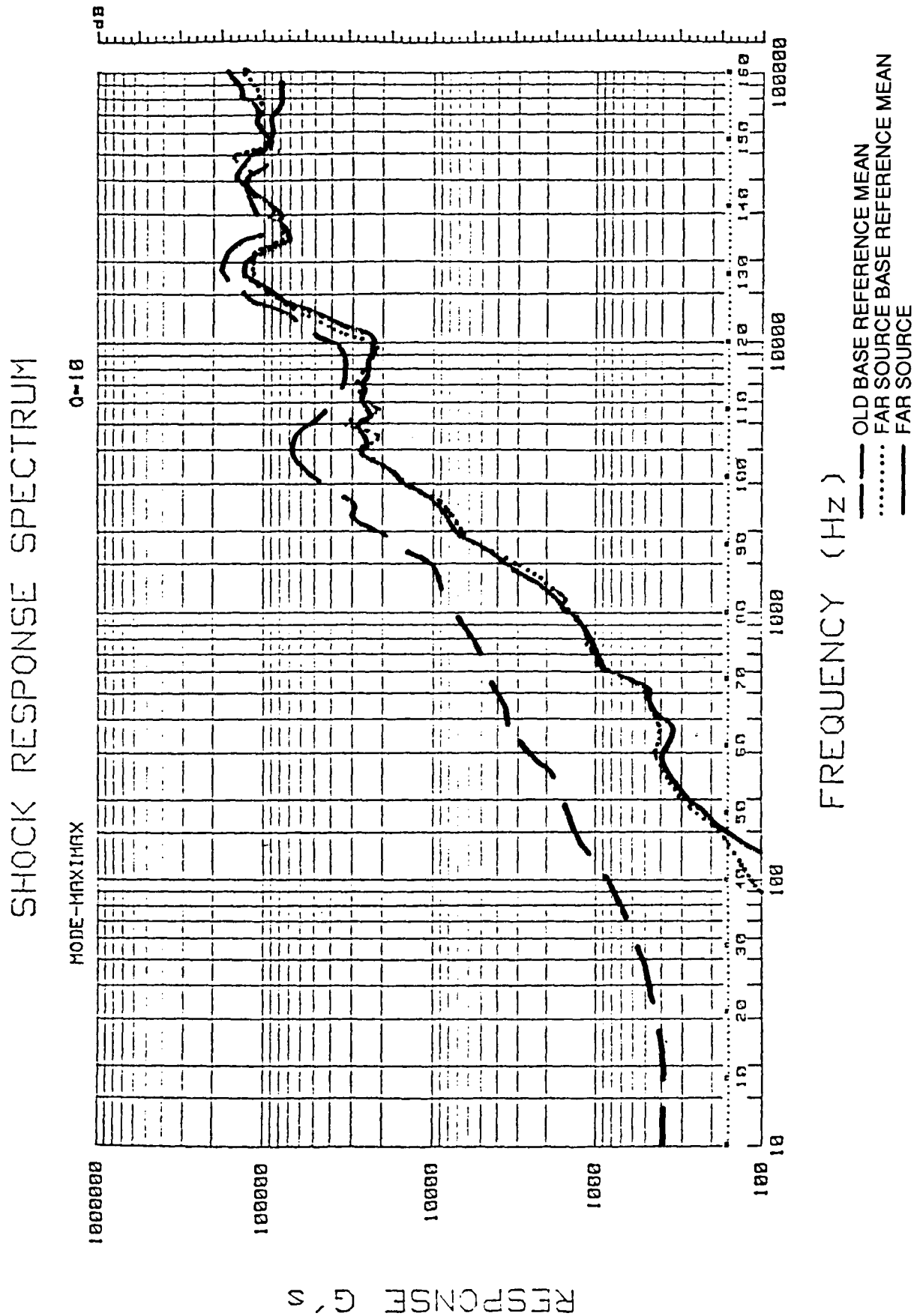

Figure 79. SRS: Rigid test – plate No. 9, far source versus far source and old base reference means.

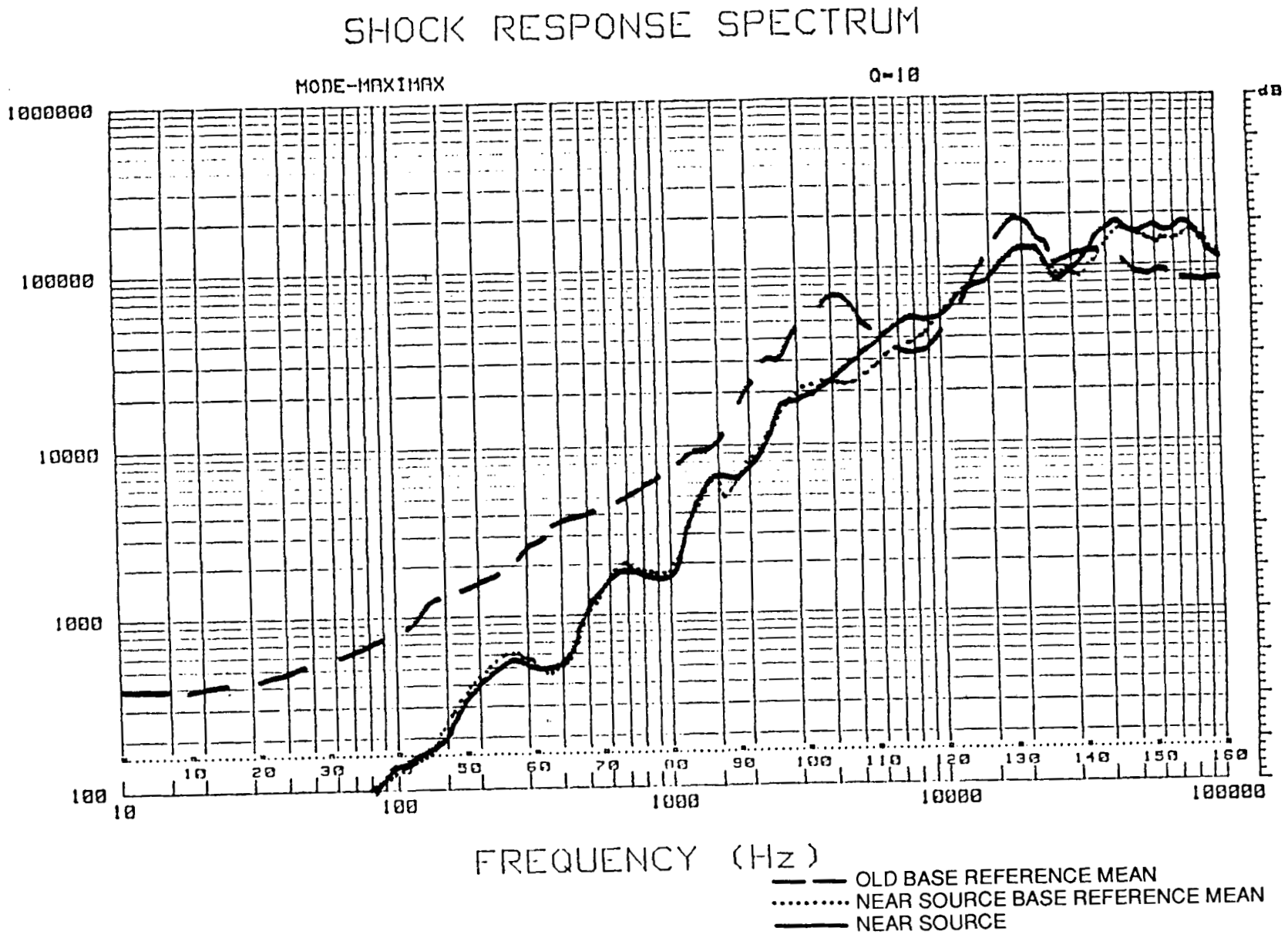

Figure 80. SRS: Rigid test – plate No. 10, near source versus near source and old base reference means.

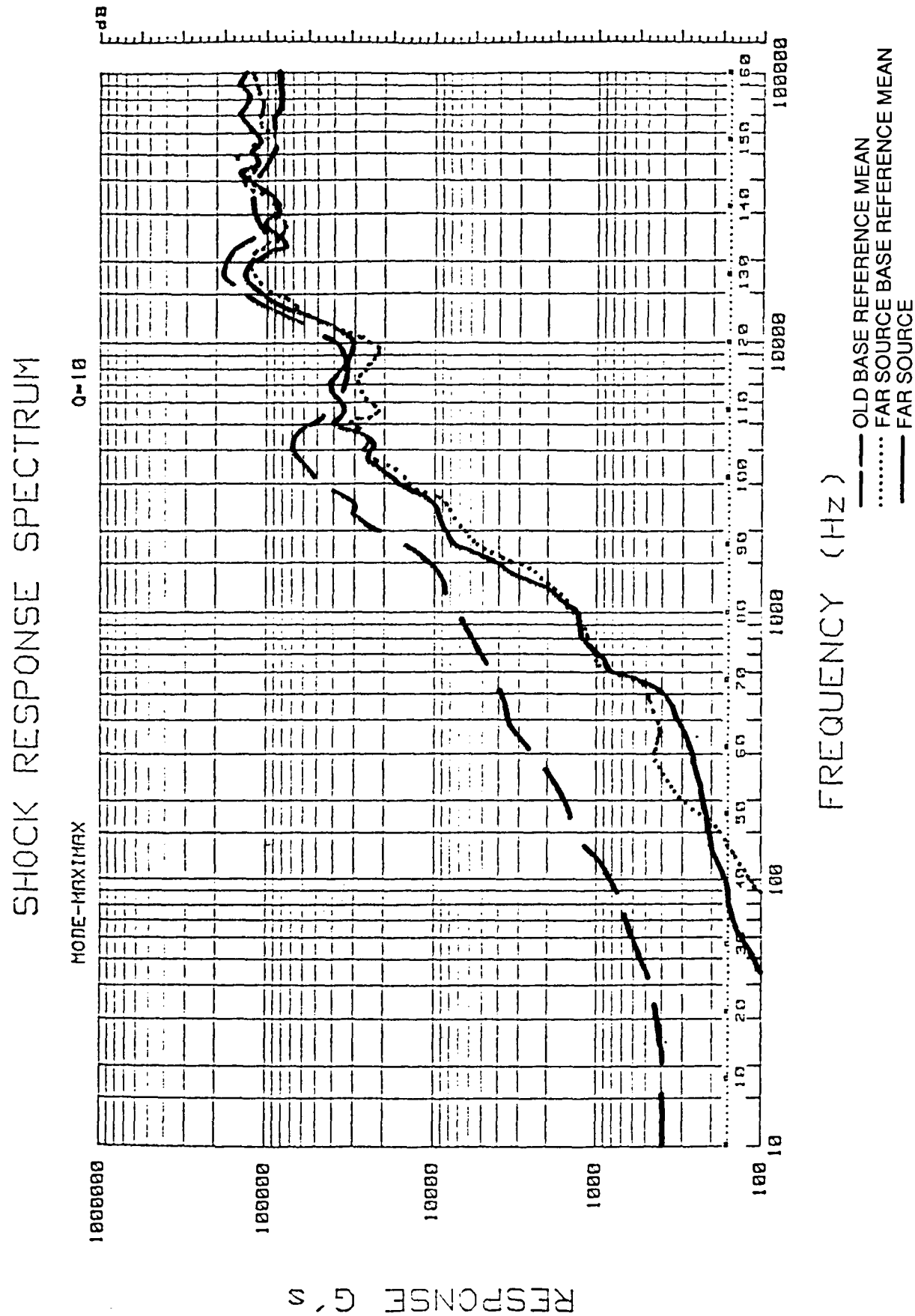

Figure 81. SRS: Rigid test – plate No. 10, far source versus far source and old base reference means.

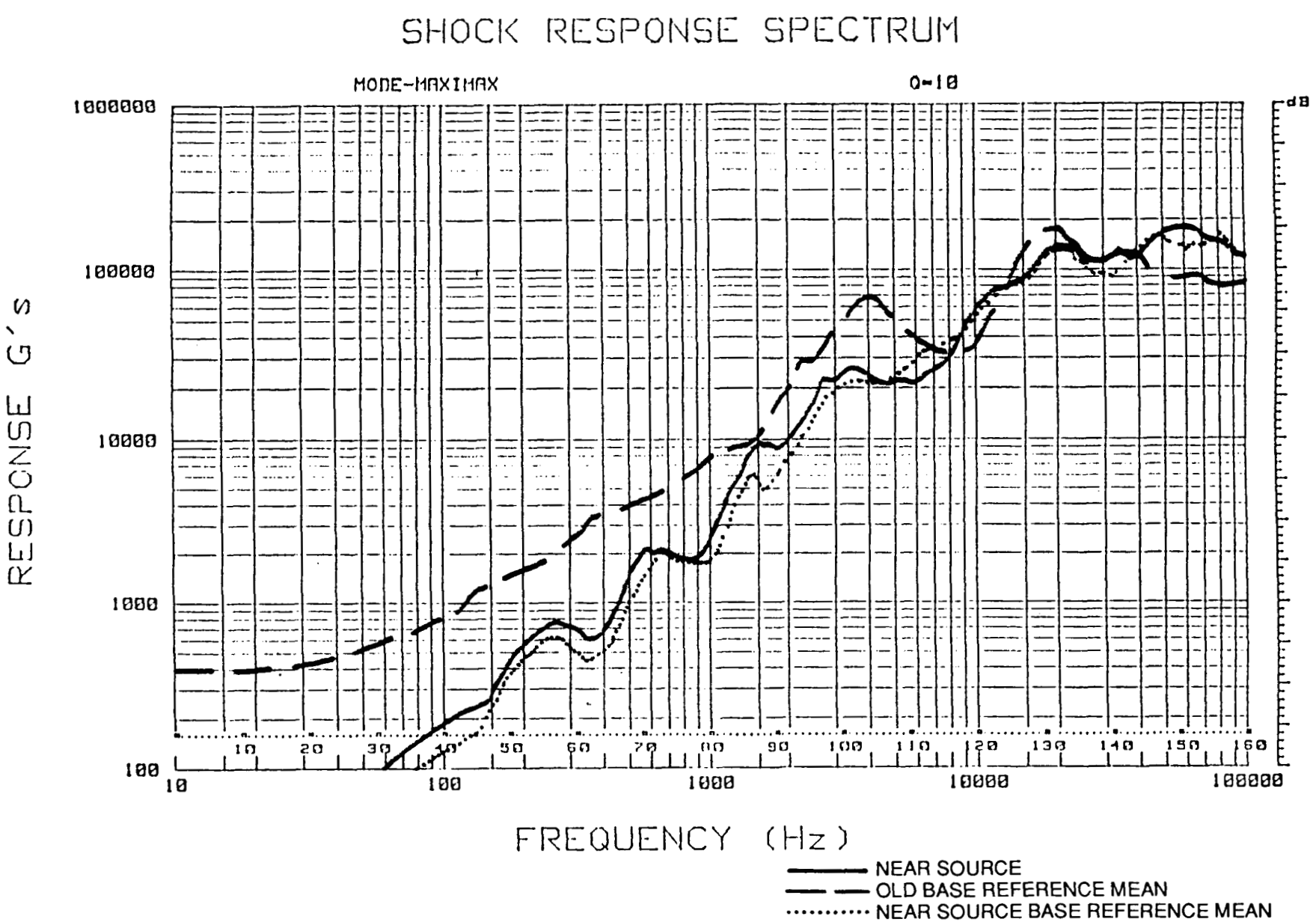

Figure 82. SRS: Rigid test – plate No. 11, near source versus near source and old base reference means.

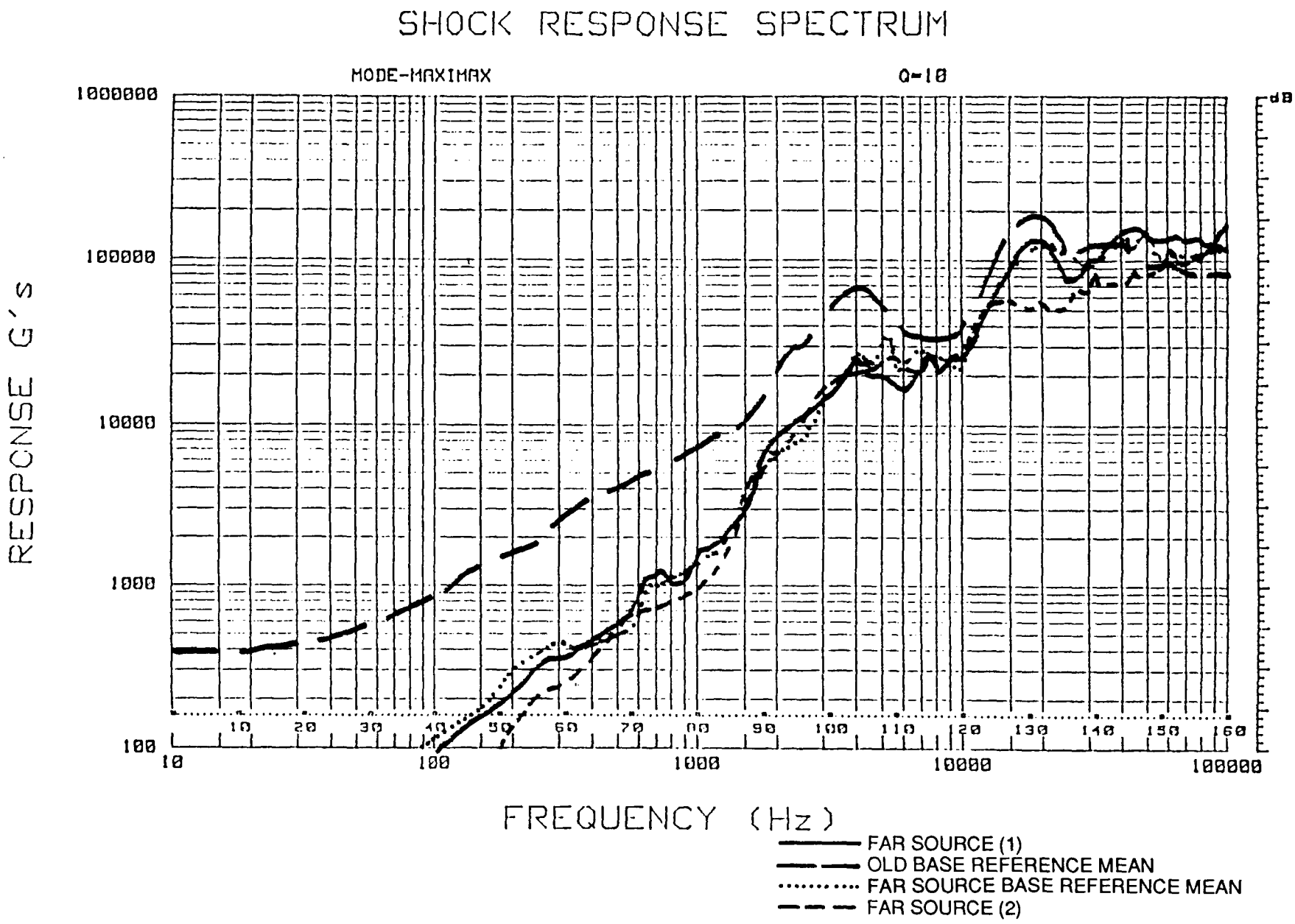

Figure 83. SRS: Rigid test – plate No. 11, far source versus far source and old base reference means.

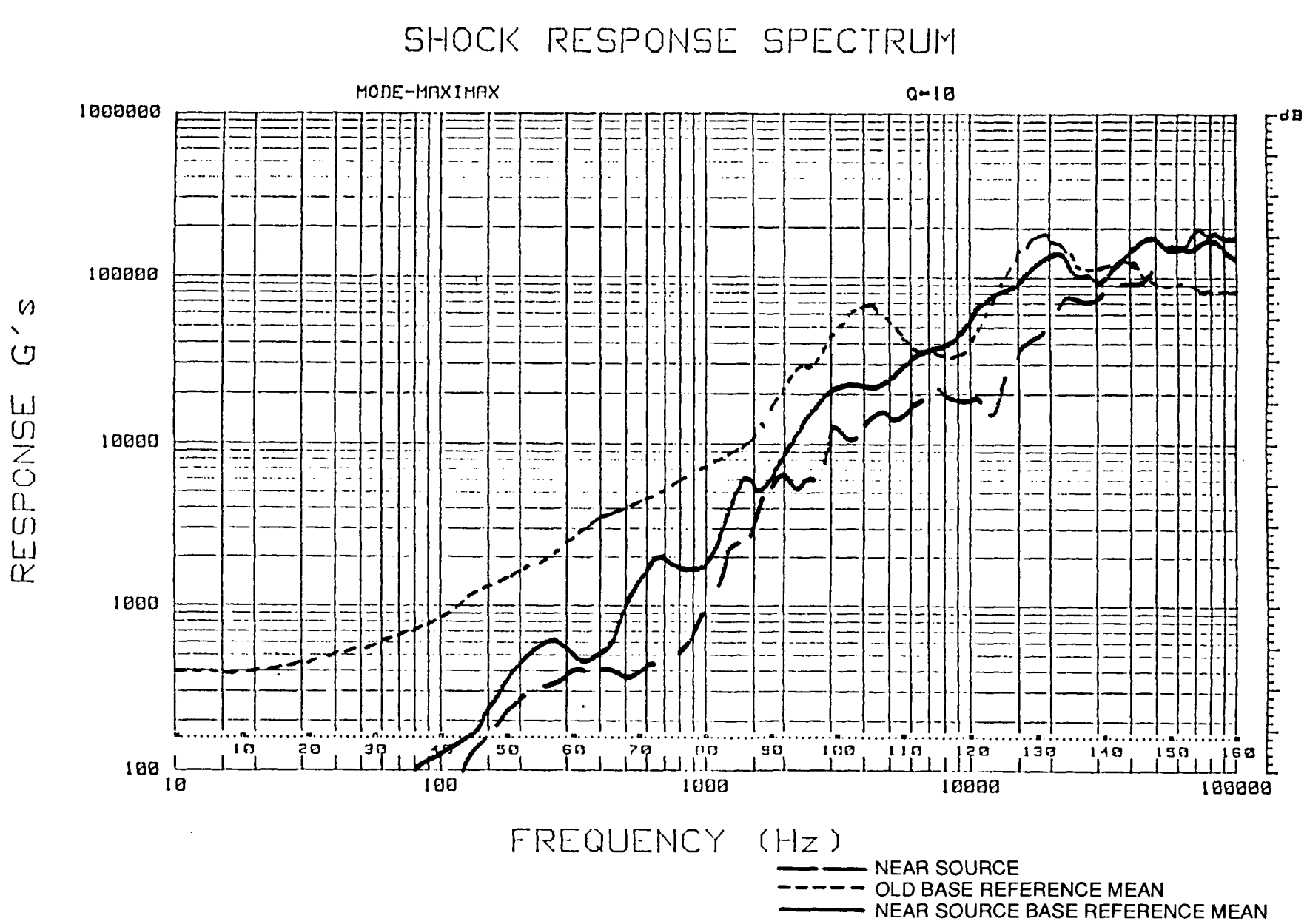

Figure 84. SRS: Mass loaded test.

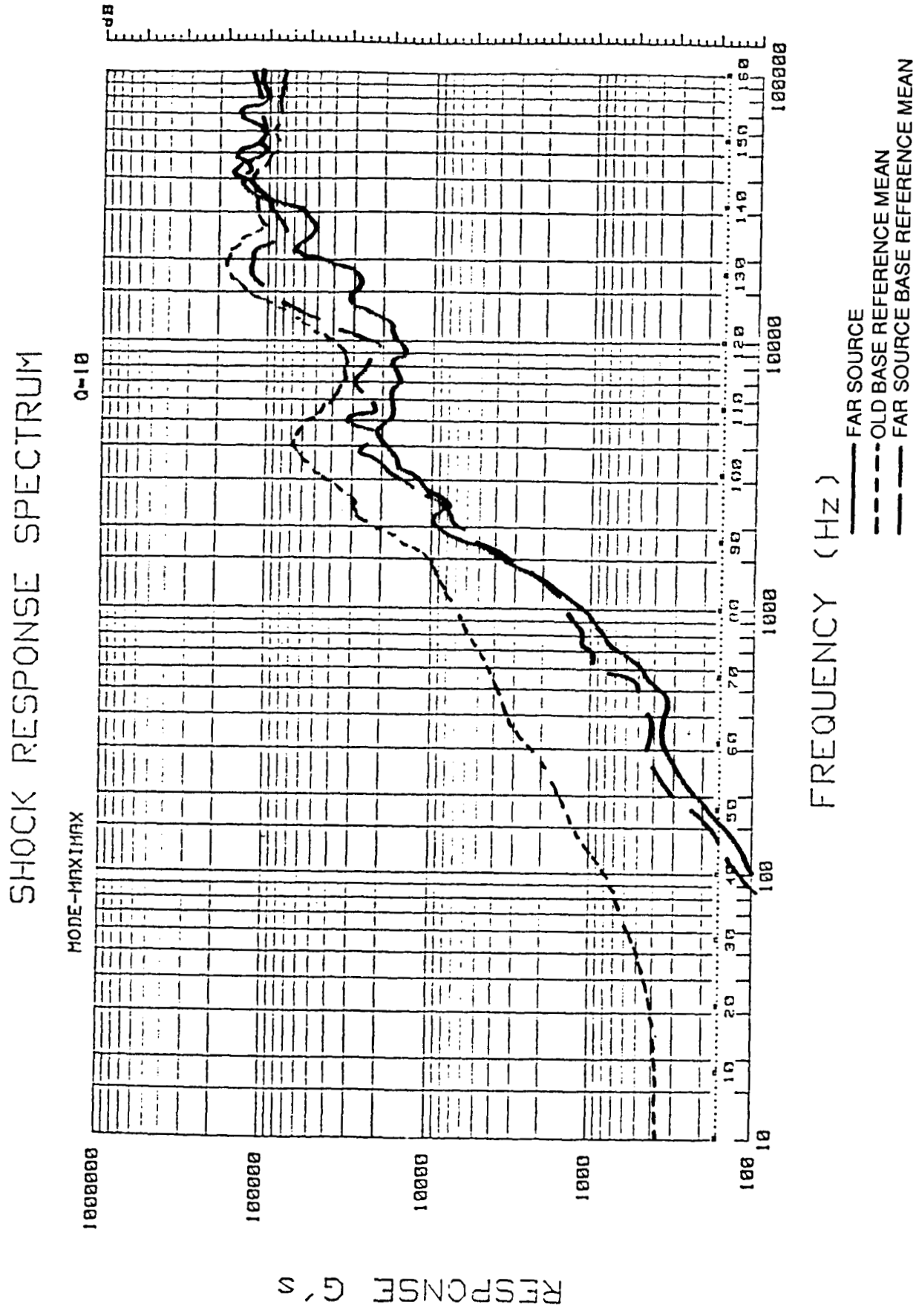

Figure 85. SRS: Mass loaded test.

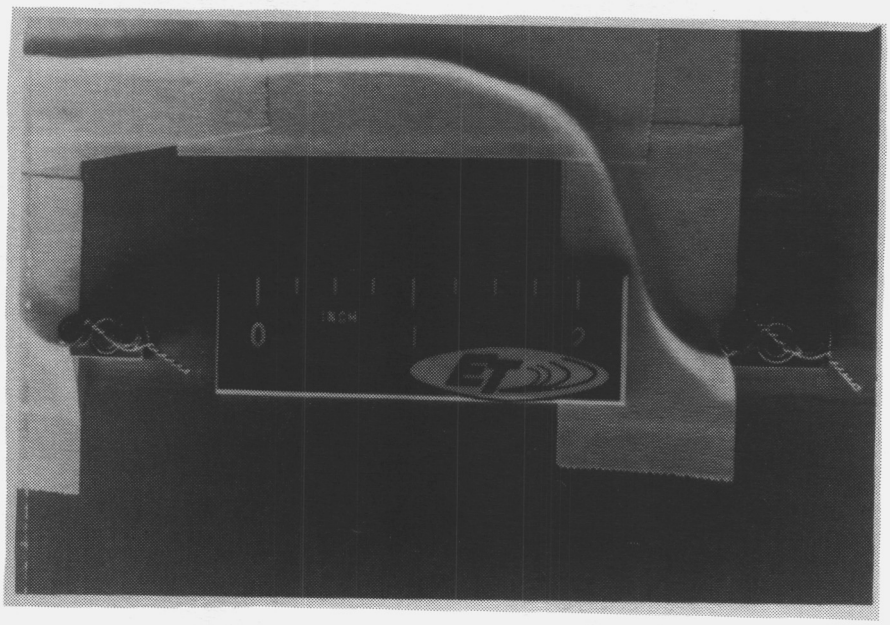

Figure 86. Side-by-side accelerometers.

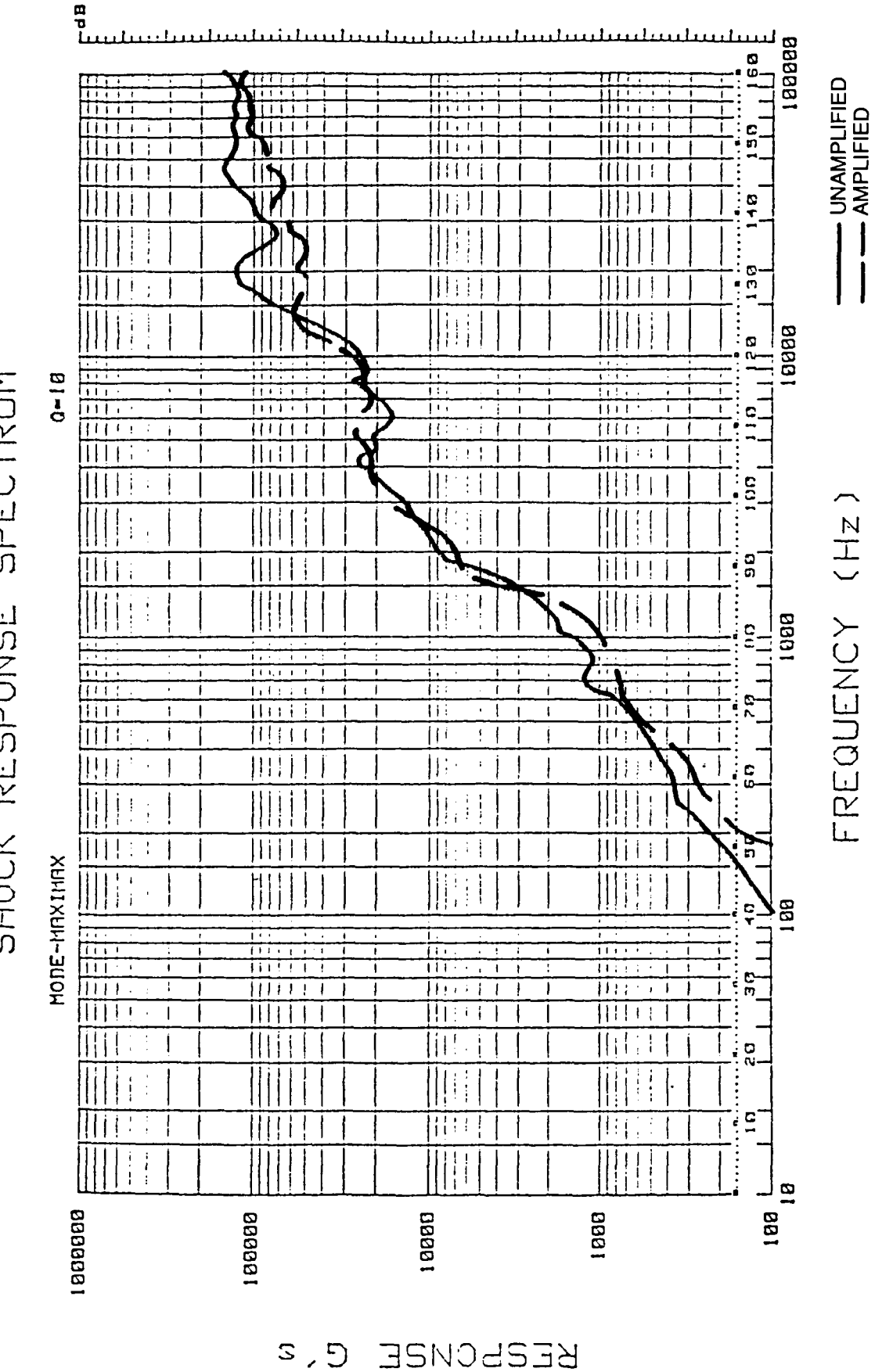

Figure 87. SRS: Unamplified versus amplified side-by-side measurements.

A. Summary

This study evaluated LSC induced shock dissipation through various spacecraft structural joint types and LSC induced shock variation for various manufacturing and assembly variables on clamped boundary test plates. Data was also collected for the next phase of the study: To verify that data correction techniques are capable of accurately recovering pyrotechnic shock data from distorted data records. This study was a direct outgrowth of a previous research and can be traced back to problems encountered early in the STS program.

Eleven pyrotechnic test plates were manufactured utilizing the SRB FSA. Five clamped boundary test plates were designed to investigate manufacturing and assembly variables and mass loading effects. Six free-free boundary test plates were designed to investigate shock energy dissipation across various spacecraft joints.

Each free-free boundary test plate was center severed by an LSC. Two test joints were located symmetrically between the center charge and the ends of the plate. One joint was located on each half of the plate. Clamped boundary test plates were end severed, just as in the original research program alluded to above. Data from the clamped boundary tests should be directly comparable to data from the first research effort.

All eleven tests were successfully performed completing the test portion of the research effort. Time histories were captured and stored on disc. Fourier transforms and SRS were calculated and plotted for each time history.

Data from all eleven tests and from the previous study were analyzed. Results from the joint energy dissipation test will be used to reformulate tables for energy dissipation across joints. Results from the manufacturing and assembly variables tests were used to determine variations in shock levels for both free-free and clamped boundary plates. The minimum and maximum shock perturbation for these variables were investigated.

B. Conclusions

Several conclusions may be drawn from the study. For both free-free and clamped boundary test plates, the shock source is very repeatable – even when the coreload is varied. Shock levels are unaffected by distance on free-free test plates; shock levels decrease with distance on clamped boundary test plates.

Added plate mass due to joint weight does not affect shock levels on free-free test plates. Shock decreases across all 3-in. and 6-in. joints is the same except for the joints with the shims. This could be mass related, but more likely is due to the "Sandwich Theory." Levels from the joint test in the previous shock study are comparable even though the previous study used end-severed plates. Joints do act as mechanical filters filtering out high frequency energy.

SRS from the rigid tests are significantly lower than the free-free SRS from the previous study using the same variables. Near source, the high frequency appears to depend upon the source, with the

C-2

low frequency more a function of the plate characteristics. Mass loading of rigid mount plates does significantly lower shock levels but only near the mass loaded area on the plate. None of the manufacturing and assembly variables affect the shock levels.

Unamplified accelerometers may be used to obtain data. The unamplified channel contained less noise and was slightly lower in the high frequency region.

C. Recommendations

The author recommends that the data correction techniques study, that is in progress, be continued by NASA. Two sets of distinct findings have developed in the 1984-1986 study and the 1987-1988 study. Characteristics of the free-free tests are in many cases exact opposites of the characteristics of clamped boundary plates. The problem at hand is that "real-world" hardware are somewhere in between. At this time we have no choice but to use the most severe case: the free-free plate tests.

Further study is warranted utilizing actual flight hardware or prototypes. Significant energy exists above 20,000 Hz. The author feels that SRS plots should be extended up to 100,000 Hz. These energy levels become critical when electronics, instrumentation, etc., are involved. Extending SRS to 100,000 Hz might prevent some future aerospace failure.

REFERENCES

1. Hieber and Tustin: Understanding the Shock Response Spectrum. Sound and Vibration, 1974, pp. 42-54.

2. Kacena, W. J., McGrath, M. B., and Rader, W. P.: Aerospace Systems Pyrotechnic Shock Data-Ground Test and flight. Volumes 1 through 6, Martin Marietta Corporation, 1970.

3. Engelsferd, I. K., and Rader, W. P.: Aerospace Systems Pyrotechnic Shock Data/Ground Test and Flight. Volume 7, Martin Marietta, 1970.

4. Clark, N. H.: How Accurate is Your Accelerometer. Vibration and Noise Control Eng., Sydney, Australia, 1976, pp. 105-106.

5. DeVorst, V. F. and Hughes, P. S.: Piezoelectric Accelerometer Signal Error in Complex Shock Recordings. U. S. Naval Ordnance Laboratory, Paper NOLT67-194, 1967.

6. Keller, Leo A., Jr.: Linear Vibration Techniques for Measuring the Cross Axis Error Coefficient in an Accelerometer. AIAA Paper, No. 80-1763, New York, 1980, pp. 297-308.

7. Sawyer, G.: Transducer Reliability – Who is to Blame? Noise and Vibration Control Worldwide, Vol. 13, No. 3, 1982, pp. 118-120.

8. Harris, Cyril M. and Crede, Charles E.: Shock and Vibration Handbook. Second Edition, McGraw-Hill Book Co., 1976, pp. 1-23.

9. Thomson, William T.: Theory of Vibration with Applications. Prentice-Hall, Inc., Englewood, New Jersey, 1981.

10. Luhrs, H. N.: Pyrotechnic Shock Testing – Past and Future. IES: Proceedings of Annual Technology Meeting, 1981, pp. 17-20.

11. Bai, M., and Thatcher, W.: High G Pyrotechnic Shock Simulation Using Metal-to-Metal Impact. SVB, No. 49, Part 1, 1979, pp. 97-100.

12. Bell, R. L.: Development of 100,000 G Test Facility. SVB, Vol. 40, Part 2, 1969, pp. 205-214.

13. Conway, J. J., Pugh, D. A., and Sereno, T. J.: Pyrotechnic Shock Simulation. Proc. IES, 1976, pp. 12-16.

14. Conway, J. J. and Sereno, T. J.: Pyrotechnic Shock Testing of Components. Proc. IES, 1977, pp. 109-112.

15. Luhrs, H. N.: Pyrotechnic Shock Transmission in Component Versus S/C Testing-Vibration Table Compared with Instrumented Spacecraft Model. Proc. IES, 1975, pp. 3-27 to 3-44.

16. Fandrich, R. T., Jr.: Bounded Impact – A Repeatable Method for Pyrotechnic Shock Simulation. SVB, No. 46, Part 2, 1976, pp. 101-107.

17. Fandrich, R. T., Jr.: Pyrotechnic Shock Testing on a Standard Drop Machine. Proceeds of IES 20th Annual Meeting, 1974, pp. 269-273.

18. Davie, Neil: Personal interview. Sandia National Laboratories, 1985.

19. Sill, Robert: Personal interview. Endevco Corporation, 1985.

20. Sill, R. D.: Testing Techniques Involved with the Development of High Shock Acceleration Sensors. Endevco Corp., San Juan Capistrano, CA, 1983.

21. Nilsson, L. and Nilsson, B.: Method for Testing Components in the High Acceleration Frequency Range. Luleaa University, Tulea-1981-18, 1981.

22. Keegan, W. B. and Bangs, W. F.: Effects of Various Parameters on Spacecraft Separation Shock. SVB, No. 42, Part 3, 1972, pp. 131-148.

23. Lieberman, P.: Pyrotechnic Plate Analysis and Test Results of Missile and Space Vehicle Hardware. Internal Instrumentation Symposium, 25th, 1982.

24. Liebermann, P.: Pyrotechnic Simulation Techniques to Test Missile and Space Vehicle Hardware. IES No. 84-45551 22-14, 1983, pp. 153-158.

25. Powers, D. R.: Development of a Pyrotechnic Shock Test Facility. SVB, No. 44, Part 3, 1974, pp. 73-82.

26. Schoessow, T. D.: Deviation of Sock Environmental Criteria-Characteristics of Barrel Tester for Shock Test Environment Generation. Proceedings of Aerospace Testing Seminar – Conference on Reliability Engineering and Quality Control Testing of Aerospace Vehicle Components, Sunnyvale, CA.

27. Kyuma, Kazuo, Shuici Tai, and Masahiro Nunoshita: Fiber-Optic Sensing Systems. Central Research Lab., Denshi, Tokyo, No. 21, 1982, pp. 98-101.

28. Hicho, M. D.: Logical Engineering Approach to Vibration Transducer Selection. Noise and Vibration Control Worldwide, Vol. 13, No. 3, 1982, pp. 109-113.

29. Pilcher, James O., II: Acceleration Measurements in High G Environments. U.S. Army Ballistic Research Lab., Technical Report BRL-TR-2610, 1984.

30. Lauer, R.: Accelerometers Using Piezoelectric Ceramic Sensors. Electronic Applications Bulletin, Vol. 35, No. 2, 1978, pp. 105-116.

31. Bouche, R. R.: Accelerometers for Shock and Vibration Measurements. ASME AMD, Vol. 12, 1975, pp. 25-59.

32. Kulkarni, V. P. and Ramakrishna, Rao K.: Design and Development of Piezoelectric Accelerometers. Journal of Industrial Engineering (India), Vol. 55, Pt. ET1, 1974, pp. 1-5.

33. Orlacchio, Anthony W.: Shock and Vibration Transducers. Electronic Design, Vol. 22, No. 21, 1974, pp. 68-75.

34. Schelby, F.: Systems Approach to Measuring Short Duration Acceleration Transients. Sandia National Labs., Report SAND-82-1730, 1983.

35. Schelby, F.: Systems Approach to Measuring Short Duration Acceleration Transients. Sandia National Labs., Report SAND-82-1730C, 1983.

36. Schelby, Frederick: Personal interview. Sandia National Laboratories, 1985.

37. Ball, R. and Lewis, C. P.: Effect of Noise When Driving Signals from Accelerometers. Measurement and Control, Vol. 15, No. 2, 1982, pp. 59-61.

38. Purdy, D.: Vibration Measurements – An Introduction to Piezoelectric Accelerometers and Associated Instrumentation. Noise Control and Vibration Isolation, Vol. 10, No. 5, 1979, pp. 178-181.

39. Marples, V. and Graham, N. A.: Dependence of Piezoelectric Accelerometer Response on Method of Attachments. Journal of the Society of Environmental Engineers, No. 56, 1973, pp. 19-20.

40. Mondshein, Lee F.: Observability of Accelerometer Test-Input Errors. AIAA Paper, No. 80-1762, 1980, pp. 290-296.

41. Brown, G. W. and Drago, G. A.: Shock Calibration of Accelerometers Using Hopkinson's Bar. University of California at Berkeley, 1977.

42. Walston, William H. and Federman, Charles: Fourier Transform Techniques for the Calibration of Shock Accelerometers. National Bureau of Standars, NTIS PB-258982, 1975.

43. Brown, G. W.: High G. Calibration of Accelerometers. University of California at Berkeley, 1975.

44. Bouche, R. R.: High Frequency Shaker for Accurate Accelerometer Calibrations. Journal of Environmental Sciences, Vol. 13, No. 3, 1970, pp. 10-15.

45. Bouche, R. R.: Calibration of Shock and Vibration Measuring Transducers. Bouche Labs., Tujunga, CA, undated.

46. Cannon, J. E. and Rimbey, D. H.: Transient Method of Calibrating a Piezoelectric Accelerometer for the High G Level Range. ASME, Paper 71-Vibr-43, 1971.

47. Clark, N. H.: Developments in Absolute Calibration of Accelerometers at the National Standards Laboratory. Monash University, Department of Mechanical Engineering, Clayton, Victoria, Australia, 1974.

48. Ecker, W.: New Calibration Method for Accelerometers with Wide Ranges. Messtechnik, Vol. 81, No. 12, 1973, pp. 385-393.

49. Ecker, W.: New Procedure for Calibrating High Range Accelerometers. NTIS, UCRL-TRANS-10906/XPS, 1973.

50. Floor, R. Z.: Field Calibration of Accelerometers. International Congress on Acoustics, 6th, Tokyo, Japan, Reports, Vol. 4, 1968, pp. 77-80.

51. Godt, P. W. and Pyle, H. S.: Application of a Laser Interferometer System for Calibrating Accelerometers and Dynamic Pressure Transducers. Journal of Environmental Sciences, Vol. 13, No. 5, 1970, pp. 9-12.

52. Gregory, H.: An Absolute Method of Piezoelectric Accelerometer Calibration. A.Q.D. Labs., Harefield, England, NTIS No. AD729705, 1970.

53. Licht, Torben R. and Yaveri, K.: Calibration and Standards: Vibration and Shock Measurement. Bruel and Kjaer Technical Review, No. 4, 1981, pp. 16-27.

54. Licht, Torben R. and Yaveri, K.: Calibration and Standards: Vibration and Shock Measurement. Measurement and Control, Vol. 15, No. 1, 1982, pp. 9-13.

55. Macinante, J. A.: Recent Developments in Accelerometer Calibration. Monash University, Department of Mechanical Engineering, Clayton, Victoria, Australia, 1974, pp. 381-392.

56. Ramboz, John D.: Comparison and Absolute Calibration of Shock Accelerometers. Proceedings of Shock Symposium and Workshop, Howard Community College, Columbia, MD, 1973.

57. Webster, H. L.: Precision Shock Accelerometer Calibrator. Sandia National Labs., Report CONF-760513-3, 1976.

58. Wittkowski, Ulrich: Shock Pendulum Method for Calibrating and Testing Accelerometers. Tech. Mess TM, Vol. 46, No. 9, 1979, pp. 323-328.

59. Yu, Zhong-Min, Li, Wen-Long, and Dong, Xian-Quan: Absolute Calibration of Accelerometers at High Frequencies. Strain, Vol. 17, No. 1, 1981, pp. 26-27.

60. Luhrs, H. N.: Equipment Sensitivity to Pyrotechnic Shock. Proc. IES, 1976, pp. 3-4.

61. Albers, L.: Pyrotechnic Shock Measurement and Data Analysis Requirements. Proc. IES, Vol. II, 1975, pp. 11-18.

62. Moore, Donald Baker: Memorandum 4DBM-113, Explosive Technology, Fairfield, CA, 1984.

63. Smith, James Lee: Recovery of Pyroshock Data from Distorted Acceleration Records. NASA TP 2494, 1985, pp. 1-14.

64. Moore, Donald Baker: Personal interview. Explosive Technology, 1985.

65. Smith, James Lee: Effects of Variables Upon Pyrotechnically Induced Shock Response Spectra. NASA TP 2603, 1986.

66. Smith, James Lee: Pyrotechnic Shock: A Literature Survey of the Linear Shaped Charge (LSC). NASA TM-82583, May 1984.

67. Final Report, Shock Measurement and Evaluation Study. Explosive Technology, OEA, Inc., ET Report 0231(01)FTR, June 12, 1986.

68. Test Report, Follow-On CDDF Shock Study. Explosive Technology, OEA, Inc., ET Report 0837(01)TR, July 16, 1987.

69. Operating Procedure Manual, Explosive Technology Standard Test Firing Panel. Explosive Technology, OEA, Inc., Manual PN80012.

1. REPORT NO.	2. GOVERNMENT ACCESSION NO.	3. RECIPIENT'S CATALOG NO.
NASA TP-2872		

4. TITLE AND SUBTITLE	5. REPORT DATE
Effects of Variables Upon Pyrotechnically Induced Shock Response Spectra – Part II	November 1988
	6. PERFORMING ORGANIZATION CODE
7. AUTHOR(S)	8. PERFORMING ORGANIZATION REPORT #
James Lee Smith	
9. PERFORMING ORGANIZATION NAME AND ADDRESS	10. WORK UNIT NO.
George C. Marshall Space Flight Center Marshall Space Flight Center, Alabama 35812	M-600
	11. CONTRACT OR GRANT NO.
	13. TYPE OF REPORT & PERIOD COVERED
12. SPONSORING AGENCY NAME AND ADDRESS	Technical Paper
National Aeronautics and Space Administration Washington, D.C. 20546	14. SPONSORING AGENCY CODE

15. SUPPLEMENTARY NOTES

Prepared by Structures and Dynamics Laboratory, Science and Engineering Directorate.

16. ABSTRACT

Throughout the aerospace industry, large variations of 50 percent (6 dB) or more in shock response spectra (SRS) derived from pyrotechnic separation events continue to be reported from actual spaceflight data and from laboratory tests. As a result of these variations, NASA funded a research program for 1984 through 1986. The purpose of the 1984-1986 project was to analyze variations in pyrotechnically induced SRS and to determine if and to what degree manufacturing and assembly variables and tolerances, distance from the shock source, data acquisition instrumentation, and shock energy propagation affect the SRS. Sixty-four free-free boundary plate tests were performed. NASA funded an additional study for 1987-1988. This study was a continuation of the previous study. This paper is a summary of the additional study. The purpose of this study was to evaluate shock dissipation through various spacecraft structural joint types, to evaluate shock variation for various manufacturing and assembly variables on clamped boundary test plates, and to verify data correction techniques. Five clamped boundary plate tests investigated manufacturing and assembly variables and mass loading effects. And six free-free boundary plate tests investigated shock dissipation across spacecraft joint structures.

17. KEY WORDS	18. DISTRIBUTION STATEMENT
Shock Response Spectra Frustum Separation Assembly Linear-Shaped Charge Pyrotechnic Shock	Unclassified – Unlimited Subject Category 39

19. SECURITY CLASSIF. (of this report)	20. SECURITY CLASSIF. (of this page)	21. NO. OF PAGES	22. PRICE
Unclassified	Unclassified	108	A06

For sale by National Technical Information Service, Springfield, Virginia 22161

NASA-Langley, 1988